GC871
C38
no.6

UC-NRLF
C 3 138 828

PHYSICAL
SCIENCES
LIBRARY

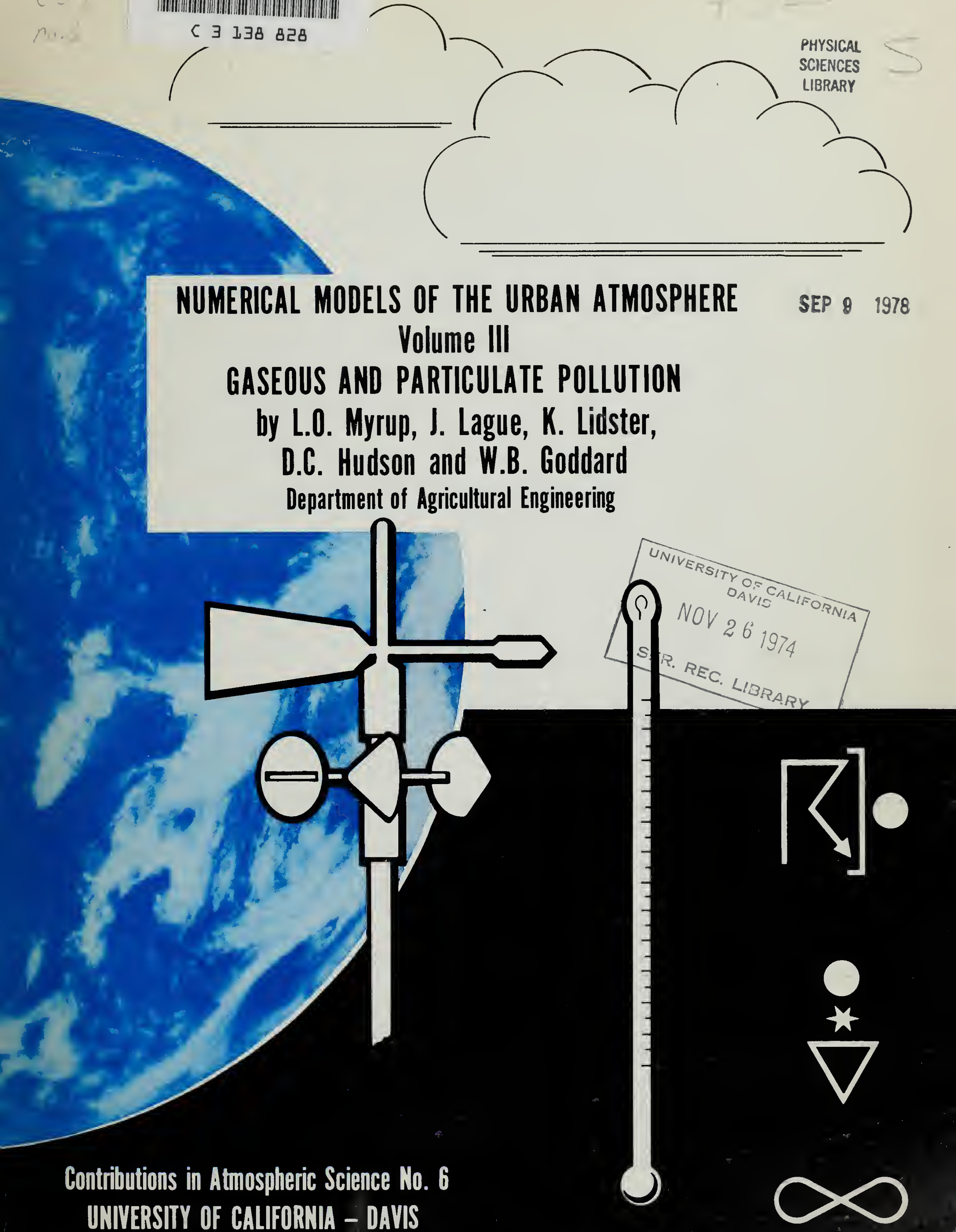

NUMERICAL MODELS OF THE URBAN ATMOSPHERE

Volume III

GASEOUS AND PARTICULATE POLLUTION

by L.O. Myrup, J. Lague, K. Lidster,
D.C. Hudson and W.B. Goddard
Department of Agricultural Engineering

SEP 9 1978

UNIVERSITY OF CALIFORNIA
DAVIS
NOV 26 1974
SER. REC. LIBRARY

Contributions in Atmospheric Science No. 6
UNIVERSITY OF CALIFORNIA – DAVIS

NUMERICAL MODELS OF THE
URBAN ATMOSPHERE

Volume III

Gaseous and Particulate
Pollution

by

L. O. Myrup, J. Lague,
K. Lidster, D. C. Hudson and
W. B. Goddard

Department of Agricultural Engineering
Department of Water Science and Engineering
University of California, Davis

February 1974

Contributions on Atmospheric Science, No. 6
Funded by Air Pollution Control Office,
Environmental Protection Agency

TABLE OF CONTENTS

Chapter		Page No.
	Preface	v
1	The Impact of Highways On Air Quality	1
2	Air Pollution Climatology for Sacramento, California	77
3	Drift, Diffusion and Fallout of an Instantaneous Line Source of Heavy Particles in the Atmospheric Boundary Layer	103

PREFACE

This volume is the third and last of a series reports of a project funded by the Environmental Protection Agency. An overview of the project objectives and accomplishments is given in Chapter One in Volume One. In the present volume, the first chapter was written by L. O. Myrup, the second by L. O. Myrup and J. Lague and the third by L. O. Myrup, K. Lidster, D. C. Hudson and W. B. Goddard. Publication of this report has been delayed for over a year in order that verification of the line source model discussed in Chapter Three could be included. Unfortunately, this was not possible due to the complexity of the appropriate experiments. Therefore, Chapter Three consists only of a description of the development of the model. We plan to include verification information when the model is published in the literature.

Digitized by the Internet Archive
in 2012 with funding from
University of California, Davis Libraries

http://www.archive.org/details/contributionsina06univ

CHAPTER ONE

"THE IMPACT OF HIGHWAYS ON AIR QUALITY"

L. O. Myrup
August 1972

Background

The twentieth century has been a time of constantly increasing energy use in the United States and throughout the world. In the United States since 1925 the rate of increase has been about 3% per year (Darmstadter, 1971). At the same time there has been a major shift from coal to petroleum products as the major source of energy in this country and throughout the world. Pollution is inherent in the production and utilization of energy. Ultimately, we must bow to the Second Law of Thermodynamics and recognize that waste heat is the cleanest kind of pollution we can possibly hope to achieve. Of course, the relative efficiency of various kinds of energy production and use varies and is directly related to resultant pollution. In general terms, the most inefficient uses which we make of energy resources are (1) the conversion process to electric power and (2) transportation by means of the internal combustion engine. Both in terms of waste heat and pollution, power generation and transportation lead all other categories (Darmstadter, 1971; List, 1971).

The subject of this paper is pollution associated with transportation, in particular that emitted by motor vehicles traveling on highways. In the course of the discussion we shall also consider the relative importance of pollution emitted by residential and arterial streets in addition to highways. The processes which lead to a specified air quality level in the air which we all breathe is complex. Figure 1-1 is a rough sketch of the kind of perspective which is useful in considering this problem. The diagram suggests, and we are all aware, that the meteorological influences are highly important in determining air quality. I have chosen to emphasize in this paper the meteorological aspect of the problem, particularly the current state of our ability to model and predict the pollution emission to air-quality part of the process. In addition, I will discuss the influence of land-use patterns on the microclimate and pollution emission. I will not attempt to deal with the

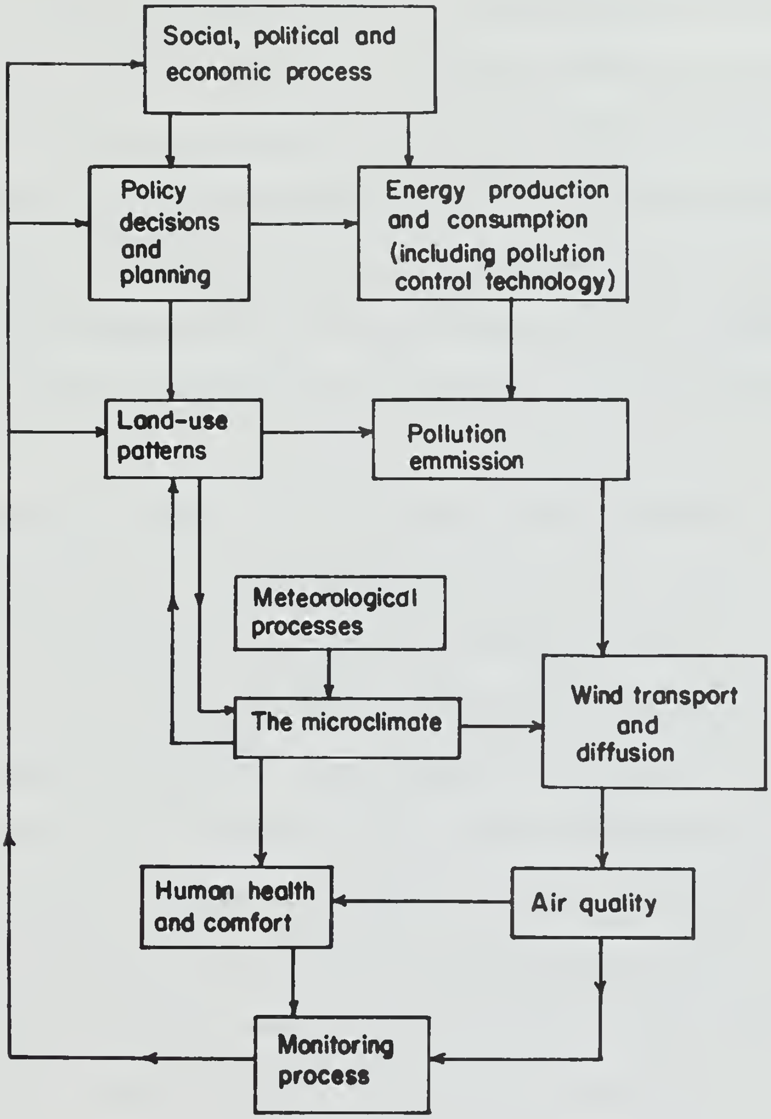
Social, political and economic process
Policy decisions and planning
Energy production and consumption (including pollution control technology)
Land-use patterns
Pollution emmission
Meteorological processes
The microclimate
Wind transport and diffusion
Human health and comfort
Air quality
Monitoring process

Figure 1-1. The air pollution system.

human health problem associated with air pollution.

Much of this paper is meant to have implications for and to be useful to the policy decision and planning processes in society. One of the benefits of making a diagram like Figure 1-1 is that it forces you to consider the problem from a broad perspective. From this point of view, it becomes clear that, say, the inventory process or land-use patterns are also critical components in determining the net result of the entire process which I take as human health and comfort. The policy-decision-making and planning processes are particularly important, for it is there that we have some hope that accurate information and our best estimates of the consequences of changes in specific portions of the system may have significant impact for the common good.

In this context, I would like to point out that the transportation industry has a unique advantage and role to play. In contrast to many portions of society, the advance planning component of transportation is strong and accustomed to making us of the best available engineering information in its operations. Consequently, the additional considerations which are necessary to protect and manage air quality come naturally, in my opinion, to highway engineers and administrators. My optimistic view is then that the transportation industry has an excellent opportunity to lead the way in rational planning to simultaneously satisfy both the innemse demands which society makes for goods and services and also to protect environmental quality.

Discussion of the Problem

Since we are dealing with pollutants emitted from motor vehicles, we may technically define the problem from a meteorological point of view as transport and diffusion of material emitted from a line source near the surface of the earth. The problem is not really this simple, as we shall see, but the geometry strongly suggests this approach. One of the problems is that of

TABLE 1-1.

Highway height z(m)	%Improvement per meter height $- \frac{100}{C} \frac{\partial C}{\partial z} = 100/z \ln z/z_o$
1	43.5
2	16.7
3	9.8
4	6.8
5	5.1
6	4.1
7	3.4
8	2.9
9	2.5
10	2.2

scale. Like most complex systems, the factors which are important to small-scale processes in the atmosphere are very different from those which determine the larger scales. The phenomena which effect the transport and dispersion of highway pollution include the micro- and mesoscale, in the the meteorological terminology. In this section, we will develop this distinction and its significance to highway air quality.

Eschenroeder (1971) has shown the existence of a zone above highways in which the air is well mixed by the energy of the moving vehicles. This zone has the dimensions of twice the height of the average vehicle times the highway width and is called the mechanically mixed cell. This mixing zone or cell can be thought of as the cumulative effect of all the turbulent wakes which are formed behind each object moving along the highway. Within the mechanically mixed cell, pollution is dispersed uniformly, to a first approximation, and this state is the effective initial distribution of air pollution which is acted upon by micro- and mesometeorological processes to affect air quality downwind of the highway.

It should be noted that in this simple model the quality of the air which drivers and passengers breathe directly above the highway is completely determined by the properties of the vehicles and their motors and is independent of meteorological processes. At sufficiently high winds, this certainly cannot be true. The extent to which the mechanically mixed cell is affected by external meteorological influences has not been studied in sufficient detail to allow any general statements at this time. This is an important point because it determines the pollution levels which highway travelers are subjected to and should be the object of an intensive experimental effort.

One operational conclusion which can be drawn from the mixing cell concept is that the effective height of emission of highway pollutants is the average height of the vehicles. For the remainder of this section, we shall imagine that the actual highway emission pattern may be replaced by a line source concentrated at that height. This material, whether gaseous or particulate, is now subjected to the microscale wind transport and diffusion processes. Under most conditions, the wind near the ground varies logarithmically with height according to

$$U = \frac{U_*}{k} \ln \frac{z}{z_o} \quad ,(1)$$

where U is the wind speed at height z, k is the von Karman constant, U_* is a micrometeorological parameter called the friction velocity, and z_o is the aerodynamic roughness and is directly related to the geometrical roughness of the surface. These last two parameters are important to the processes by which atmospheric turbulence is generated near the ground. U_*, which is defined by

$$U_* = \sqrt{\frac{\tau}{\rho}} \quad ,(2)$$

where τ is drag force which the wind exerts on the surface and ρ is air density, can be thought of as representative of the turbulent velocity fluctuations which arise from the roughness of the surface and which do most of the work in diffusing material near the surface. The significance of the logarithmic wind law for highway air quality lies in the fact that in all theoretical and empirical treatments of air pollution, air concentration is found to be inversely proportional to wind speed. Consequently, the air quality downwind of a freeway must be closely related to the effective height of emission and elevated highway configuration would be expected to result in significantly improved downwind air quality compared to at-grade highways. Again, we must qualify this statement with the fact that highway measurements adequate to verify this prediction are only now being made.

I have made an order of magnitude calculation of the wind dilution effect on local air quality to be gained from elevating freeways. Assuming a logarithmic wind profile and all other factors constant, I calculated the effect of raising the highway to height z on the air concentration of pollution, C, at the same height at some arbitrary distance downwind. I obtained the relationship

$$\frac{100}{C}\frac{\partial C}{\partial z} = \frac{-100}{z \ln z/z_o} \quad .(3)$$

If we take $z_o = 0.1$ m, a value typical of suburban-land use, this formula gives the following results. (See Table 1-1)

As can be seen, large improvements in air quality would be expected downwind for the first one to two meters of elevation but with decreasing effect after that. It should be emphasized that this is only a rough order-of-magnitude estimate and neglects other effects which may be more important in some cases, but would be expected to work in the same sense.

A second qualifying remark should be made at this point. The logarithmic wind law is strictly valid only for conditions in which the atmosphere is well mixed. Under other conditions, corrections must be made to this relationship (Morgan, Pruitt and Lourence, 1971) which are, however, not large in magnitude and are well known providing a parameter called the Richardson Number, which we will discuss in the following section, is measured or estimated.

At the same time that highway pollution is being transported by the wind, it is being diffused by atmospheric turbulence. It is useful to consider the energetics of turbulence at this point. We may define the kinetic energy per unit mass, e, of the field of turbulence at a point as

$$e = \overline{1/2\ (u)^2} \quad ,(4)$$

where u is the turbulent component of the wind speed near the ground such that

$$U = \overline{U} + u \quad ,(5)$$

where $\overline{U}$ is the average wind speed. In both equation (4) and (5), the overbar signifies a spatial or a sufficiently long time average. Since we have chosen to consider turbulence as energy, it is instructive to look at the sources and sinks of turbulence energy neat the ground. This problem was first treated by Richardson (1920) who was particularly interested in the special case when turbulence vanishes in the atmosphere, a situation of critical significance to the air pollution problem.

The rate at which turbulence energy is generated mechanically by wind shear associated with surface roughness is given by (Lumley and Panofsky, 1964)

$$U_*^2 \frac{\partial U}{\partial z} = K_m \left(\frac{\partial U}{\partial z}\right)^2 \qquad ,(6)$$

where K_m is the turbulent diffusivity for momentum in the atmosphere and arises from the definition of U_*. The rate at which turbulence is suppressed by stable temperature gradients near the ground is given by

$$\frac{-g}{T} \frac{H}{\rho c_p} = \frac{g}{T} K_h \frac{\partial \theta}{\partial z} \simeq \frac{g}{T} K_h \frac{\partial T}{\partial z} \qquad ,(7)$$

where g is the acceleration of gravity, T is air temperature in degrees Kelvin, c_p is the specific heat capacity per unit mass, H is the flux of sensible heat carried upward by turbulence (negative for stable conditions in which heat is diffused downwards), K_h is the turbulent diffusivity for heat and θ is the pttential temperature, which in most practical cases may be replaced by temperature. It is apparent that the sign of this term changes if the sensible heat flux is upward, which corresponds to the normal condition during the day when heat is being transferred upwards by convection from the warm ground. In this case, the temperature stratification is unstable and turbulence is being generated by buoyant forces rather than being suppressed. For stable stratification, Richardson reasoned that turbulence would disappear when

$$\frac{g}{T} K_h \frac{\partial T}{\partial z} > K_m \left(\frac{\partial U}{\partial z}\right)^2$$

or

$$\frac{\frac{g}{T} K_h \frac{\partial T}{\partial z}}{K_m \left(\frac{\partial U}{\partial z}\right)^2} > 1 \qquad ,(8)$$

that is, when the turbulence sink exceeds the source. The Richardson number, Ri, has come to be defined by

$$Ri = \frac{\frac{g}{T}\frac{\partial T}{\partial z}}{(\frac{\partial U}{\partial z})^2} \qquad ,(9)$$

where potential temperature must be used in the numerator if large height increments are used in evaluating the temperature gradient. Experimentally, it has been found that turbulence vanishes at Richardson numbers around 0.3 (Townsend, 1957). That fact that the critical Richardson number is not unity reflects experimental (Morgan, Pruitt and Lourence, 1971) observations that the ratio K_h/K_m is considerably less than one under stable conditions.

In the years since Richardson's pioneering work, the parameter which bears his name has assumed an overwhelming significance in micrometeorology. It has been shown experimentally (Deacon, 1949) and theoretically (Batchelor, 1953) that the Richardson number is the most important single parameter in all micrometeorological processes. That is to say, Ri is more important than, say, wind speed or the temperature stratification, considered alone. In particular, the Richardson number has been found to be enormously useful in organizing data into simple and understandable patterns. Figure 1-2 shows some typical micrometeorological data organized into useful functional relationships by the use of the Richardson number.

The Richardson number has the disadvantage that its numerical value varies with height so that measurements of this parameter must be made at a standard height to be comparable. Another equivalent parameter, more useful in some ways, may be obtained by forming the ratio of the two energy source/sink terms as before but now using the most fundamental definition on the left of equations (6) and (7),

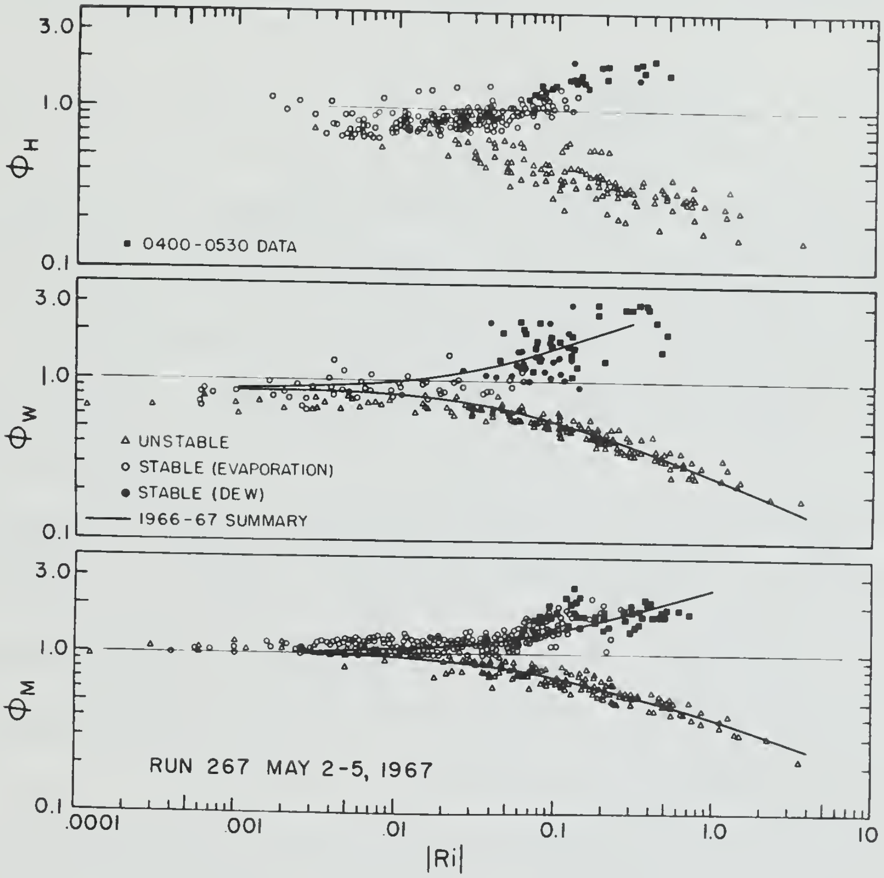

Figure 1-2. Micrometeorological measurements of the "phi functions" plotted as functions of the Richardson number.

$$\frac{\frac{-g}{T}\,\frac{H}{\rho c_p}}{U_*^2\,\frac{\partial U}{\partial z}} = \frac{z}{\left[\frac{-\rho c_p\,T\,U_*^3}{k\,g\,H}\right]} \quad ,(10)$$

where we have used the vertical derivative of the logarithmic wind law in this transformation. The quantity in brackets, which has the dimension of length and is approximately constant with height, is called the Monin-Obukhov length, L, where

$$L = \frac{-\,\rho c_p\,T\,U_*^3}{k\,g\,H} \quad .(11)$$

Under stable conditions (downward, negative heat flux, H), the Monin-Obukhov length has the interpretation of being roughly the height at which turbulence is suppressed. Under stable conditions, then, pollution emitted near the ground would be expected to diffuse to height L. Under very stable conditions, L becomes small and air pollution concentrations high. Under unstable conditions, L is negative and has the physical interpretation as being the height at which convectively-produced turbulence energy compares with mechanically produced energy. Above L, convection predominates and, under these conditions, turbulence levels are higher, atmospheric diffusion more efficient, and air concentrations of pollution are less.

We shall discuss the mathematics of diffusion in the next section. In qualitative terms, it is permissible to visualize atmospheric dispersion as a process similar to molecular diffusion in a solid or liquid body. The random motion of the molecules acts on superimposed gradients to transport properties, such as heat, "down the gradient" from regions of high concentration to low. In the analogy with turbulent motion in fluids, turbulence is thought of as essentially random motion which acts to mix or equalize distribution of fluid properties and, thus, the net result is a transport process in which one region of the fluid gains at the expense of another. Formally we can define diffusivity, K_s, of a fluid property, s, expressed in units per unit mass of fluid by

$$F_{sx} = -\rho K_s \frac{\partial c}{\partial x} \qquad ,(12)$$

where F_{sx} is the flux (transport per unit area and time) of s in the x direction resulting from the diffusion process, and c is the concentration per unit mass of air. The diffusivity so defined is formally equivalent to molecular diffusivity and, indeed, may be regarded as the sum of the molecular and turbulent processes. The size of the turbulent component of the diffusivity is, however, many orders of magnitude larger than the molecular term in natural fluid systems. The conclusion to be drawn is then that turbulence is vastly more efficient at transporting fluid mass and whatever properties associated, including pollution, than is molecular diffusion. That is the central significance of turbulence and also, as far as we know, the fundamental reason for its existence.

The molecular analogy is useful only in a very general sence. Unlike molecular properties, such as conductivity or viscosity which can be tabulated as physical constants for many systems, turbulent diffusivity is a complex function of the state of the flow. It is, for instance, a function of the Richardson number. The property of turbulence which makes it particularly difficult to deal with both practically and theoretically is that the diffusivity cannot, in principle, be treated as constant even in situations where the measured Richardson number is constant. The reason is that diffusivity is observed to be a function of the scale of fluid motion. If one follows a puff of smoke emitted from a source near the ground, it is easy to observe a rapid increase of size of the puff as it entrains (mixes with) fluid from the environment. This process is a function of the energy which is contained in scales of motion (or "eddies") which are smaller than the puff. It is a fundamental property of the atmosphere, and all turbulent flow systems, that if measurements are made of the amount of kinetic energy available in the various scales of motion present in the turbulence, it is invariably found that more energy exists at large scales than at small scales. Consequently, as our smoke puff grows, it is subjected to more and more energetic diffusion by the scales of turbulent motion smaller than its current dimensions. The larger it gets, the faster it diffuses. L. F. Richardson (1926) was the first to recognize this remarkable phenomenon, and he proposed that this variation could be well represented by

$$K_s \approx \text{constant} \times l^{4/3} \quad ,(13)$$

where l is a representative size of the "eddy" or identifiable diffusing substance. "Richardson's law" has stood the test of time and now constitutes a primary objective of any new turbulence theory.

There are several consequences of these properties of turbulence which are of significance to the practical objective of modeling the dispersion of pollution in the atmosphere. If one clooses to model the dispersion of effluent by following individual "puffs" or identifiable portions of the polluted air, it is not possible to consider the diffusivity as constant. Richardson's law must be taken into account. Second, if one considers the distribution of turbulence energy with height above the surface of the earth, it is reasonable to expect that as you gain altitude, larger and larger scales of motion will exist because there is more "room". This has been found to be true observationally (Myrup, 1967) along with the logical corollary that diffusivity increases strongly with height. Hence, if the Richardson number at a given height is constant in time, it is permissible to consider the diffusivity as constant at that height. However, if the process extends over a considerable range in height, as diffusion does, the diffusivity is not a constant but a function of height. Thus, the common assumption in air pollution meteorology that the diffusivity is a constant quantity is an approximation whose limitations should be explicitly recognized.

At this point, I wish to point out that the dispersion of particulates, large enough to fall out near their source, has certain unique properties. Since particulates emitted from any source have a spectrum of sizes, the fallout is differential; big particles reach the ground first. This effect alone, in the absence of any turbulence or wind shear, is enough to produce a wide dispersion of the material which falls out and is deposited at the surface of the earth. This effect is illustrated in Table 1-2 in which we list the terminal velocity for various sized particles and a single order-of-magnitude calculation of the distance downwind at which a particle of the indicated size would be deposited if the average wind speed was 2 ms^{-1} and the release height was 2 meters. As can be seen, the dispersion due to differential fallout is considerable. This is also a stability-dependent process, since the shape of the wind profile (and hence the average value of the wind) and the turbulent diffusivity between the release height and the surface are a function of the Richardson number.

The magnitude of the differential fallout effect is heavily dependent on the shape of the particulate size spectrum. To my knowledge, insufficient measurements have been made of the size distribution of particulates emitted by motor vehicles to allow modeling of this process with any degree of confidence.

The horizontal dimensions of cities are such that many properties of the atmosphere above them belong to those of the meteorological meso-scale. The term "air pollution meteorology" usually refers to the phenomena of the meso-scale and, indeed, most air pollution studies have been concerned with this scale. The reason for making this distinction is that many of the fundamental properties of this scale of motion are different from those of the micro-scale. Table 1-3 is a schematic summary of the contrasting properties of the two scales

TABLE 1-2.

Particle radius(μ)	Terminal velocity(cms^{-1})	Deposition point downwind(m)
5	.3	133.3
10	1.3	30.8
50	32.0	12.5
100	136.0	2.94
400	340.0	1.18

TABLE 1-3.

Phenomena	Microscale	Mesoscale
Pollutant	Primary gaseous and particulate pollutant	
		Products of photochemical reactions
Space scale	1 - 100 m (highway corridor)	0.1 to 100 Km (city, air basin)
Time scale	1 - 60 minutes	1 hr. to 1 day
Primary Transport processes	Prevailing (geostrophic) wind	
	Turbulence	Diurnal wind systems (sea breezes, etc.)
Source of transport energy	Surface roughness, wind shear, convection	Horizontal temperature contrasts, topography
Primary parameters	Wind speed, Surface roughness	
	Richardson Number	Latitude, stability (inversion height)
Typical model	Line-source Goussian	Box

from which their differing significances to pollution derive. Meso-scale wind systems arise because of horizontal gradients in the temperature of the earth's surface. Sea and lake breezes are familiar examples of this phenomenon. These wind systems have the properties that the strongest wind speeds are usually near the surface of the earth, and wind direction often exactly reverses with height. Figures 1-3 and 1-4 show examples of pollution transport in the Los Angeles basin by the sea breeze, and Figure 1-5 illustrates the typical reversal of wind direction with height. Since meso-scale wind systems are strongly associated with the 24-hour period of the sun, the wind flow develops slowly enough that the component of the earth's rotation about the local vertical (Coriolis parameter), which is a function of latitude, becomes an influence. Measurements of the Richardson number are difficult to make in the free atmosphere. Consequently, atmospheric stability is usually specified by means of the lapse rate alone. Elevated inversion (temperature increase with height) layers are usually present in diurnal wind systems and the height of the base of the inversion is an important parameter for meso-scale air pollution modeling. Within inversion layers, the Richardson number often becomes large enough that all turbulence ceases, and hence inversions are effective barriers to atmospheric dispersion. Figure 1-6 is a typical temperature sounding in the Los Angeles basin and shows the famous inversion layer which is usually present over that area during the summer and fall months.

In qualitative summary, we may say that the most important physical processes and parameters which determine the concentration of pollution in the air which we breathe, are the following (not necessarily in order of importance): rate at which pollution is emitted into the atmosphere("source strength"), distance downwind from the source of pollution, wind speed, atmospheric stability near the ground (Richardson number), height of elevated inversion layers and topography.

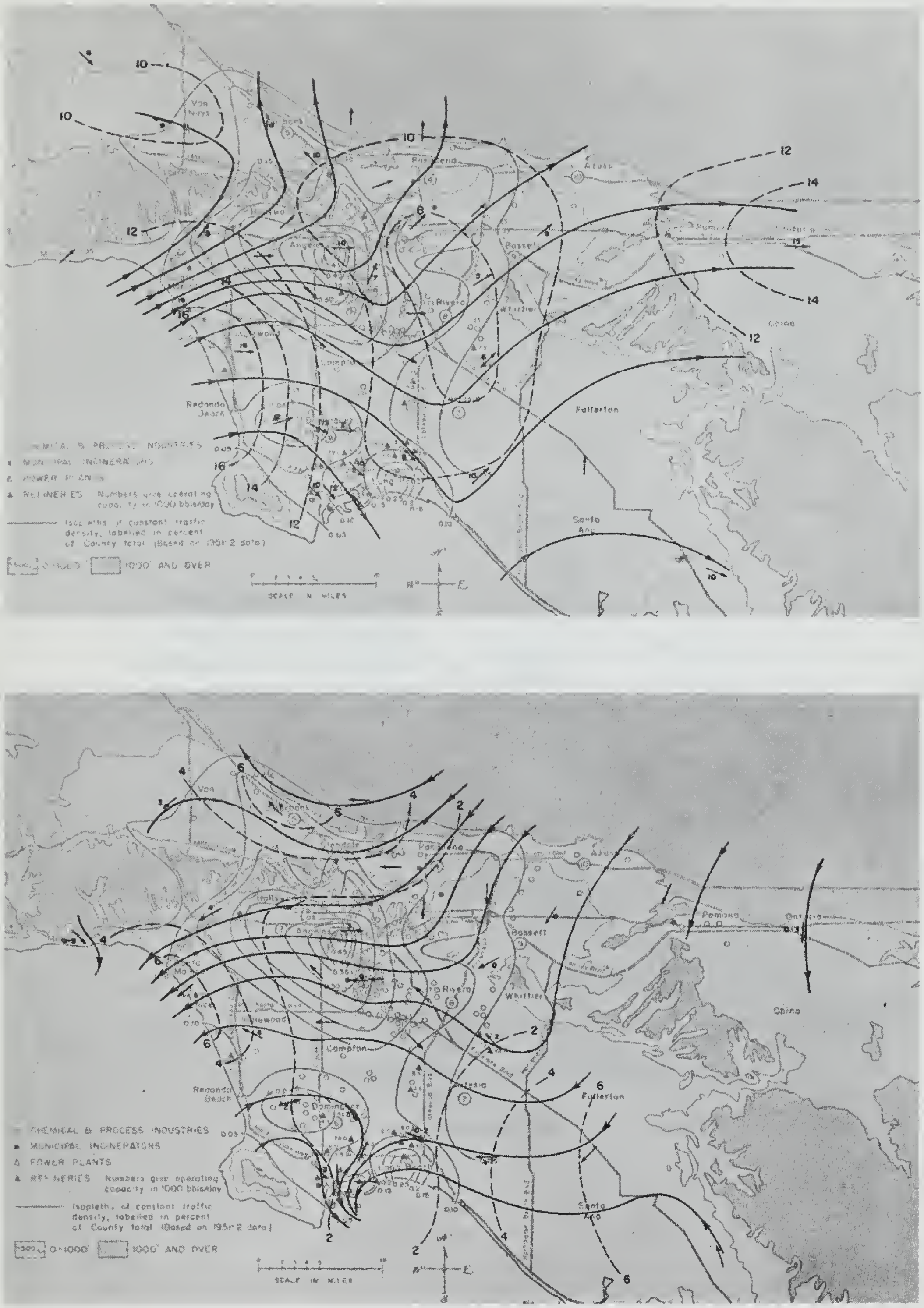

Figures 1-3 and 1-4. The Los Angeles sea breeze. (Neiburger et al, 1956).

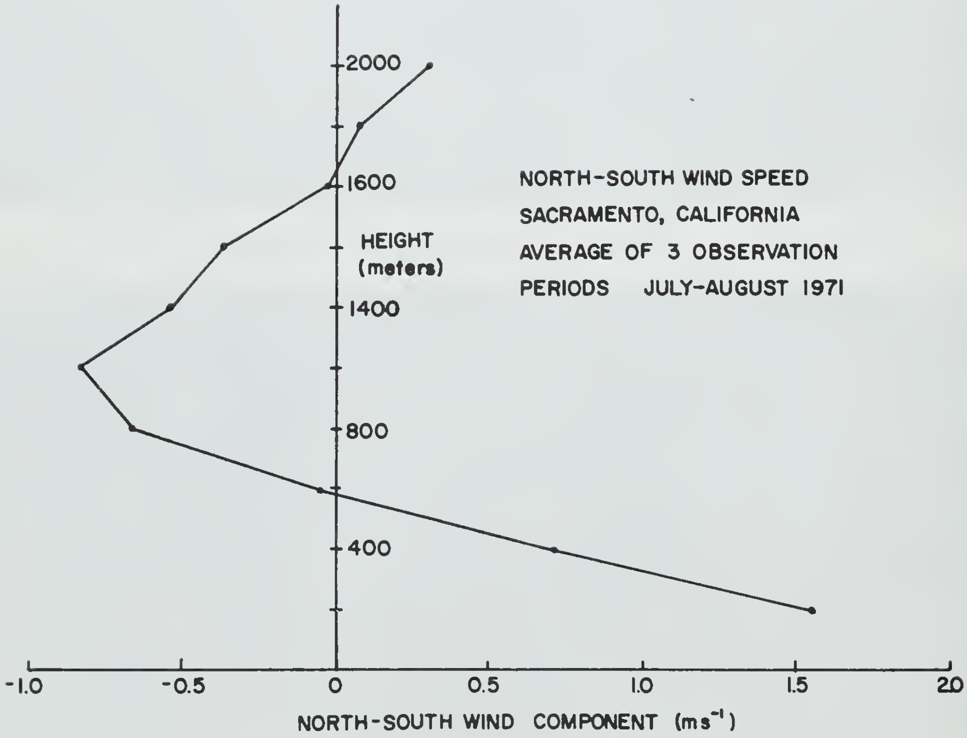

Figure 1-5. Typical meso-scale wind-speed profile.

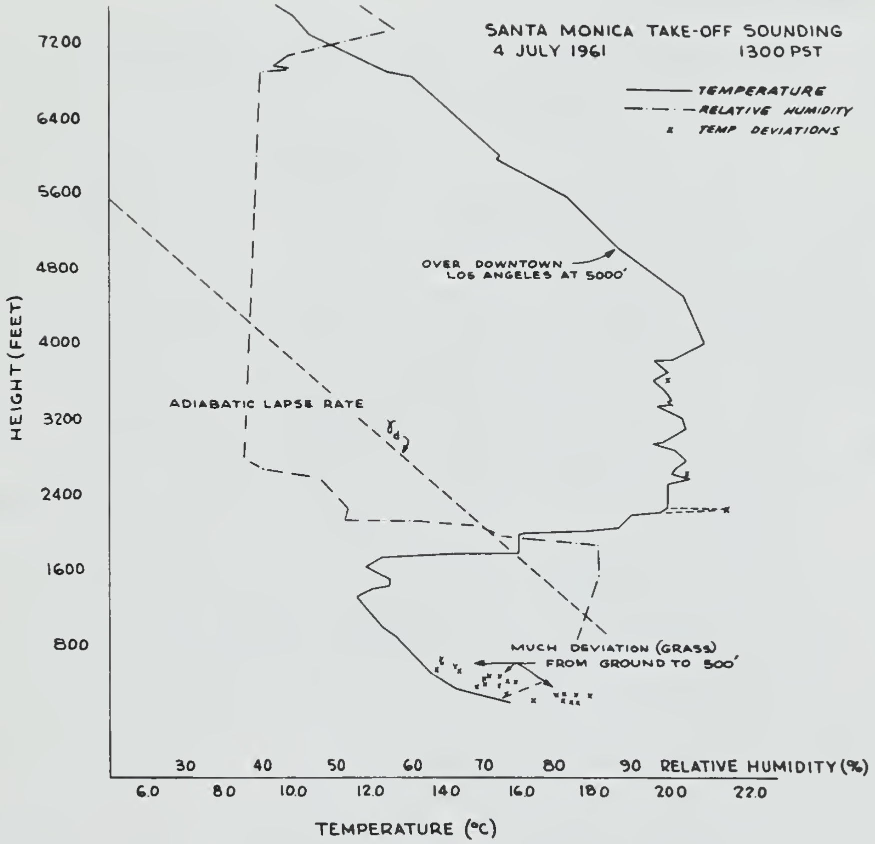

Figure 1-6. Typical sounding of temperature and humidity over Los Angeles.

Mathematical Modeling of Air Quality

In this section we shall discuss the application of mathematical and numerical techniques to the problem of estimating air quality given information on pollution emission. With reasonable generality, we can state the governing equation for the concentration, C, of some pollutant as

$$\frac{\partial C}{\partial t} = -u \frac{\partial C}{\partial x} -v \frac{\partial C}{\partial y} -w \frac{\partial C}{\partial z} + \frac{\partial}{\partial x} (K_x \frac{\partial C}{\partial x}) + \frac{\partial}{\partial y} (K_y \frac{\partial C}{\partial y}) + \frac{\partial}{\partial z} (K_z \frac{\partial C}{\partial z})$$

$$+R(t)C +S(x,y,z,t) \qquad ,(14)$$

where u and v are the horizontal and w the vertical components of the velocity of the air in the x,y, and z directions, K_x, K_y, and K_z are turbulent diffusivities associated with turbulent transport in the three coordinate directions, R(t) is a chemical reaction function for the case in which the pollutant is chemically active, and S(x,y,z,t) is a completely artibrary source function which expresses the rate at which pollutant is emitted into a unit volume. Many different approaches can be adopted in obtaining analytic or numerical solutions to this equation. We shall concentrate on the most common solutions and methods which are currently in operational use in estimating air quality.

As it stands, equation (14) is formidable and solutions are only possible if it is greatly simplified. For instance, if the mean wind is in the x direction, the vertical velocity is neglected, diffusion in the x direction is neglected relative to wind transport, the pollutant is non-reacting, and the diffusivities are taken as constants, the equation (10) reduces to

$$\frac{\partial C}{\partial t} = -u \frac{\partial C}{\partial x} + K_y \frac{\partial^2 C}{\partial y^2} + K_z \frac{\partial^2 C}{\partial z^2} + S(x,y,z,t) \qquad .(15)$$

For this case, application of boundary conditions appropriate for certain source configuration allows explicit analytic solutions to be found. Equation (15) is, in fact, essentially the molecular or Fickian diffusion equation and numerous solutions are available in any text on heat conduction or molecular diffusion (Crank, 1956). For instance, one of the most commonly used solutions, which is valid for a point source of pollution emitted at height h is

$$C = \frac{Q}{2\pi\ \sigma_y\ \sigma_z\ U}\ \mathrm{Exp}\left[-\frac{1}{2}\left(\frac{y}{\sigma y}\right)^2\right]\left\{\mathrm{Exp}\left[-\frac{1}{2}\left(\frac{z-h}{\sigma z}\right)^2\right]\mathrm{Exp}\left[-\frac{1}{2}\left(\frac{z+h}{\sigma z}\right)^2\right]\right\}, \tag{16}$$

where Q is the rate of release of the pollutant, $\overline{U}$ is the average wind speed, and σ_y and σ_z are the standard deviations of the concentration from the plume axis as functions of distance downwind. This formula is formally analogous to normal or Gaussian bivariate probability distribution, and the term "Gaussian" is usually applied to models which use equations of this sort. Turner (1963) used this solution in an air pollution model for computing the sulfur dioxide concentration in Nashville, Tennessee.

The key to success for this or any other Gaussian formula is selection of the appropriate σ's as functions of distance downwind. These terms are, in fact, functions of the diffusivity and hence functions of surface roughness and atmospheric stability, as measured by the Richardson number. Turner (1969) has published a practical system for making air quality estimates based on procedures developed by Pasquill (1961) and Gifford (1961). In this scheme stability is estimated from meteorological conditions, such as wind speed, cloud cover, and intensity of solar radiation, in terms of six stability classes, A(strongly unstable) to D (neutral) to F(strongly stable). The dispersion parameters, σ_y and σ_z are then taken from graphs which specify downwind variation as a function of stability. Figure 1-7 shows the set of curves for K_z.

Equation (16) includes the assumption that the surface acts like a perfect reflector, i.e., no deposition or absorption takes place. Clearly this assumption is appropriate only for chemically inactive gases. The presence of elevated inversion layers can be handled by assuming that when the plume dimensions have become comparable to the height of the base of the inversion, H, this becomes a lid preventing further vertical growth and thereafter mixing

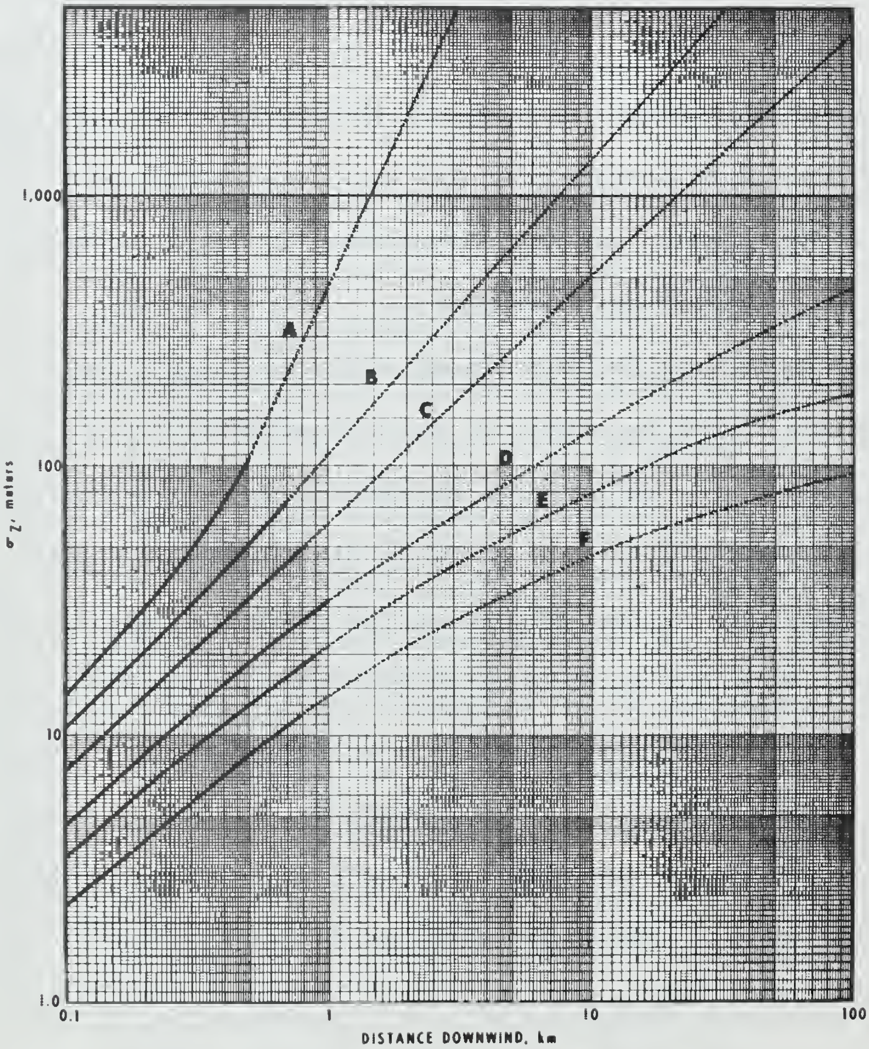

Figure 1-7. Vertical dispersion coefficient as a function of downwind distance from the source.

Estimates

338-901 O - 88 - 2

in the vertical is complete. If this distance downwind is assumed to be twice that at which one-tenth of the plume has penetrated the inversion, then the formula for air concentration becomes

$$C = \frac{Q}{\sqrt{2\pi}\,\sigma_y\, H\, \bar{U}}\ \mathrm{Exp}\left[-\frac{1}{2}\left(\frac{y}{\sigma_y}\right)^2\right] \qquad ,(17)$$

where the concentration is now independent of the vertical direction and this relation is supposed to be valid when $\sigma_z > 0.94H$.

The Gaussian approach is easily extended to other source configurations. For a continuously emitting infinite line source, the solution at ground level is

$$C = \frac{2Q}{\sqrt{2\pi}\,\sigma_z\, U \sin\phi}\ \mathrm{Exp}\left[-\frac{1}{2}\left(\frac{h}{\sigma_z}\right)^2\right] \qquad ,(18)$$

where ϕ is the angle between the wind direction at the line (zero at right angles).

Equations (16) and (18) are the working formulae for the great majority of practical schemes for estimating air concentration from air pollution source inventory information. In order to calculate the air concentration at a specific point in an urban area, the city is divided up into a set of equal areas defined by a grid and an appropriate source strength assigned to each. For instance, in his Nashville study, Turner obtained SO_2 source strengths for each square mile in a 17 x 16 mile rectangle. Downwind concentrations resulting from SO_2 emitted within a given square mile were calculated from the point source formula, assuming that the area emission was concentrated at a point. This calculation was repeated for each of 272 square mile sources and the results summed to give the net result. Observed wind speeds and σ's estimated from observed meteorological conditions were used. Comparison between observed and computed 24-hour averages showed that 58% of all computed values were within ±1 pphm, a result which was taken as demonstrating the feasibility of the approach.

Several other investigators have made calculations similar to those of Turner. Koogler, et al. (1967) used Turner's equation with the addition of an exponential decay to account for SO_2 removal processes for Jacksonville, Fla. Koogler obtained 95% of his calculated SO_2 concentrations within ±1 pphm of observed values. Hilst (1967) used essentially the same approach for the state of Connecticut using an improved method of incorporating observed winds. 5,600 square area sources were used, each 5,000 feet on a side, and important individual sources, such as large power plants, were treated individually.

The most sophisticated air pollution model now in existence is, to our knowledge, that which is being developed by Neiburger and Lamb (1968). This model includes improved solutions to the diffusion equation for point, finite line, and area sources, absorption of pollutants at the ground, simple chemical reactions whose rates may be given as arbitrary functions of time, and horizontally- and time-varying winds. In this model, the diffusion coefficients are constants and wind does not vary with height, and vertical motion is neglected. Preliminary calculations with this model, using observed winds and traffic data, were made for carbon monoxide. The results, while considered encouraging, revealed a major source of error associated with the neglect of vertical motion. Unrealistically large values of carbon monoxide concentration were calculated to occur in regions of horizontal convergence of the wind indicating that removal of pollutant by vertical motion is an important process which cannot be neglected. This model is in an active state of development and important and high quality results are anticipated in the near future.

Since we can illustrate most of the points we wish to make by reference to the models we have already discussed, we shall limit our presentation of the remaining major approaches to brief outlines. In addition to the Gaussian models and Neiburger's and Lamb's improved version of this technique, there are four other major approaches to the problem of calculating air quality from measurable parameters. One is based on the statistical theory of turbulence, originally introduced by G. I. Taylor (1921). In this approach, emphasis is placed on the statistical properties of velocity fluctuations of ensembles of passively floating particles or marked fluid. The statistical theory deals directly with the spread of a group of particles with respect to a frame of reference moving with the fluid (Lagrangian frame) which is the most fundamental manner in which to treat turbulent diffusion. Since measurements are almost always made with respect to a fixed (Eulerian) frame of reference, a central problem in applying the statistical theory to practical dispersion problems is to establish the correspondence between Lagrangian and Eulerian turbulence parameters. The statistical theory may be the most fundamental but is probably the most remote from immediate practical application at this time.

Another major approach which is only now being developed and hopefully represents a useful compromise between the unashamed empiricism of the Gaussian models and more satisfying basic theory is the hydrodynamics approach (Knox, et al., 1971). In this technique, the fundamental equations of meteorological dynamics and thermodynamics are numerically solved on a three-dimensional grid using approximate topography as a boundary condition to provide the mesoscale flow and stability. Smaller scale flow features, or "turbulence ", are handled by means of diffusivity parameters, such as we have been discussing. A less satisfying variant of this approach would be to use observed three-dimensional winds to specify the mesoscale flow. This alternative appears less satisfying to us because of the extraordinary measurement problem.

Three-dimensional numerical integrations are so demanding of computer storage and computational speed that only relatively crude models can be solved at this time. It remains to be seen whether computer capabilities develop fast enough for this approach to be of practical utility in the near future.

The next of the major approaches to our problem is the similarity theory, introduced by Monin (1959) and developed further by Batchelor (1959, 1964), Gifford (1962) and Pasquill (1966). In this technique, a semi-empirical framework based on dimensional analysis is adopted to organize pollutant data in terms compatible to micrometeorological practice. We present some results in the next section obtained with what is essentially a similarity approach, so we will not develop this approach further at this time.

The last approach to be discussed here is the so-called box model, which is almost trivially simple but nevertheless useful for mesoscale applications. In situations where a well-defined inversion acts as an effective lid on vertical dispersion and when pollution is emitted more or less uniformally over a large urban area, it may often be acceptable to calculate concentration from

$$C = \frac{kQ}{\overline{U}H} \quad ,(19)$$

where $\overline{U}$ is the average wind speed between the surface and the height of the base of the inversion, k is a constant, and Q is an emission rate per unit area. Hanna (1971) has shown that simple formulae like equation (19) are often as accurate as much more sophisticated approaches, as near as can be told from the available data.

The modeling approaches we have been discussing are meant to be used in a practical, engineering sence. They must ultimately be judged in this spirit. Before attempting an overall evaluation of the state of the art of highway air quality modeling, it is instructive to look at an operational attempt to use some of the techniques we have presented.

In the last two years the California Division of Highways has been conducting an extensive environmental impact program to evaluate the effect on air quality of current highways in the state and to make projections of the effect of future planning decisions regarding highway construction. At present, this program is limited to an evaluation of the probable air quality impact of the decision to build or not to build highways whose routes and configurations were planned well before the overriding significance of environmental impact became clear. There were four major objectives for the program. One was to generate reliable data on the current state of air quality near highways. A second objective was to develop and verify practical highway air quality models. The third was to develop models for assessing highway impact on the air quality of entire mesoscale air basins. A fourth was to use verified models to estimate air quality in twenty years time for the built and not-built cases for particular highway plans. At present, several contracts have been awarded to research and development groups in the private sector to perform these impact studies. I shall briefly outline the results of the first of the studies to be completed, which was an air-quality analysis and impact study of proposed routes 92/238 near Hayward, California. The Hayward area lies on the coastal plain to the east of the southern portion of the San Francisco Bay. The immediate topography is uncomplicated; on a larger scale, Hayward lies in the basin which encloses the Bay. The firm which was awarded the contract collected all available air quality and meteorological data for the area, established additional meteorological and air pollution monitoring stations, developed a Gaussian transport and diffusion model, verified the model with data taken during a special concentrated observation period, and performed calculations with the model to estimate air quality in the region for the year 1990 with and without the proposed freeways. On the whole, there is no doubt that this was a highly professional piece of applied science and is well representative of the current state of our measurement techniques and modeling capability. For these reasons, whatever criticism we make of the techniques employed or results obtained in this study are to be taken as applying to the field as a whole.

Figure 1-8 shows an example of the basic data which was collected in the Hayward area by the contractor. The pollutant is carbon monoxide averaged over 24 hours. The numbers attached to the data points refer to the various sites

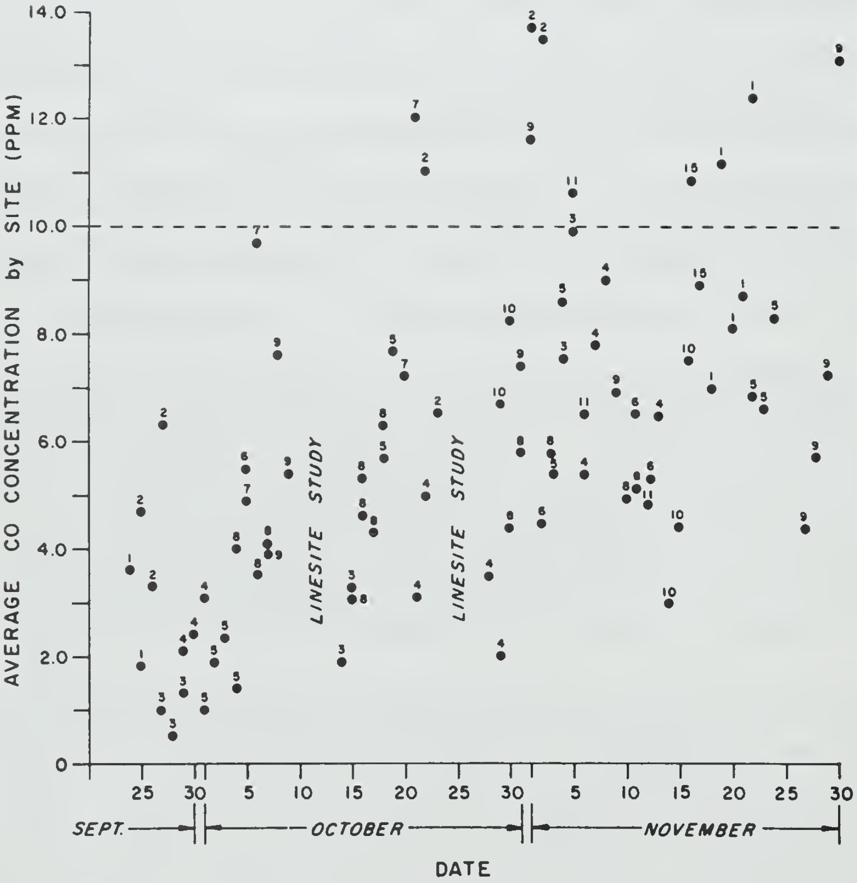

Figure 1-8. Time variation of carbon monoxide concentration at various sites in the vicinity of Hayward, California in 1971.

used in the study. The extreme day-to-day variability is typical of pollution data. The horizontal dashed line is the ambient air quality standard for carbon monoxide (12 hours at 10 ppm). Figure 1-9 shows a cumulative frequency diagram derived from the 1063 hourly measurements of CO made during the two and a half months of this study. The diagram shows, for instance, that hourly average CO concentrations of 10 ppm were equalled or exceeded 18% of the time during this study. Figure 1-10 shows the non-cumulative frequency distribution for the same data but now broken down by site. The variability from site to side and the apparent bimodal character of these curves is striking. In addition, it could be said that these curves do not have the usual smooth appearance of well-defined and stable statistics. The question must be asked as to whether the conditions of this study allowed time for sufficient data to be gathered to allow reliable statistical generalizations to be made. Figure 1-11 shows a similar analysis of weekday versus weekend data for all sites. The same comments apply.

The investigators state, although the analysis is not presented in sufficient detail to allow evaluation, that a significant correlation was found between carbon monoxide and the product $\overline{U}H$, where these parameters have the same meaning as in the box-model approach discussed above, so that the result amounts to be partial validation of that approach.

Figure 1-12 shows a summary of a concentrated microscale study in the immediate vicinity of an existing freeway section which ran approximately North-South. All data are shown from a variety of meteorological and traffic situations and it is difficult to see a clear pattern such as simple models such as the line-source Gaussian would lead you to expect. Figure 1-13 shows a typical individual case for downwind data and Figure 1-14 for upwind data. While these displays appear to be more reasonable than the previous scatter diagram, serious methodological questions arise from consideration of these data. The measurements

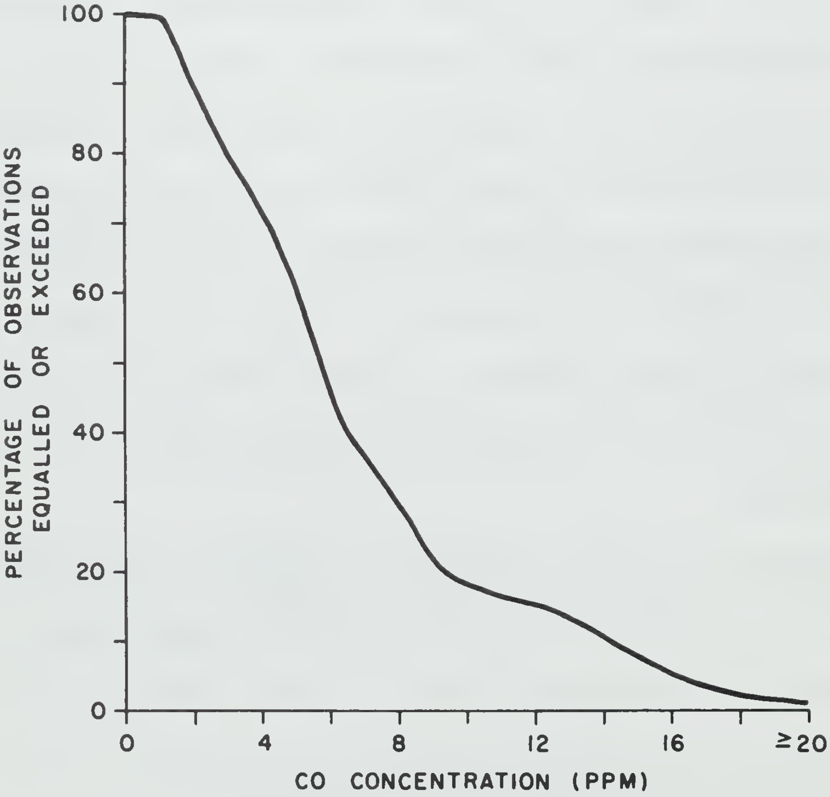

Figure 1-9. Cumulative probability distribution for carbon monoxide concentration at Hayward, California.

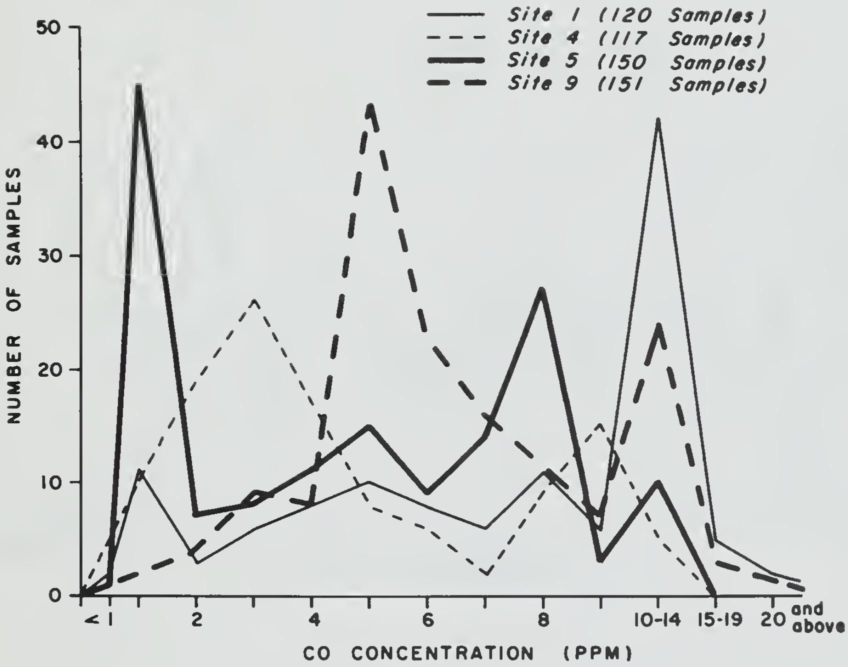

Figure 1-10. Frequency distribution of CO concentration for various sites at Hayward, California.

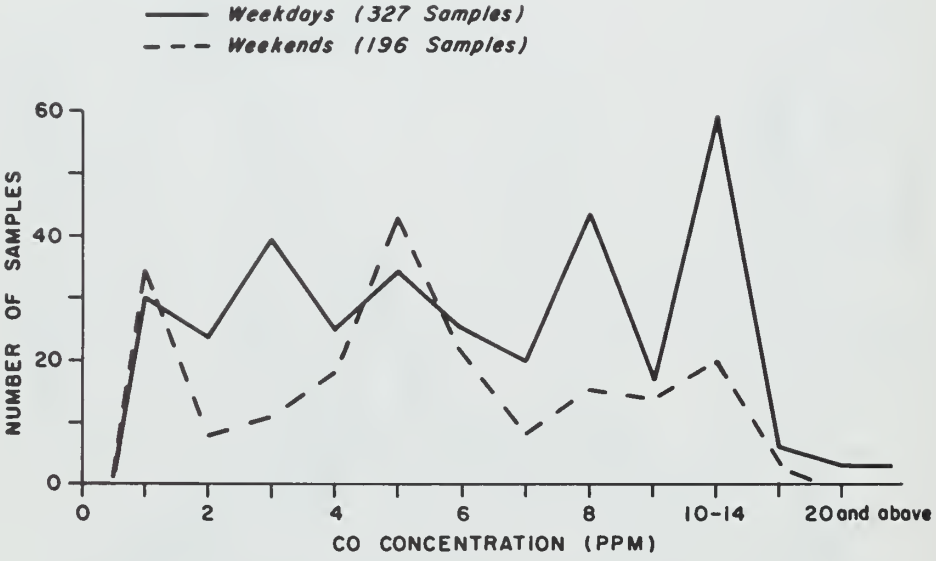

Figure 1-11. Frequency distribution of CO concentration on weekdays and weekends for Hayward, California.

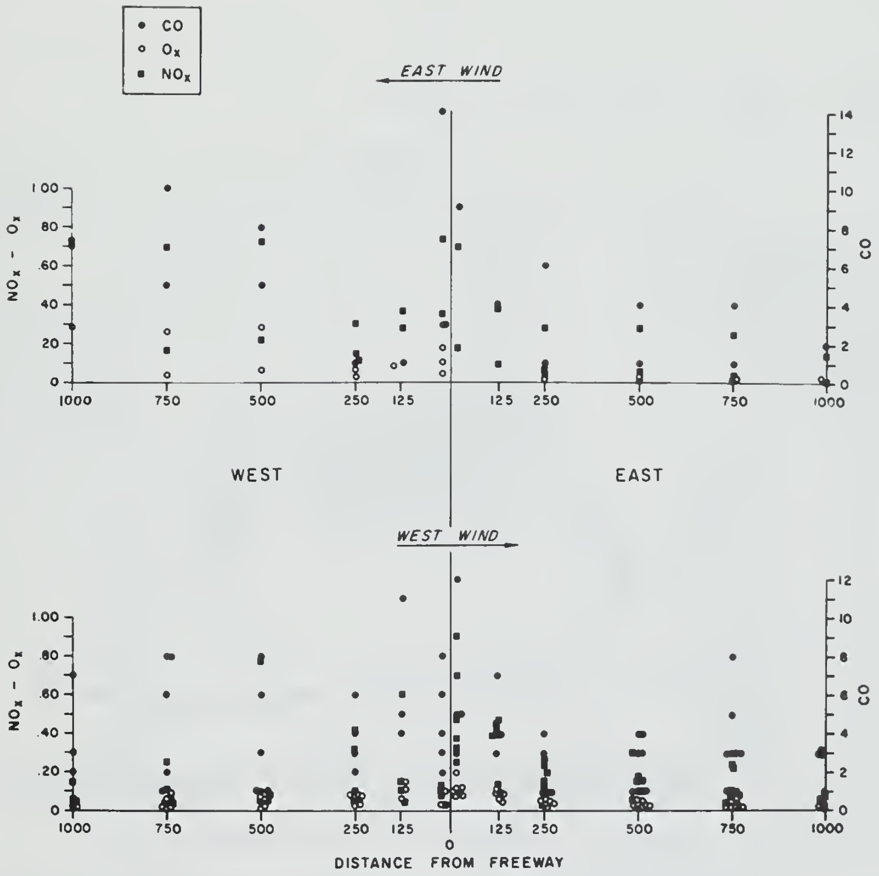

Figure 1-12. CO concentrations in the immediate vicinity of the Nimitz Freeway near Hayward, California. All measurements shown.

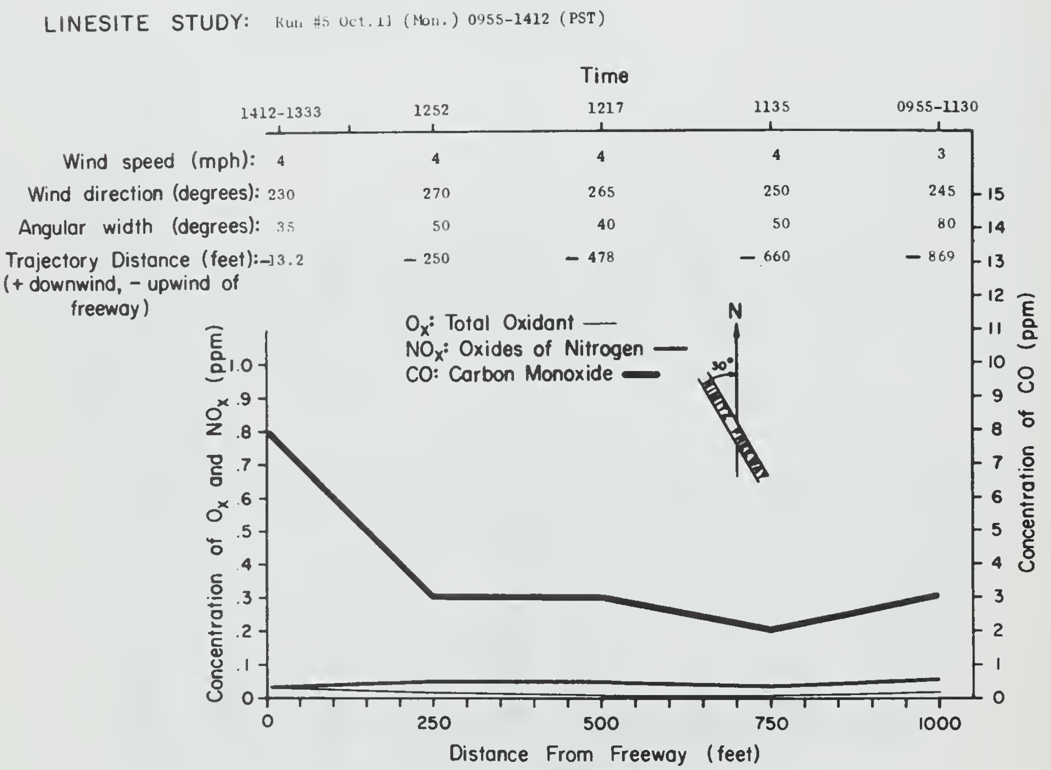

Figure 1-13. Pollution measurements made upwind of Nimitz Freeway near Hayward, California, Oct. 11, 1971.

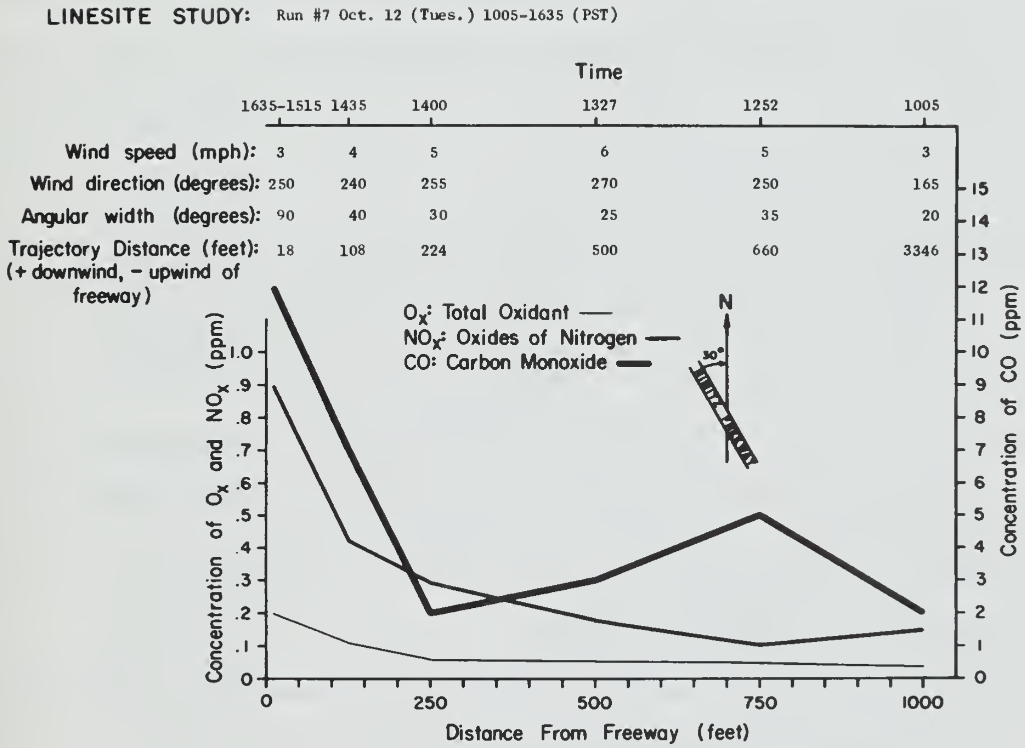

Figure 1-14. Pollution measurements made downwind of Nimitz Freeway near Hayward, California. Oct. 12, 1971.

were made by moving a van containing air pollution sensing apparatus from point to point. Thus, the data are not simultaneous and contain large variations of meteorological parameters from point to point. Such a procedure would not be acceptable in any professional micrometeorological study. Measurements must be simultaneous to be comparable. I have no doubt the contractor did the best job possible with the time and resources available. Nevertheless, it must be said that we need to do much better than this.

A validation analysis was made of the highway diffusion model, and this is shown in Figure 1-15. The objective was to estimate the contribution to carbon monoxide concentration at specific locations from an existing freeway alone. As can be seen, the "background" concentrations are larger than the calculated freeway contributions. It is difficult to have confidence in the modeling approach on the basis of this analysis alone.

An additional criticism can be made concerning the lack of analysis of the properties of the model itself. At a minimum, a sensitivity analysis of any operational model should be made to determine the relative importance of the various input data and the degree of precision needed. For instance, how sensitive are the validation calculations discussed above to uncertainties in, say, the wind speed or freeway emission rate? Without such information, it is difficult to interpret a validation analysis.

To fulfill the final portion of the study, the contractor used the developed models to make air-quality projections for the year 1990. On the mesoscale a number of calculations were made for various wind directions and stabilities for the cases in which the proposed routes 92/238 were built and not-built. In general, the mesoscale calculations showed little difference between these two cases.

On the microscale, within a thousand feet of the highway corridor, relatively large differences were found between the built and not-built cases.

Figure 1-15. Test of an air pollution transport and diffusion model.

Date	NAWC Model	Background	Computed	Observed
(A) - WSW Flow				
9-30-71 (1400-1700 PST)	0.2	1.4	1.6	1.5
10-1-71 (0800-1100 PST)	0.4	2.4	2.7	2.8
10-21-71 (1200-1600 PST)	0.3	2.8	3.1	3.8
11-7-71 (0900-1100 PST)	0.4	4.7	5.1	5.0
(B) - WSW Flow				
10-29-71 (1400-1500 PST)	1.5	3.5	5.0	6.5
(C) - Drainage Flow				
10-3-71 (0400-0700 PST)	1.9	1.2	3.1	4.6
11-4-71 (0400-0700 PST)	2.4	2.4	4.4	8.4

Figure 1-16 shows typical results which indicate lower upwind concentrations of carbon monoxide and considerably higher downwind concentrations of carbon monoxide for the built case in comparison with not-built. In view of the uncertainties in the validation program discussed above, it becomes doubly uncertain as to how to interpret or use these microscale projections. An important point to note is that these calculations are presented, as is appropriate, in the form of air concentrations at various distances from the freeway. The validation measurements, however, were made only at one point, and we have no way of knowing the ability of the model to predict spatial variation.

It is difficult to assess the overall state of the field of air pollution modeling. The field is moving very fast and many complex problems are involved and must be considered. In particular, the measurement phase is critically important and must be discussed in connection with the modeling effort.

First of all, it is clear the physical rigor of all operational and research models is not high. The treatment of diffusion parameters, for instance, is usually highly arbitrary and unconnected with what we know of the physics and energetics of turbulence. In particular, diffusion coefficients are almost never given as functions of the Richardson number and surface roughness, despite extensive micrometeorological experience that this is so. Nevertheless, it is our opinion that this is of far lessor importance than the measurement and methodological questions to be discussed next.

Typical measurement programs in air pollution meteorology are grossly inadequate. The example discussed above was a good state-of-the-art effort which attempted to apply, with great energy and professional competence, known techniques and standard methods to the problem. Nevertheless, it is clear that the information and results obtained are not adequate for the purpose of making future projections. Thus, a general and serious constraint must be faced. If we wish to make reliable projections of the air-quality impact of highway

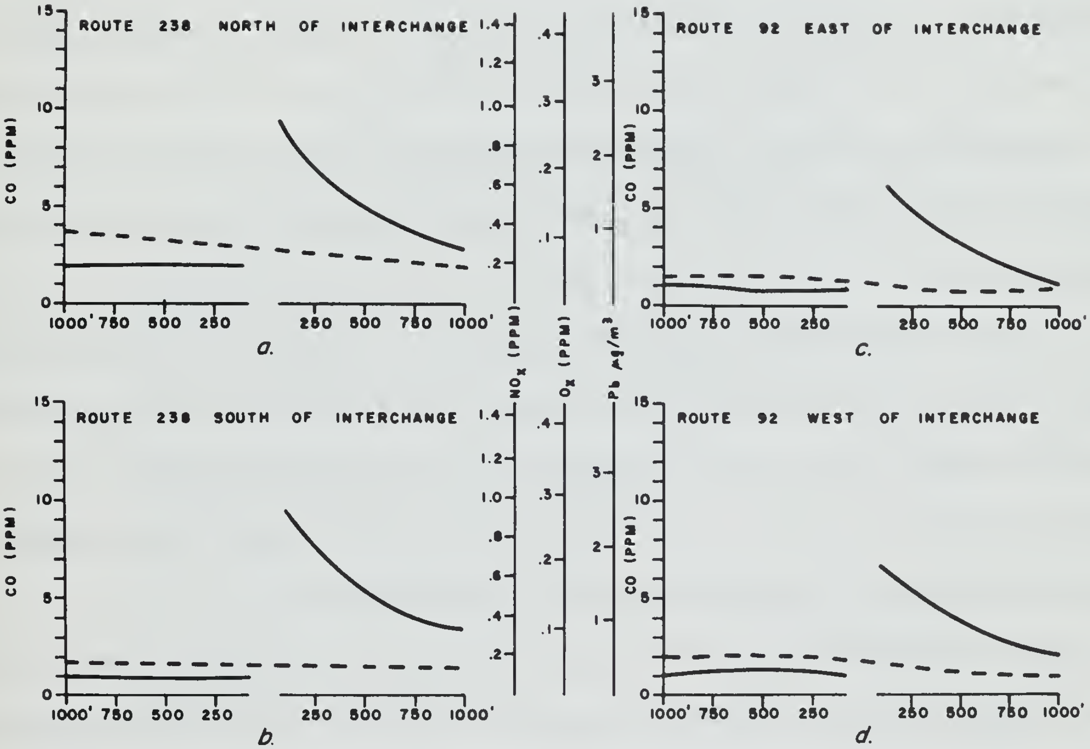

Figure 1-16. Projections to the year 1990 for air quality with and without a proposed freeway.

development, we must do better than we are now.

Specifically, present measurement programs have the following faults. Air concentration of pollutants, diffusion, and standard meteorological parameters are measured, but the Richardson number is not. This deficiency ensures lack of repeatability in the results and makes an unacceptably large scatter in the data inevitable. The Richardson number has been shown to be the single most important parameter governing all micrometeorological processes. It should be a standard part of any air-quality measurement program. Secondly, measurements are not adequately extensive either in time or space. Two and a half months is not a sufficiently long time to develop reliable meteorological or air-quality statistics. Likewise measurements of air quality at various distances from a highway must be simultaneous or, again, the data will not be interpretable.

It may be argued that the measures which are implied in the criticism above, i.e., more sophisticated and extensive measurements, would be too expensive to fund. The counter argument is that present practices are not producing the results we need. It would be better to run far fewer measurements on a higher plane; the results would be far more useful.

Until adequate measurements are available, the question of model validation remains academic. However, considerably more effort could and should be spent in analysis of the properties of the models themselves. Intensive sensitivity studies reveal acceptable and unacceptable properties of models. In addition, such sensitivity information helps put the instrumental and observational effort in better perspective. For instance, it doesn't make sense to make an expensive effort to measure an input parameter which has little effect on the final model output.

An Integrated Microclimate/Diffusion Approach

In the previous sections, we have presented a survey of the factors which control wind transport, diffusion and fallout of pollutants emitted by motor vehicles. In this section, I shall describe the research approach of the atmospheric environment group at the University of California, Davis. This effort was a cooperative effort among the Departments of Agricultural Engineering, Geography, Water Science and Engineering, Civil Engineering, the Division of Environmental Studies and the Atmospheric Science group. The work I shall be outlining here is largely a group effort and my colleagues, Donald Morgan, Wilson Goddard, Vinaya Sharma, and David Rogers, share in the credit for our results.

Our overall objective was to study the fundamental processes which give rise to the diverse microclimates which are observed in urban areas. We wished to develop, as consequences of the most basic theory available, means for calculating atmospheric stability and diffusion parameters and hence, air quality. One final objective of our research programs, which we have only partially achieved, is to develop models, not only of air pollution concentration, but also of human comfort and health.

We selected the city of Sacramento, California as the target area for this study because of topographic simplicity, relative isolation from other urban areas, stable summer meteorological conditions and proximity to the Davis Campus. Figure 1-17 shows the geographical location of Sacramento within the Central Valley of California, and Figure 1-18 shows a map of the city with the grid we used to describe the properties of the city. Each rectangle measures 6,000 to 8,000 feet and hence the area is 48 million square feet or approximately 1.7 square miles.

We began our study by dividing the city into 13 conventional land-use categories. Table 1-4 shows the 13 categories and their relative abundance in

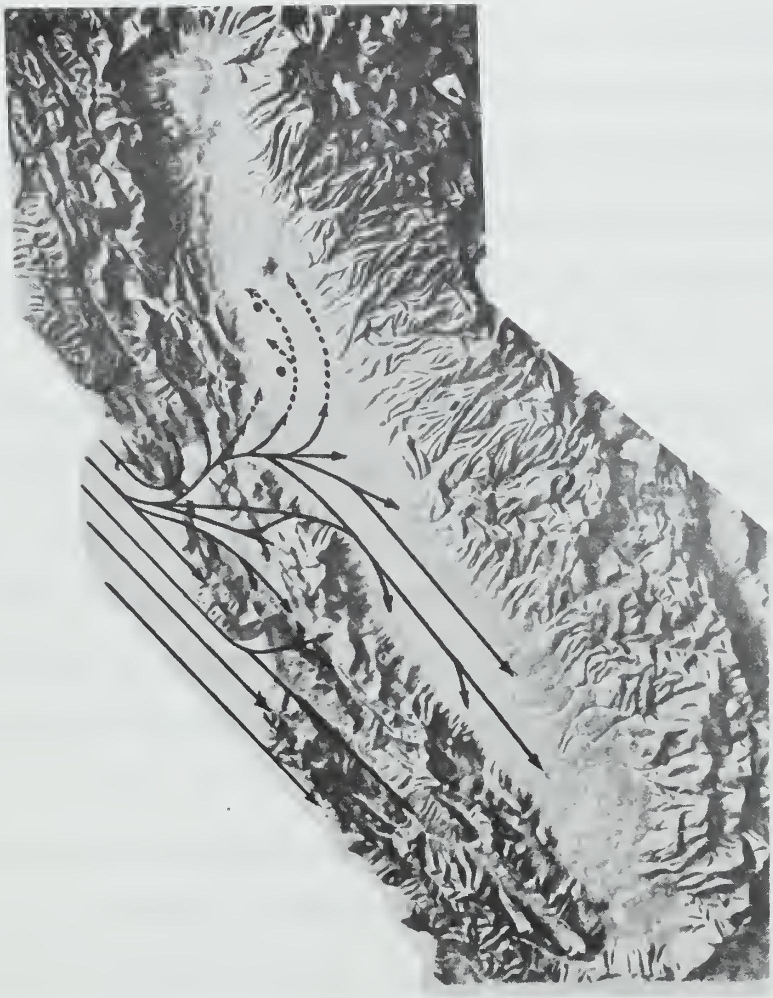

Figure 1-17. Wind flow in the Central Valley of California.

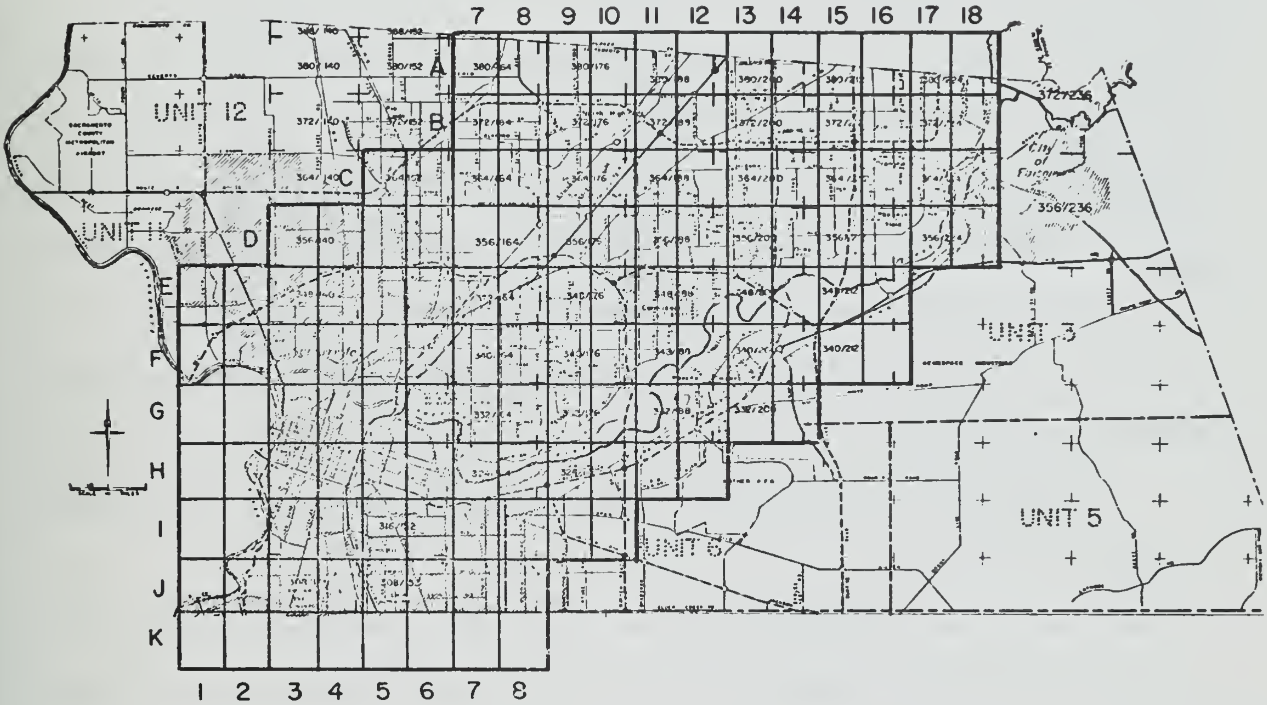

Figure 1-18. The City of Sacramento showing the spatial grid used in the microclimate/diffusion study.

TABLE 1-4.

Category	Abbreviation	% of City
Light-Density Residendial	LDR	43.6
Medium-Density Residential	MDR	1.3
Heavy-Density Residential	HDR	0.6
Schools	SCH	3.2
Shopping	SHP	8.7
Office Buildings	OFF	0.6
Parks	PRK	8.2
Central Business District	CBD	0.3
Industrial	IND	15.0
Freeways	FWY	2.7
Open Green	PGR	1.5
Seasonal Green	SGR	11.8
Water	WTR	2.5
		100.0

our target area as a whole. As can be seen, the categories of Light-Density Residential, Industrial, and Seasonal Green (agricultural land) occupy over 70% of the study area. From either the known properties of each land-use category or field measurements of our own, we were able to attach numbers to each category describing its fundamental physical properties. Table 1-5 shows the result of this effort. The aerodynamic roughness length, z_o, was obtained by means of a technique due to Lettau (1969) in which geometric measurements of the average properties of the roughness elements (buildings and trees) can be used to infer this parameter. The "wet fraction" is, in fact, the percentage area occupied by green, transpiring plants in a given land-use category.

All micrometeorological experience (Sutton,1953; Sellers,1965 ; Munn,1966) indicates that these are the fundamental physical and biological characteristics of the surface of the earth which determine the "response" of a given area to large-scale meteorological processes, such as radiation load, wind speed, or temperature and humidity well away from the surface. The "response" is, in fact, the microclimate which determines, in turn, atmospheric stability, diffusion parameters, and human comfort. Given detailed information about the nature of the surface of the earth, it is possible to calculate microclimatic parameters. The heat-budget equation for the surface of the earth,

$$R_N = H + LE + G \qquad ,(20)$$

which is an expression of the first law of thermodynamics, is the single most powerful principle which determines the microclimate. In equation (20), R_N is the net flux of radiation absorbed at the surface of the earth (positive during the day, negative at night), H is the flux of heat carried upward from the warm surface of the earth by turbulent convection, E is the evaporation rate (including transpiration), and L is the latent heat of evaporation, so that the product, LE, is the flux of energy required to allow evaporation rate, E, and G is the flux of heat into the ground. The net radiation term can be

TABLE 1-5. CITY INTERFACE PARAMETERS BY LAND-USE CATEGORY

	Albedo	Infrared Emissivity	Heat Conductivity [cal cm^{-1} sec^{-1}°C^{-1}]	Heat Capacity [calcm^{-3} °C^{-1}]	Wet Fraction	Roughness, z_o [cm]
Light-density Residential	.20	.88	.0023	.45	.43	108
Medium-density Residential	.23	.86	.0024	.43	.56	532
Heavy-density Residential	.25	.88	.0022	.40	.43	370
Schools	.15	.90	.0023	.50	.35	41
Shopping	.20	.86	.0022	.42	.04	36
Office	.22	.85	.0025	.45	.13	175
Park	.16	.89	.0030	.58	.93	127
Central Business District	.26	.86	.0024	.42	.07	321
Industrial	.26	.86	.0024	.42	.01	13
Freeway	.30	.80	.0030	.60	.00	4
Open Green	.35	.90	.0006	.30	.05	2
Seasonal Green	.15	.90	.0030	.60	1.00	2
Water	.09	.93	.0014	1.00	1.00	.001

thought of in simplified terms as the energy input rate while the terms on the right determine how the energy is used. For instance, over water or surfaces completely covered with freely transpiring plants, the majority of the incoming solar energy goes into evaporating water (LE) and, hence, is not available to heat the air or underlying surface. On the other hand, for surfaces which are dry and do not evaporate, most of the sun's energy goes into heating the air (H) or surface material (G). This simple mechanism explains most of the microclimatic variability found in mesoscale systems such as the urban environment. A glance at our "wet fraction" data shows that very large contrasts exist between the various land-use categories in the amount of evaporation which must be occurring. This also is largely the basis for contrasts in stability, diffusion, air quality and human comfort.

Solution of the energy budget equation is feasible using micrometeorological formulae for each of the various terms. The technique has been successfully used by Halstead (1957), Myrup (1969), Goddard (1971), and Outcalt (1972). The output of these models includes air and surface temperature as well as the energy-budget components and the friction velocity, U_*, discussed earlier. It should be remembered that the only two important variables which enter into the definition of the Monin-Obukhov length, L, are H and U_*. Hence, we are in a position to calculate the microclimate and atmospheric stability from interface characteristics.

We have performed this calculation, using the microclimate simulation model, CLISIM, developed by Goddard (1971). CLISIM requires, as input, the interface parameters as listed above, meteorological parameters (temperature, wind speed, and humidity) well away from the surface, and latitude and date (to determine the solar radiation).

As a preliminary feasibility study, we have performed the CLISIM calculations for each of our 13 land-use categories for August 24, 1971. Table 1-6

TABLE 1-6. FRICTION VELOCITY AND MONIN-OBUKHOV LENGTH BY LAND-USE CATEGORIES FOR AUGUST 14, 1971

	U_*(cm s^{-1})		L(meters)	
	0500	1400	0500	1400
LDR	29.7	53.1	56.29	- 55.01
MDR	38.7	60.5	50.60	-243.40
HDR	37.5	59.3	58.49	-127.00
SCH	15.7	47.7	12.20	- 40.00
SHP	--	55.1	--	- 29.70
OFF	41.4	61.8	84.53	- 52.71
PRK	14.4	44.6	9.04	-139.49
CBD	40.0	69.8	94.62	- 62.26
IND	--	49.0		- 24.56
FWY	5.8	44.9	3.06	- 19.64
OGR	--	42.5	--	- 17.69
SGR	5.9	31.9	3.26	- 27.17
WTR	9.7	26.5	20.94	- 86.50

shows the result of this operation for the friction velocity, U_*, and the Monin-Obukhov length, L, at 0500 and 1400 PST. Pronounced variation among the various land-use categories is apparent.

The real city is not made up of neatly arranged parcels of pure land-use categories. Instead every one of our 138 1.7-square mile zones contained several categories. We have measured the percent of each land-use category in each rectangle. With this information, we can form a weighted average for the pure land-use parameters and produce a number which should be representative of the entire 1.7-square mile area. Figure 1-19 shows the result of such an analysis for the roughness parameter, z_o. The city appears as a rough oasis in the midst of relatively smooth agricultural lands. Z_o values are particularly big in the vicinity of the central business district due to the presence of many large buildings. We have made similar analyses of all the interface parameters listed above and for the energy-budget components. Figure 1-20 shows the result for R_N, net radiation, and Figure 1-21 for the evaporation term, LE, for the 1400 PST time period. At this time, the city is absorbing less radiation than the surrounding agricultural lands due to higher reflectivity and greater emission of infrared energy. In the evaporation display, the city appears as a dry island surrounded by large evaporation from the agricultural areas.

We have now reached the point where we have developed the capability of calculating the atmospheric stability from measurable surface properties, including its roughness. The next step would be to specify the air pollution emission process and finally the transport and dispersion. This we have done, and we briefly describe our approach in the remainder of this section. Figure 1-22 shows the emission of carbon monoxide from motor vehicles in Kilograms per day per 1.7 square miles. These figures were estimated as follows. For each rectangle, the total miles of residential, arterial, and highways were

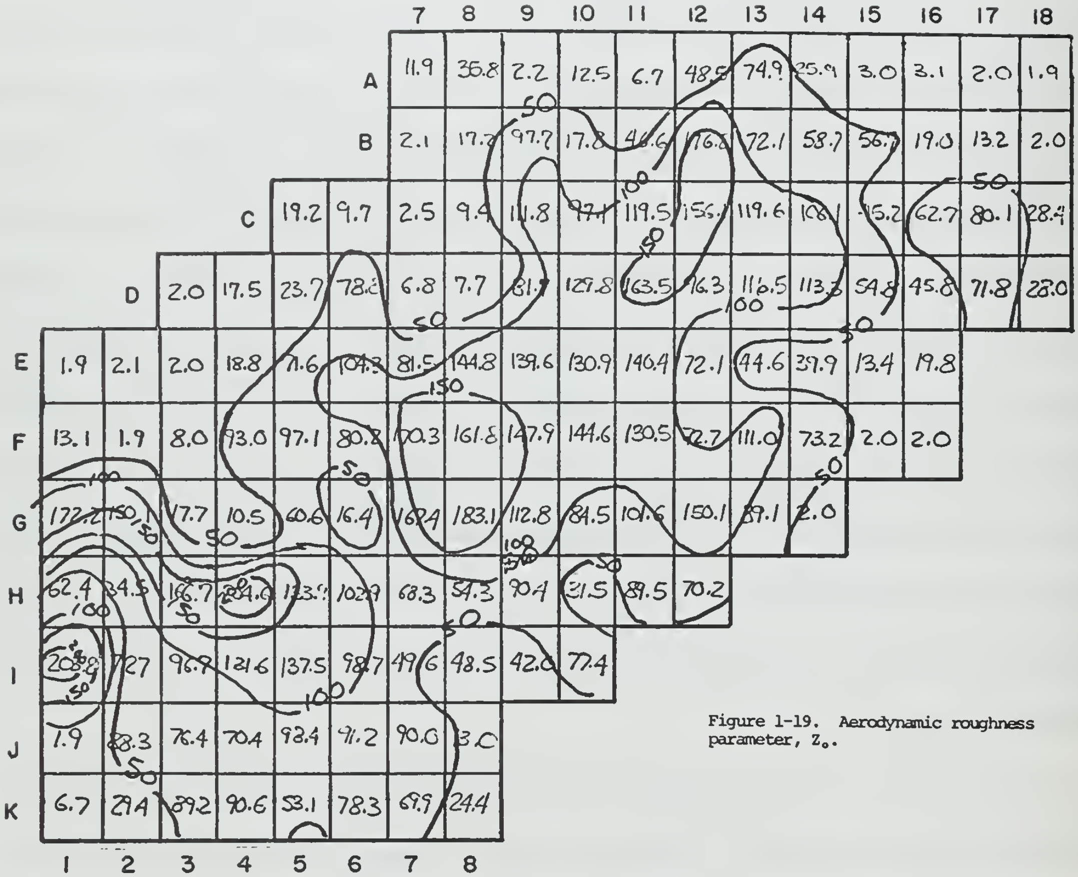

	1	2	3	4	5	6	7	8	9	10	11	12	13	14	15	16	17	18
A							11.9	35.8	2.2	12.5	6.7	48.5	74.9	25.9	3.0	3.1	2.0	1.9
B							2.1	17.2	97.7	17.8	46.6	176.8	72.1	58.7	56.7	19.0	13.2	2.0
C					19.2	9.7	2.5	9.4	111.8	97.1	119.5	156.1	119.6	108.1	45.2	62.7	80.1	28.4
D			2.0	17.5	23.7	78.2	6.8	7.7	81.7	129.8	163.5	76.3	116.5	113.3	54.8	45.8	71.8	28.0
E	1.9	2.1	2.0	18.8	71.6	104.3	81.5	144.8	139.6	130.9	140.4	72.1	44.6	37.9	13.4	19.8		
F	13.1	1.9	8.0	93.0	97.1	80.2	170.3	161.8	147.9	144.6	130.5	72.7	111.0	73.2	2.0	2.0		
G	172.2	150.1	17.7	10.5	60.6	16.4	162.4	183.1	112.8	84.5	101.6	150.1	89.1	2.0				
H	62.4	34.5	166.7	284.0	123.9	102.9	68.3	54.3	90.4	31.5	89.5	70.2						
I	208.9	72.7	96.9	121.6	137.5	98.7	49.6	48.5	42.0	77.4								
J	1.9	88.3	76.4	70.4	93.4	91.2	90.0	3.0										
K	6.7	29.4	89.2	90.6	53.1	78.3	69.9	24.4										

Figure 1-19. Aerodynamic roughness parameter, Z_o.

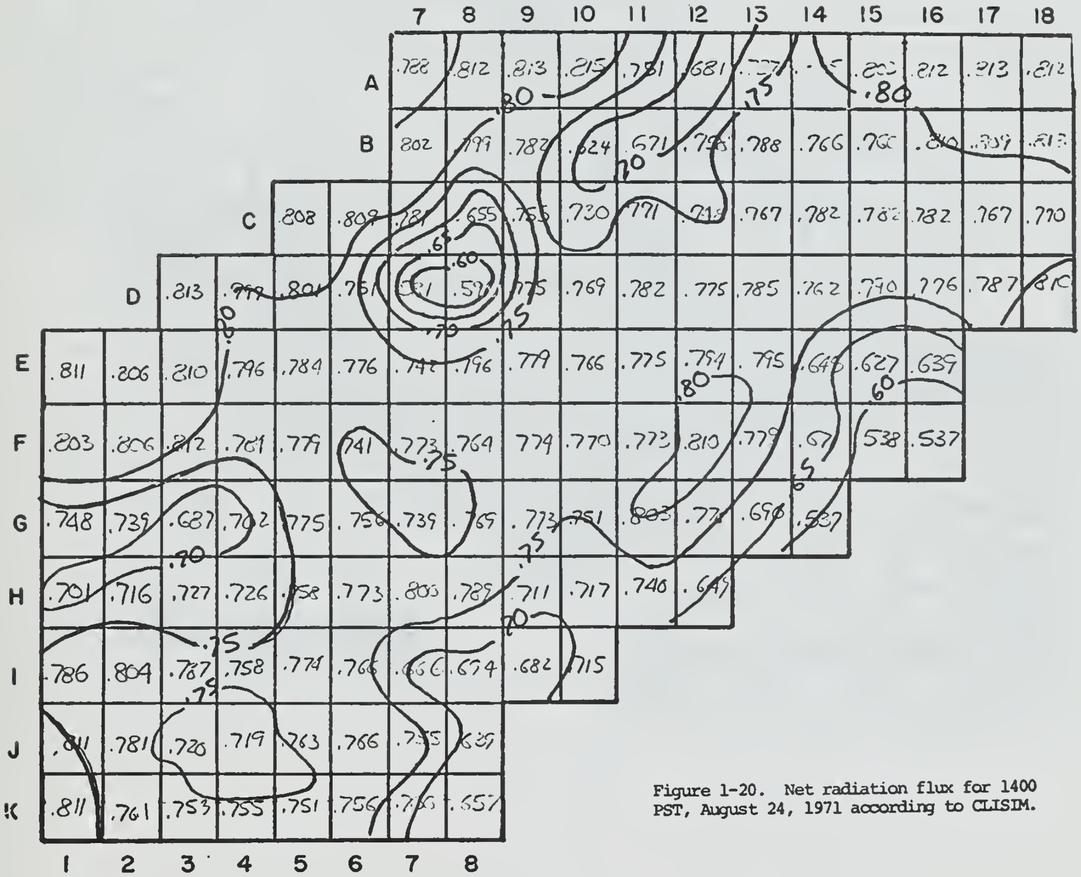
7 8 9 10 11 12 13 14 15 16 17 18
A .788 .812 .813 .815 .781 .681 .812 .813 .812
B 802 .799 .782 .624 .671 .788 .766
C .808 .809 .781 .655 .755 .730 .771 .767 .782 .782 .767 .770
D .813 .801 .751 .59 .775 .769 .782 .775 .785 .762 .790 .776 .787
E .811 .806 .810 .796 .784 .776 .196 .779 .766 .775 .794 .795 .648 .627 .639
F .803 .806 .812 .761 .779 .741 .773 .764 774 .770 .773 .810 .779 .67 538 .537
G .748 .739 .687 .702 .775 .756 .739 .769 .773 .751 .803 .77 .696 .537
H .701 .716 .727 .726 .758 .773 .800 .789 .711 .717 .740 .649
I .786 .804 .787 .758 .774 .766 .666 .674 .682 .715
J .811 .781 .720 .719 .763 .766 .755 .639
K .811 .761 .753 .755 .751 .756 .657
1 2 3 4 5 6 7 8
.80
.80
.80
.75
.70
.65
.60
.70
.75
.80
.60
.75
.65
.70
.75
.70
.75
.75
.70

Figure 1-20. Net radiation flux for 1400 PST, August 24, 1971 according to CLISIM.

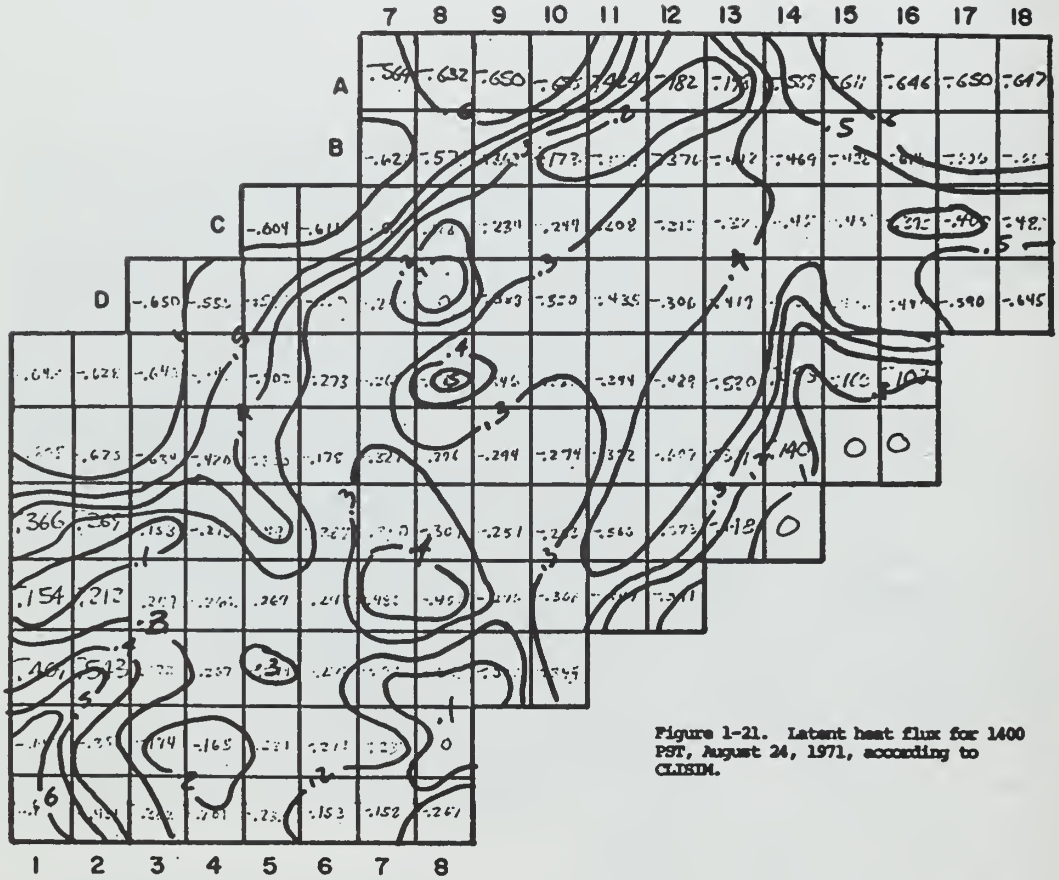

Figure 1-21. Latent heat flux for 1400 PST, August 24, 1971, according to CLISIM.

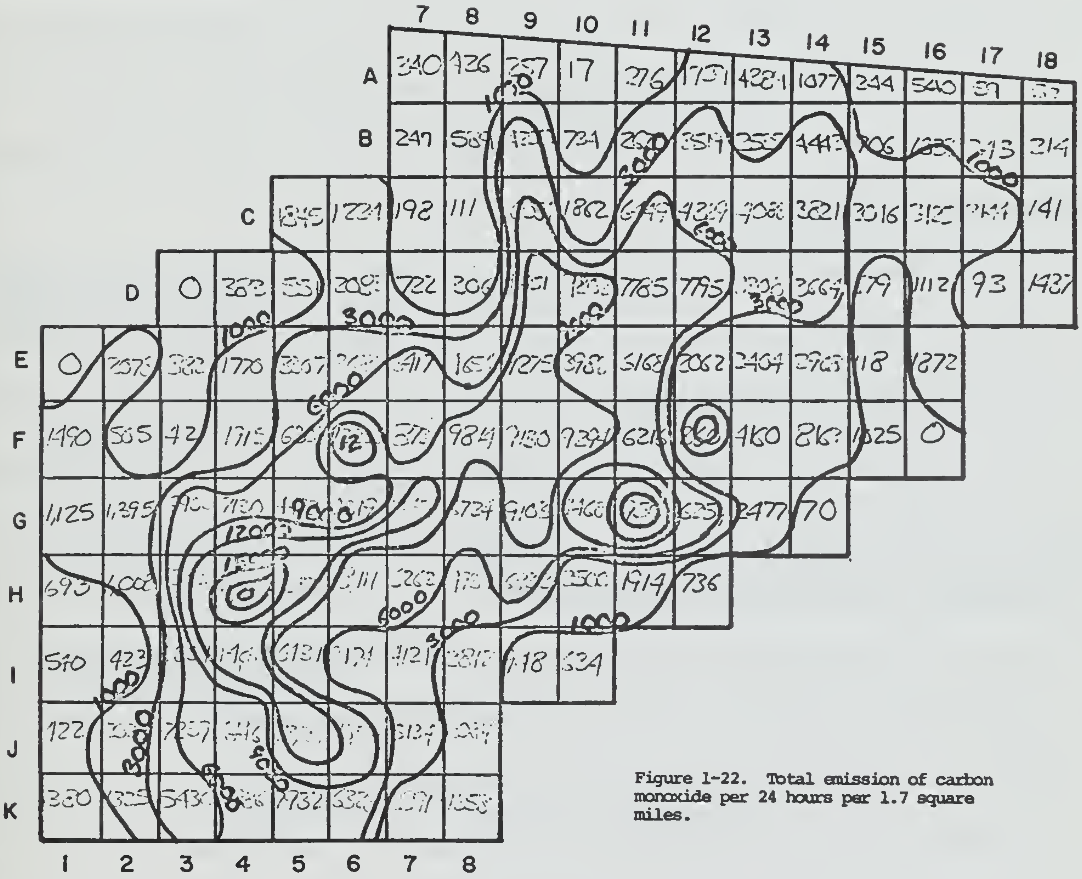

Figure 1-22. Total emission of carbon monoxide per 24 hours per 1.7 square miles.

measured from maps. The average traffic volume for each of the three types of streets was obtained from the California Division of Highways and car-mile factors computed. Application of vehicle emission factors (U. S. Env. Protection Agency, 1972) at appropriate average vehicle speeds, then yields the total amount of each kind of pollution emitted by the three kinds of streets, and, after summation, the total emitted by the rectangle in question.

The pattern of carbon monoxide emission from motor vehicles varies immensely from area to area. The traffic concentration observed in the central business district results in the largest value found, 21,258 Kilograms per day. At the edge, in some agricultural areas, we show zero values although this is undoubtedly an underestimate if only because we did not take agricultural vehicles into consideration.

We have developed a preliminary air pollution transport and diffusion model which is designed to take, as input, the kind of information which we have developed for the state area. The model, which was the subject of a portion of Dr. Sharma's dissertation, is related to the work of Monin (1959) and can be considered to be a member of the similarity family of diffusion models. It presently exists in a form which neglects the effects of elevated inversion layers and has been formulated only for an infinite line source configuration. These restrictions, however, are not inherent in the approach, and extension of the model to include more realistic features is planned.

The central physical phenomenon of interest is the behavior of the plume of pollutant which is emitted by a highway line source. The vertical propagation by turbulent diffusion and horizontal transport of the plume determines the resultant air concentration of pollutant observed at some downwind location. Figure 1-23 shows the model geometry. Monin (1959) postulated that "turbulent diffusion in a horizontally homogeneous, stationarysurface layer of air obeys the similarity theory in which L and U_* are the only scales of length and

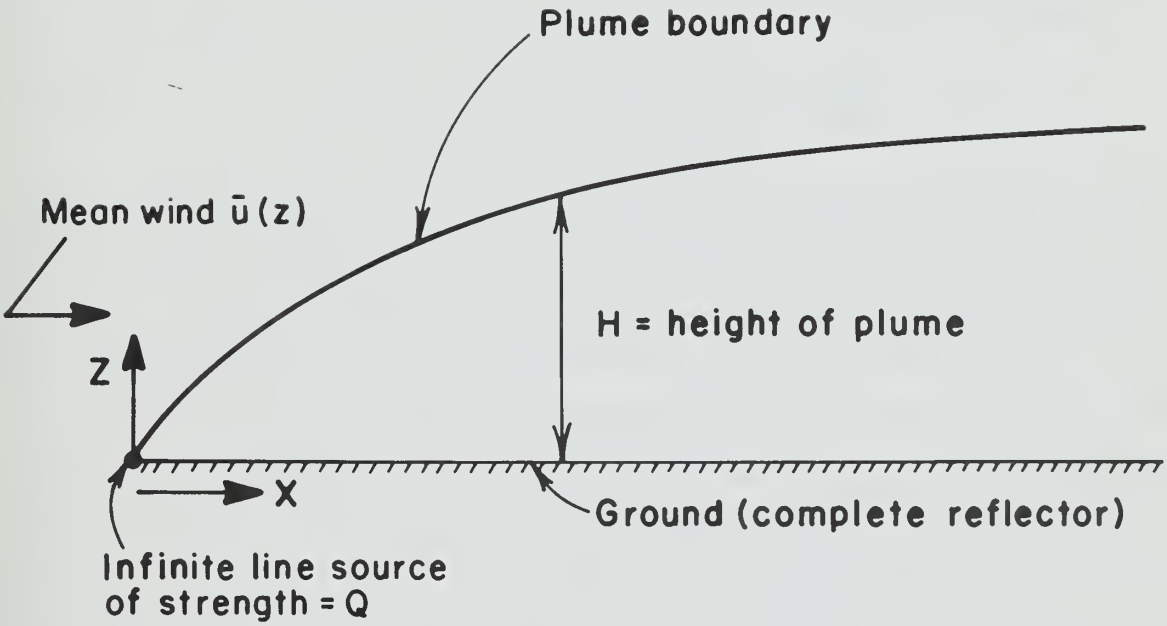

Figure 1-23. Problem description.

velocity". It follows, then, from dimensional considerations that the upward velocity of propagation of marked or polluted air, due to diffusion, W_*, is given by

$$W_* = \lambda U_* \phi (z/L) \qquad ,(21)$$

where U_* and L are defined as before, λ is a constant with the value of W_*/U_* for neutral stratification ($z/L = 0$). The equation which governs the height, Z, of the upper boundary of plume, is

$$\frac{dZ}{dx} = \frac{W_*}{U} \qquad ,(22)$$

where x is downwind distance. Monin assumed the "log-linear" relationship for U (a stability-corrected form of the logarithmic wind law) and obtained

$$\frac{dz}{dx} = \frac{k \lambda \phi (z/L)}{\left[(\ln(z/z_o) + \beta (\frac{z-z_o}{L})\right]} \qquad ,(23)$$

where β is another constant. From this formulation, Monin further postulated that "The shape of the boundaries of the plume (in particular, their inclination to the horizontal) does not depend upon the wind velocity but does depend upon the stratification of the atmosphere". Monin went on to integrate the above equation using empirical information for the ϕ-function and claimed good correspondence between calculations and smoke-plume observations. We have followed the general principles proposed by Monin but have chosen to use different techniques to specify the plume shape and velocity profiles.

The model is constrained to obey the principle of conservation of mass as stated by

$$Q = \int_o^z U(z)\ C(z)\ dz \qquad ,(24)$$

where Q is the source strength. For mathematical convenience, and also in hopes of validity at greater heights, we represent the wind by a power law form

$$U = U_1 \left(\frac{z}{z_1}\right)^p \qquad ,(25)$$

where U_1 is the wind speed at height z_1. The exponent must be a function of surface roughness and stability. Davenport (1965) gives empirical values for p which range from 0.1 for open sea, to 0.16 for flat open country to 0.28 for forest to 0.4 for urban areas. Reliable information on the stability dependence of p is not available. In the absence of such information, we were forced to use the log-linear formula to generate p-values as functions of both stability and roughness. This procedure is only an interim measure until better data are available. The values of p, so obtained, do have the virtue of allowing convenient mathematical manipulations in the model and yield reasonable extrapolations to heights where the log + linear form alone fails. Figure 1-24 shows p-values for stable stratification as a function of z_o and L, and Figure 1-25 shows the same display for the unstable case. Most surprisingly, these values correspond quite well to Davenport's values.

In our approach we obtain the height of the top of the plume by means of an analytical solution, due to Roberts (1923), of the plume-diffusion equations with wind speed and diffusivity varying according to a constant power of height (power law). After considerable manipulation, a result is obtained for the height, z, of the plume

$$z = a\ x^{b} \qquad ,(26)$$

where b = 1/(2p + 1) and a is a known function of stability and roughness. Figure 1-26 shows an example of the growth of a polluted plume over an area of large roughness (z_o= 100 cm) for various stabilities.

The air concentration observed at any point within the plume depends on the form of the vertical distribution of pollutant. The available data are not particularly helpful in this respect. Figure 1-27 shows measurements of smoke density from Monin (1959),and Figure 1-28 data from the Fort Wayne experiment conducted by the Traveler's Research Center (Hilst and Bowne, 1966). In both cases, and in all others we have inspected, the data could be represented by a linear decrease with height as well as any other function. We have chosen, therefore, to assume a linear decrease of concentration with height

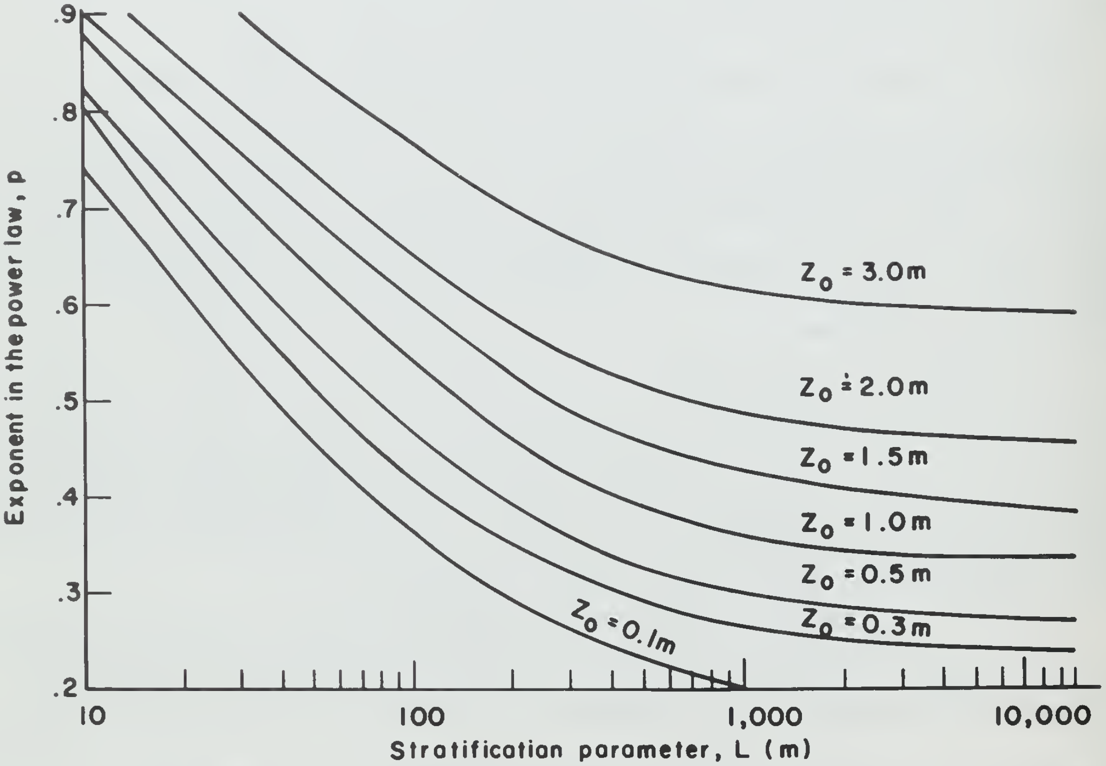

Figure 1-24. The exponent in the power law, p, vs. the stratification parameter, L, for different roughnesses, Z_o, for stable stratification.

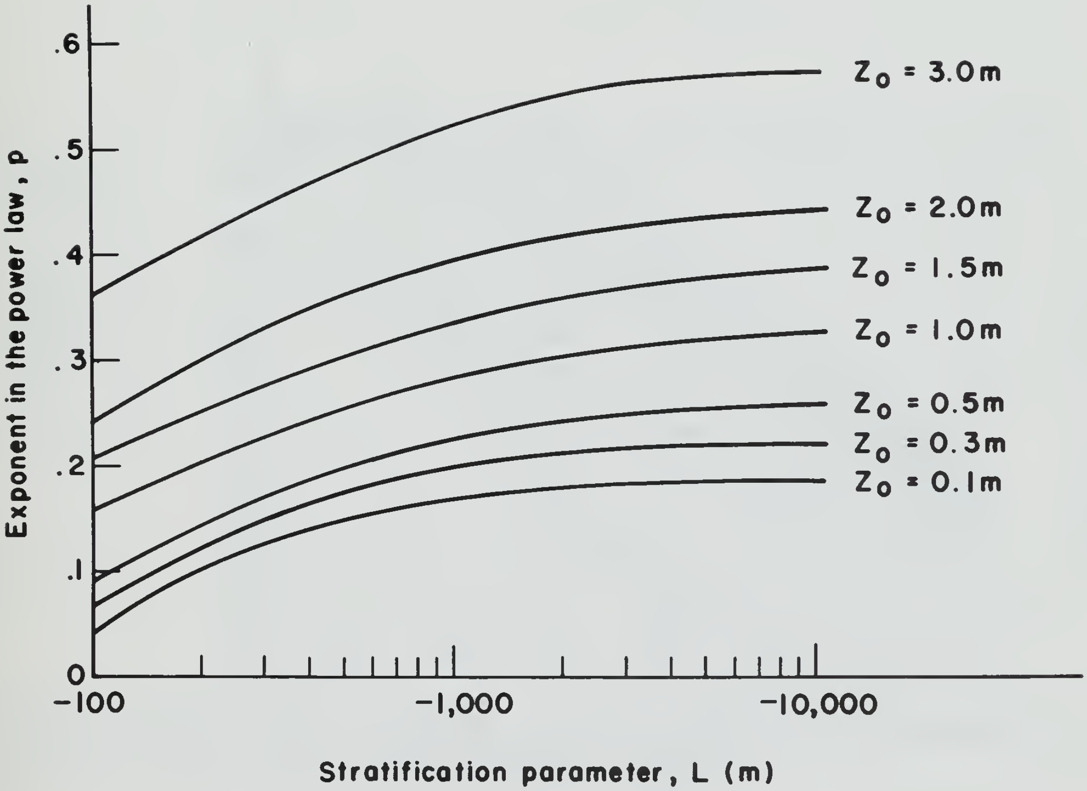

Figure 1-25. The exponent in the power law, p, vs. the stratification parameter, L, for different roughnesses, Z_o, for unstable stratification.

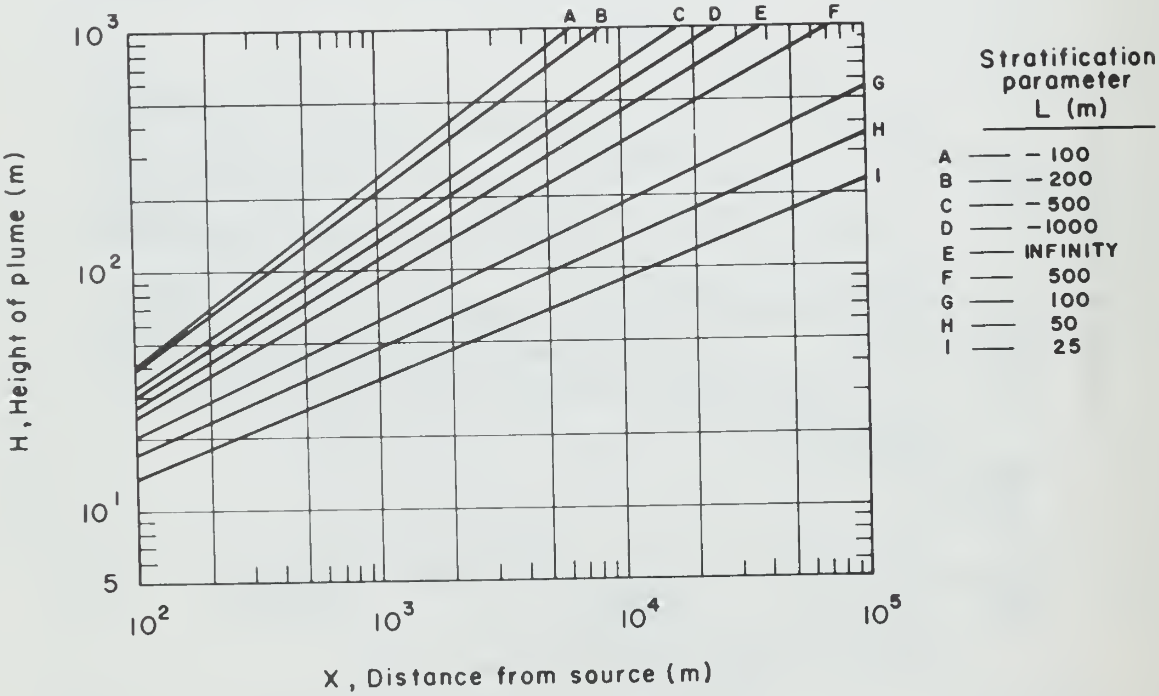

Figure 1-26. Height of the plume, H, vs. downwind distance, X for surface roughness, Z_o = 1.0 m.

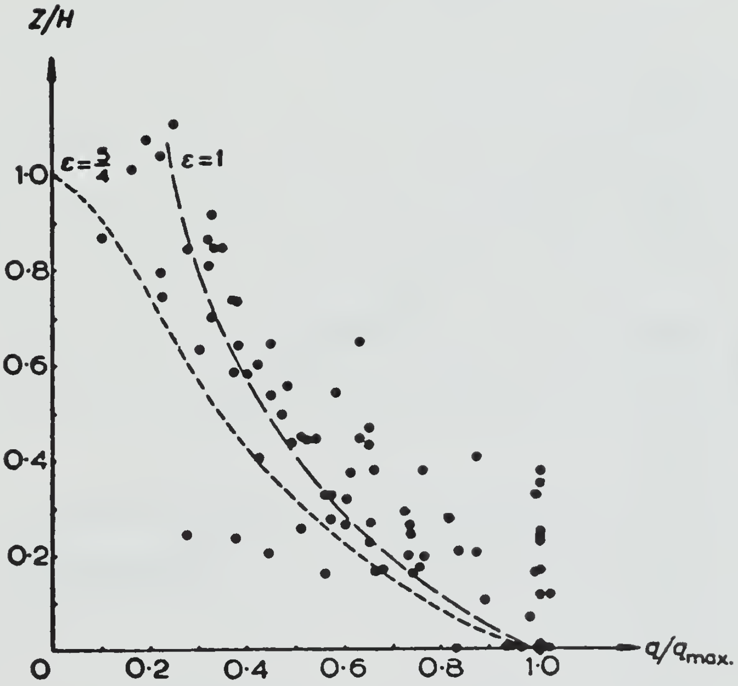

Figure 1-27. The vertical distribution of smoke density in the smoke plume, from Monin (1959).

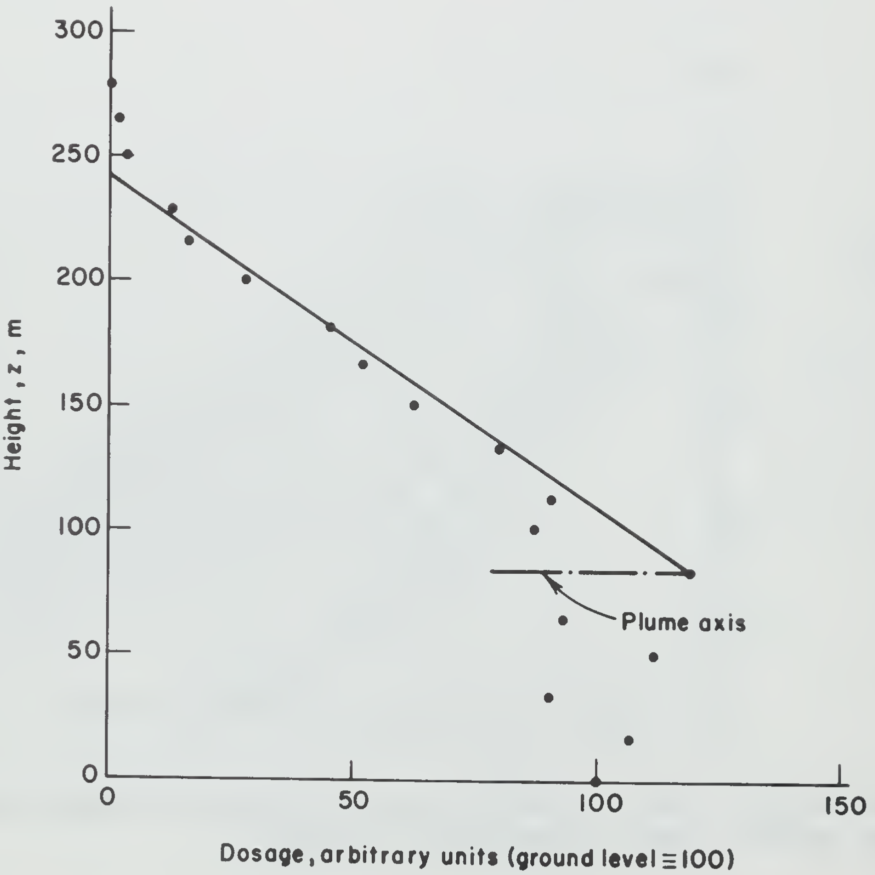

Figure 1-28. Vertical dosage distribution at WANE-TV tower, first sampling line, Ft. Wayne "check" trial TRC 65-16-G1. From Hilst and Bowne (1966).

within the plume. This will probably lead to incorrect concentrations near the upper edge of the plume since the concentration must assume a more asymptotic shape there. However, the linear representation of concentration throughout the majority of the plume should be as good as the observational data. Integration of the conservation of mass equation using the assumed wind profile, plume height, and concentration profile formulae yields a relationship for the surface concentration, C_o,

$$C_o = \frac{Q}{U_1 Z} \left(\frac{z_1}{z}\right)^p \frac{(p+2)\ (p+1)}{(p+2) + a_1 (p+1)} \qquad ,(27)$$

where U_1 is the wind speed at height z, and a_1 is constant.

We have thus obtained this, a simple diffusion and transport model which requires, as input, surface roughness, stability, wind speed at a specified height and the source strength. We feel that this model is probably as good as the data and has the virtue of being explicitly dependent on the most important physical parameters which are known to govern the diffusion process in the atmosphere.

In order to analyze the sensitivity of the model to the various parameters which determine the surface concentration, we define the sensitivity of the model to parameter s, S_s, as

$$S_s = \frac{100}{C_o} \frac{\partial C_o}{\partial s} \qquad . (28)$$

The algebraic simplicity of this model allows immediate analysis of the sensitivity to wind speed, U, source strength, Q, and plume height, H. These sensitivities are given below.

$$S_u = \frac{-100}{U}$$

$$S_Q = \frac{100}{Q}$$

$$S_H = \frac{-100\ (p+1)}{H^{2p+3}} \qquad (29)$$

The model is most sensitive to parameter change or error at low wind speed, weak source strength, and low plume heights.

Sensitivity of the model to surface roughness and stability was estimated by performing calculations for specific conditions. For instance, the roughness calculation was done at a distance of 3 Km downwind for neutral stratification and for roughnesses of 10 and 200 cm. Under these conditions, the prediction was that the smooth surface concentration would be 2.4 times that of the rough surface case. A similar strategy was followed to obtain the sensitivity to stability. For this calculation, the roughness parameter was set at 200 cm, a wind speed of 1 ms^{-1} at 5 meters, and an arbitrary source strength of 1000, and we obtained the surface concentrations given in Table 1-7. The concentration calculated at L = 100 (stable) is 5.5 times that at L = -100 (unstable).

Direct verification of this or any other model is not straight forward because of the lack of definitive experimental evidence. For instance, the Fort Wayne study, reported by Hilst and Bowne (1966), is by far the best available set of data. In this experiment a long line of uniform fluorescent particles was released upwind of the city by airplane and resultant air concentrations were measured in the city at five points as well as stability and turbulence parameters. Unfortunately, the source strength was not well known in this experiment. The manner in which the particles are generated and released in the wake of the airplane results in the immediate deposition of a large fraction of the particles. For this reason Hilst and Bowne recommend, for the purposes of verification calculations, that the source strength be adjusted to yield observed values at the first sampling point downwind. Using observed wind and stability (L = -200 meters) and a roughness of 200 cm, we obtained the results given in Table 1-8 in terms of dossage, D_o. With the adjustment at 1600 meters, the correspondence between observed and calculated

TABLE 1-7.

Monin - Obukhov Length, L(m)	Calculated surface concentration, C_o
- 100	0.96
- 500	2.44
-10,000	3.12
+10,000	3.38
+ 500	3.86
+ 100	5.32

TABLE 1-8.

OBSERVED AND CALCULATED SURFACE DOSSAGE FOR FORT WAYNE TEST NO.65-06 G1

X (Km)	Observed	Calculated D_o (particle-min/m^3)	Ratio
1,600	96.2	96.2	1.0
4,800	42.0	48.6	0.87
8,000	35.3	32.4	1.09
11,200	31.5	24.8	1.27
14,400	24.5	21.2	1.15

TABLE 1-9.

OBSERVED AND CALCULATED DOSSAGE FOR FORT WAYNE TEST NO.65-13 G1

X (Km)	Observed	Calculated D_o (particle-min/m^3)	Ratio
3,200	54.5	54.5	1.0
6,400	36.2	43.2	0.84
9,600	31.2	36.0	0.87
12,800	23.0	31.0	0.74
16,000	21.6	27.0	0.78

dossages is good. For these conditions, the model generated an exponent in the wind speed power law of 0.30; the observed value from tower measurements in the city was 0.32.

A companion calculation was made for a slightly stable case in which L was measured at 510 m. Again, adjusting the source strength to force exact correspondence at the first downwind measurement point and using the observed wind speed, we obtained the results shown in Table 1-9. In this case the model appears to over-predict air concentrations by about 20% at considerable downwind distances.

This brief verification study is meant to be only illustrative. The available experimental data do not permit unambiguous conclusions to be drawn about the limits of accuracy of any model. The data do suggest that our model may be a useful addition to the tools we have at our disposal to predict and, ultimately, control air pollution. Our goal was to formulate a simple, easy to use, model which required surface roughness and stability as primary inputs and which yielded results comparable to the quality of the data available.

In particular, we wished to develop means of handling the dispersion processes which were closely related to the primary influence on turbulence near the surface, i.e., roughness and stability. It appears that we may have come close to achieving our goals.

One of our goals is to provide information, conceptual and analytical tools, which will be useful in the decision-making and planning portion of society. Figure 1-1 suggests and certainly our analysis strongly supports the idea that land-use is a particularly critical portion of the processes that air pollution is a part of. Ideally, then, we would hope to relate pollution emission and air quality to land-use categories. We are in the process of doing this. Table 1-10 presents a preliminary analysis of the emission of carbon monoxide from motor vehicles by land-use type. Emissions are presented as an emission flux of grams of CO per ft^2. The data were selected from spot readings of representative portions of our spatial array.

TABLE 1-10. PRELIMINARY ANALYSIS OF CARBON MONOXIDE EMISSION FROM MOTOR VEHICLES BY LAND-USE TYPE FOR SACRAMENTO, CALIFORNIA in grams CO/$(feet)^2$

Category	Residential	Arterial	Highway	Total
LDR	.037	.177	.024	.476
MDR	0	.203	.095	.298
HDR	.026	1.511	0	1.537
SHP	.006	.464	.165	.635
IND	.019	.434	.339	.792
OFF	0	.019	0	.019
CBD	.010	.405	0	.415
SGR	.002	.413	.036	.451

We expect the general features of this table to remain the same when the analysis is completed. In particular, the fact that the emission from arterial streets is larger than highway has been a persistent feature of our preliminary results. Largest emission fluxes are found in the Heavy-Density Residential, Industrial, and Shopping land-use categories.

It may be that emission factors like these may be typical of similar land-use categories throughout California. We plan to pursue this concept in our future research. We hope that future planning decisions regarding land-use will take into account probable emission of pollutants and resultant impact on air quality.

To close this section, we present a second preliminary result of our systems approach to air quality. The final result of the current phase of our research program has been a data base consisting of all the information necessary to make an air pollution transport and dispersion calculation with the Sharma model, presented in the previous section. In order to provide an example of the use of air quality modeling, we have performed a preliminary calculation using the Sacramento data base and CLISIM estimates of stability as inputs to the Sharma model. To do this, we assumed an overall value of 66 cm for the roughness parameter and the following values of CO emission by 18,000-foot strips (the city imagined infinite for the purpose of this calculation in the crosswind direction).

TABLE 1-11. CO EMISSION AS A FUNCTION OF DOWNWIND DISTANCE in gm CO $m^{-2}sec^{-1}$

X(ft)	Area Emission Rate
18,000	9.4×10^{-6}
36,000	16.8×10^{-6}
54,000	11.7×10^{-6}
72,000	9.6×10^{-6}
90,000	6.2×10^{-6}
108,000	2.5×10^{-6}

These emission rates were chosen to be representative of the pattern in Sacramento during the normal summertime wind flow from the Southwest. We then performed an air quality calculation for the times of 0500 and 1400 PST using average L-values generated by CLISIM for the August 24, 1971 case. These were 15 meters for the stable case and -40 meters for the unstable afternoon case. The results of this exercise, which is meant to be only illustrative, are shown in Figure 1-29 and Figure 1-30. The CO concentration is given in gm $m^{-3}x10^{3}$. The values on the vertical ordinate can be taken as ppm for sea level conditions (ignoring the factor of 10^{2}). The unstable case shows a pattern of CO concentration which follows the assumed emission rate very closely. Concentrations are low. Both these results are the consequence of the efficient dispersion characteristic of unstable stratification. In contrast, the values of concentration calculated for the stable 0500 PST case are very high and the shape of

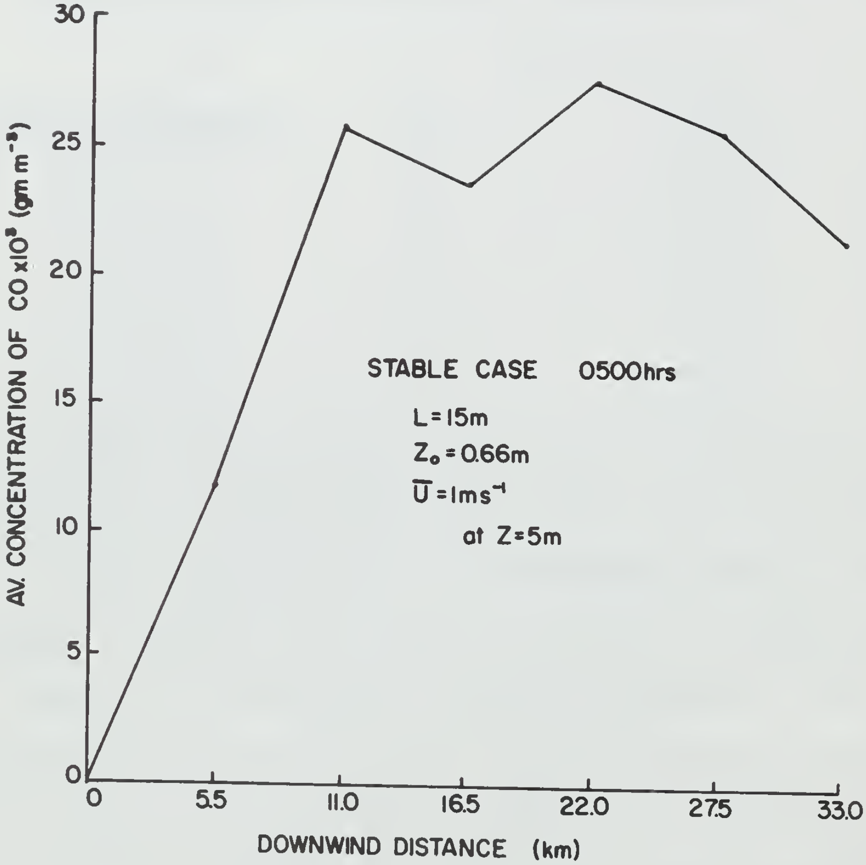

Figure 1-30. Computed Carbon Monoxide concentration. Stable case.

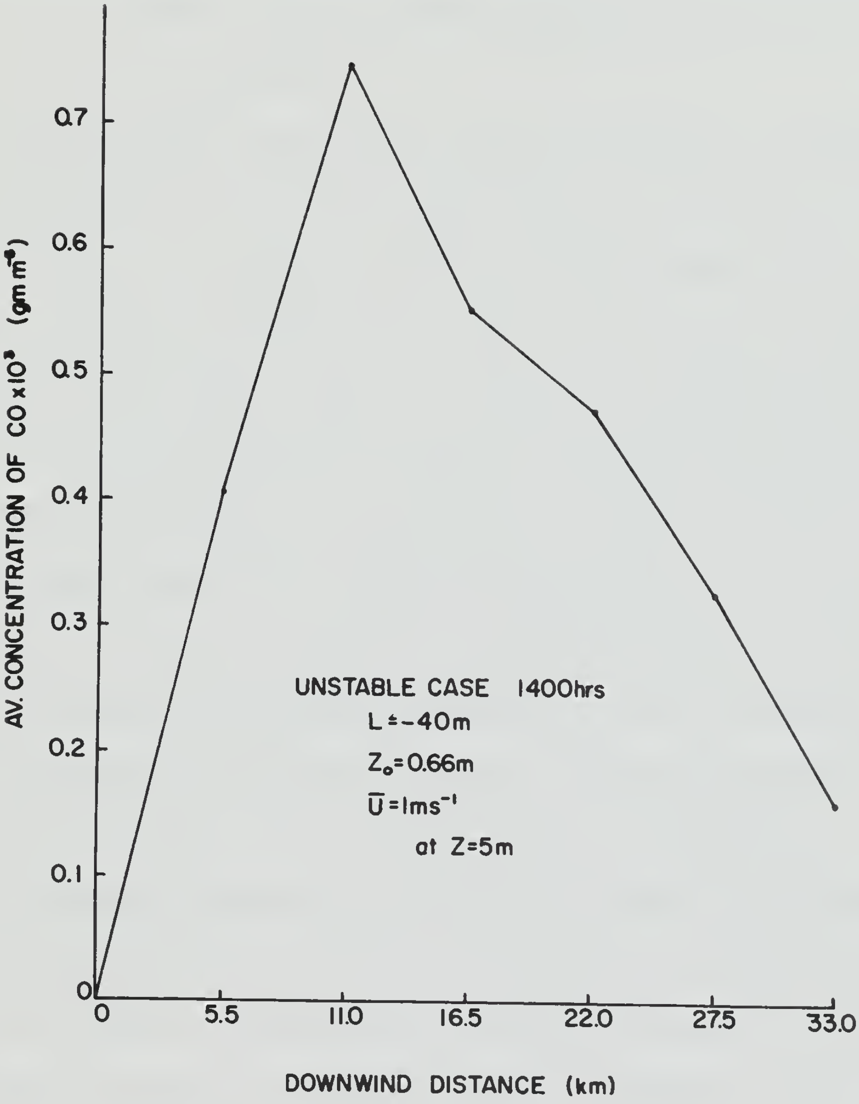

Figure 1-29. Computed Carbon Monoxide concentration. Unstable case.

the concentration curve is different. The effect of the very stable atmosphere is a downwind buildup of air concentration to levels about 35 times that calculated for unstable conditions. It should be noted that we used the same traffic density for both of these order-of-magnitude calculations.

Summary and Conclusions

In this report, we have attempted to tie together the physical processes which generate the microclimate, determine transport and diffusion processes on the micro- and meso-scale and how these are related to land-use patterns and, finally, air quality. There are four general areas in which conclusions from this review are appropriate.

(1) The microclimate emerges from this discussion as a concept of considerable importance to the problem of measuring and predicting air quality. Large horizontal variations of important physical processes, such as those represented by the flux of net radiation, exist within cities. These "neighborhood contrasts" are strongly coupled to land-use patterns and hence directly related to the planning processes in urban and regional governments. In particular, the evaporation rate, as indicated by relative abundance of green, freely transpiring plant, is the single most important parameter which determines the microclimatic response of a specific locality to a given radiation load and other large-scale meteorologic factors. Since air pollution emission from motor vehicles is also closely related to land-use patterns, the "air pollution system" as a whole is thus strongly coupled to land-use.

(2) The processes through which pollution diffuses from highways are also largely determined by the microclimate. In particular, surface roughness and atmospheric stability, as measured by the Richardson number or its equivalent, the Monin-Obukhov length, are the most important parameters controlling microscale transport and diffusion. In view of its central importance to micrometeorological and diffusion processes, an important conclusion to be drawn from this review is that measurement of the Richardson number should be a standard part of highway air quality programs. Extensive micrometeorological experience indicates that this is necessary to allow measurements made at different locations or at different times to be compared.

(3) Consideration of the multitude of air pollution models which are available to estimate air quality leads to the conclusion that the models generate far more information at greater precision than is available from field measurements. In fact, we feel the need for better and more comprehensive measurements is the most important conclusion to be drawn from this review. The measurement problem is severe because large local variability in the underlying microclimate leads to local contrasts in all processes governed by the microclimate. Hence, any measurement program must be carefully designed to ensure that the measurements are, in fact, representative of the area in question. In particular, pollution and meteorological parameters must be measured simultaneously within the study region over an adequate averaging time.

(4) We have also briefly reviewed the state of the art of air quality modeling in this report. The prevailing standard in the field, the Gaussian family of models, are deficient in the sense that the diffusion parameters which are used in these models are not derived directly from the physical processes which are known to dominate turbulent diffusion on the microscale, i.e., the microclimate - surface roughness - Richardson number parameter complex. More generally, it appears that far more attention needs to be paid to the properties of the models themselves. Comprehensive sensitivity analyses should be made in conjunction with model verification programs. Such information will allow better information as to the predictability of air quality and of the requirements of measurement and verification programs.

VOLUME III
CHAPTER 2: AIR POLLUTION CLIMATOLOGY FOR SACRAMENTO, CALIFORNIA

Objectives

As a portion of our overall program of research into the factors which influence the atmospheric environment over urban areas, we have studied the available air quality, and associated meteorological statistics, for Sacramento, California, for the period of 1961-1969. We had three general objectives for this work.

(1) During the period 1960-1970 the population of Sacramento County increased by 22% and energy consumption, in common with the state as a whole, approximately doubled. In very general terms it might be expected that phenomena associated with waste and inefficiencies, such as air pollution, would show increases somewhere between the rates for population and energy consumption, other factors being the same. This last condition is, of course, never met in practice. The major meteorological factors which determine the air concentration resulting from a given rate of emission of pollution, such as wind speed and mixing depth, are not constant in time. In addition, the technological effort to control automobile emissions of pollution began midway through the 1960-70 decade. An important practical objective in examining air quality data for this period would be to determine whether a measurable improvement can be demonstrated from these data. Therefore, one goal for this study was to determine whether or not a statistically significant trend can be found in the available air quality data. We recognize, of course, that an air pollution "climatology" may not even be a definable concept due to rapid changes with time and lack of data.

(2) One of the uses to which historical air pollution and meteorological data may be put is to provide baseline information for model development. At a minimum, the historical data sets the order of magnitude of general pollution levels, as well as maxima and minima, which any useful predictive model must be able to generate from historical emission rates. In addition, it would be hoped that sufficient historical data are available that detailed verification tests could be made for various air pollution models. Therefore, the second ovjective of our study of historical air pollution data was to compile sufficient information to test predictive models of the processes by which pollution is transported and diffused by the wind.

(3) As a third objective, we wished to subject the available data to standard statistical procedures to determine the existence of strong statistical relationships between the various pollution and meteorological parameters. Such relationships, if found at a sufficiently high level of significance, might be useful for various pragmatic applications as well as a guide to the model-generating process.

Pollution Data

Data for contaminants was available for Sacramento from the Air Resources Board from October 1, 1957 to December 31, 1969 at the time we initiated our study. The early data includes only oxidant with other pollutants appearing gradually as appropriate instrumentation became available. Pollution data for the entire period mentioned above were punched up for computer processing. However, since meteorological data were conveniently available only for

January 1, 1961 to December 31, 1969, all statistics regarding relationships between pollutant concentrations and meteorological parameters were confined to this shorter period. Data were collected for every day in the target period for the following parameters: maximum daily concentrations of particulates, total hydrocarbons, oxides of nitrogen, nitric oxide, nitrogen dioxide, carbon monoxide, and total oxidants.

Definition of terms

The following definitions are useful in the proper interpretation of the data.

1) Hourly average: The average concentration for a 60-minute period, usually the clock hour. This is an integrated value, usually read from the strip chart by eye. Some parts of the hour have lower values than the average, some higher. There are 24 such values for each day starting with hour 00 and ending with hour 23.

2) Daily maximum: The highest concentration reached during 24 hours of sampling and may be of only a few minutes duration.

3) Daily maximum hourly average: This is the highest of the 24 hourly averages reported during the day. The monthly maximum hourly average is the highest such value reported during the month.

4) Daily concentration: The recorded value is the reading for the clock hour having the highest average value. The clock hour is any one of 24 60-minute intervals beginning and ending on the hour.

Measurement techniques

1) Total oxidant - Refers to all substances which may be present in the atmosphere that oxidize potassium iodide (KI) to form iodine (I_2), such as ozone, nitrogen dioxide, and organic peroxides. Specific spectroscopic measurements indicate ozone is the principal oxidant in California air. Concentrations are measured with continuous recording analyzers using potassium iodide and are reported as parts of oxidant per million parts of air by colume. In Sacramento the instrument is colorimetric and is standardized against ozone. Oxidant measurements for Sacramento have been printed in The Clean Air Quarterly for each day beginning on August 20, 1957.

Note: The phenolphthalein method for measuring oxidant concentration was used in Sacramento until August 24, 1960 at which time the potassium iodide method came into use. The phenolphthalein method was as follows: Concentrations were determined by hand analysis of individual samples and reported as parts per million of air by volume. The method was standardized against hydrogen peroxide. Grab samples were taken once a day, usually between 1000 and 1400 hours.

2) Nitrogen oxides (NO, NO_2, NO_x) - Continuous measurement of NO_2 is performed by scrubbing the sample air with an absorbing solution (Saltzman type reagent) in an automatic recording analyzer. Reaction with the NO_2 forms a red AZO dye which is photometrically measured and recorded on the strip chart as ppm NO_2.

NO is determined by first passing the air sample through an acid permanganate bubble (oxidizer) which converts NO to NO_2. The NO plus NO_2 originally present is recorded as Oxides of Nitrogen (NO_x) in parts per million of air by volume. The NO concentration is taken as the difference between the NO_x and NO_2 concentrations.

Daily values for the concentrations of NO and NO_2 are reported in the Clean Air Quarterly beginning on October 4, 1960. The addition of Oxides of Nitrogen to the published data tables came on January 1, 1963. Since this date all three entries have been made.

3) Carbon monoxide - CO is measured continuously by measuring the absorption of nondispersed infrared radiation (NDIR) by the CO nolecule. Irradiation from a hot filament is directed to a detector through two cells: a reference cell filled with dry air or nitrogen, and a sample cell through which the air is continuously drawn. The difference in infrared absorption between the reference and sample cells creates a pressure difference in the detector. This pressure difference is transduced to CO concentration in parts per million. The principal interferences for this method are caused by water vapor and carbon dioxide. The analyzer is of the recording nondispersive infrared (Luft) gype.

4) Hydrocarbons - Hydrocarbons are measured with continuous flame ionization analyzers standardized against propane. Results are reported as parts of methane per million parts of air.

5) Suspended particulate matter - Particulate matter samples are taken by automatic AISI samplers using two-hour sampling cycles. Values are calculated by comparing light transmission through sampled areas and blank tape and are expressed as COH units* per 1000 linear feet of air passing through the filter. COH units less than 1.0 indicate relatively clean air.

Note: Particulate concentrations for dates up through February 1967 are tabulated when readings are available for at least nine (9) 2-hour cycles. Beginning in March 1967, daily averages are tabulated regardless of the number of readings reported.

Dates for which data are available

1) Oxidant
    a) 08/01/57 - 12/31/60: Listed as daily maximum concentration
    b) 01/01/61 - 12/31/62: Listed as daily concentration
    c) 01/01/63 - 12/31/69: Listed as maximum hourly average concentration by day
2) Nitric oxide and nitrogen dioxide
    a) 10/01/60 - 12/31/60: Listed as daily maximum concentration
    b) 01/01/61 - 12/31/62: Listed as daily concentration
    c) 01/01/63 - 12/31/69: Listed as maximum hourly average concentration by day
3) Oxides of nitrogen
    01/01/63 - 12/31/69: Listed as maximum hourly average concentration by day
4) Hydrocarbons
    01/01/65 - 12/31/69: Listed as maximum hourly average concentration by day
5) Carbon monoxide
    a) 01/01/60 - 06/30/60: Listed as daily maximum concentration
    b) 07/01/60 - 12/31/61: No data reported
    c) 01/01/62 - 12/31/62: Listed as daily concentration
    d) 01/01/63 - 12/31/69: Listed as maximum hourly average concentration by day
6) Particulate matter
    04/01/58 - 12/31/69: Listed as daily mean COH values by the AISI method
    Note: Particulate concentrations for dates 04/01/58 - 02/28/67 are tabulated

---

* Note: One "COH Unit" is the quantity of light scattering solids which is capable of producing an optical density of 0.01 for light at 0.4μ.

only when readings for nine (9) 2-hour cycles are available. Beginning in March 1967, daily averages are tabulated regardless of the number of readings reported.

Location of sampling stations

Most of the pollutant sampling which is reflected in our data has been measured at the downtown station (1230 J Street). Oxidants have been continuously measured there since September 16, 1961; particulate matter since June 8, 1962; NO and NO_2 since September 16, 1961; and carbon monoxide since October 5, 1961. In 1965 hydrocarbons were added. The height of the sampling point is about 25 feet above the ground.

The data which are on punched cards begin with January 1, 1961. Thus, any pollution data for the period January 1, 1961 - September 15, 1961 was measured at 2221 Stockton Blvd. where oxidants and particulates were sampled during the early years of air contaminate monitoring. The sampling point at the latter location was approximately 3 feet above ground level.

Critique of instrumentation used to obtain pollution data*

(1) Oxidant. The continuously recording colorimetric analyzers used to measure total oxidant have been calibrated semi-annually with ozone-air mixtures so that the oxidant concentrations in the air are registered as apparent O_3 concentrations. Over a 4-year period, 67% of the instruments in use in California have been found with ±10% and 83% within ±20% of the previous calibration.

The principal oxidant species besides O_3 which oxidize potassium iodide to I_2 are NO_2, PAN, organiz peroxides, Cl_2, H_2O_2, etc. The sensitivity of the KI method to interference by NO_2 increases with the concentration of the KI solution, and with a 20%KI solution (the maximum concentration used) 30 to 40% of the NO_2 present is measured as ozone. PAN concentrations in the atmosphere can be as large as .04 ppm and 50% of the PANs are recorded as apparent O_3 concentrations. Hence these species cause interference as well as doubts about the species content in the group of oxidants. SO_2 is found to interfere negatively, resulting in a decrease in the oxidant reading by an amount equal to the concentration of SO_2 present in the sample. In general, the performance of these and other instruments based on wet chemical analysis appears to depend greatly on the diligence and skill of the person tending them. Reagent quality and concentrations, air flow, and air-solution contact are regulated by non-reliable automated wet-channel devices which require close attention. The instrument in use in Sacramento is made by Beckman instruments.

(2) Oxides of nitrogen are now measured by a continuous automatic colorimetric analyzer (Beckman). The Beckman instruments used in California have been calibrated semi-annually for NO_2. In stability tests 67% of the analyzers were found to be within ±10% of the previous calibration and 85% with ±20%. The lower limit for meaningful concentration measurements was 0.01 ppm. Calibration for NO has been incomplete because of the lock of a reliable NO source. Therefore, all measurement data actually represent NO_2 equivalent concentrations.

In the parallel mode (used in Sacramento) NO_2 is lost in the oxidizer and only about 80% of the NO present is converted to NO_2. Also 50% of the concentration of PANs is measured as NO_2. Strict adherence to the Saltzmann procedure is required to avoid important interferences by SO_2 and NO with the NO_2 determination in air.

---

*This section is based on Project Clean Air, University of California, Task Force Assessments, Volume 4.

Furthermore, no information has appeared about the reliability of the NO → NO_2 conversion in $KM_n)_4$ acid solution, nor of the interferences with this process.

(3) Carbon monoxide is presently measured by the Beckman Non-dispersive Infrared Analyzer (NDIR). This device is believed to be relatively accurate and reliable. However, if proper filtering techniques are not used in the analyzers, H_2O and CO_2 cause the principal interferences and to a lesser degree CH_y and C_2H_6. The major drawback with NDIR analysis is the rather ambiguous air sampling technique. Air samples are collected in aluminized bags and then analyzed. A more direct means of air intake to the analyzing instrument at a constant regulated flow rate would be preferable. The lower limit for meaningful concentration measurements is about 1 ppm.

(4) Total hydrocarbon is now measured by Hydrogen flame ionization analysis. No performance data seem to be available for appraisal of the value of the instruments presently in use. However, once proper flame conditions and precise maintenance of flow rate have been established, the breakdown problems seem minimal. The lower limit of meaningful concentration measurement seems to be about 1 ppm of methane equivalent.

(5) Particulates - All the particulate concentrations reflected in the Sacramento data are recorded in COH units per 1000 linear feet of air sampled. While these measurements can be related approximately to the concentrations in $\mu g/m^3$ of particulates in the air sample, they depend strongly on the number, size, color, and, in particular, on the phase (liquid or solid) of the suspended matter as well as on the grade of filter material used.

Meteorological data

Meteorological data were taken from the monthly issues of the U. S. Department of Commerce, Weather Bureau, in the form of the Local Climatological Data (Supplement) January 1961 - December 1969. Following is a summary of the dates for which the various data are available and an explanation of reporting units.

1) Average dry-bulb temperature (°F)

January 1, 1961 - December 31, 1969: data available

Average appears to be $\frac{T_{max} + T_{min}}{2}$ for each day.

2) Precipitation (water equivalent) in inches

January 1, 1961 - March 31, 1962: no data
April 1, 1962 - April 30, 1962: data available
May 1, 1962 - August 31, 1962: no data
September 1, 1962 - September 30, 1962: data available
October 1, 1962 - September 30, 1962: no data
October 1, 1963 - November 30, 1963: data available
December 1, 1963 - December 31, 1963: no data
January 1, 1964 - May 31, 1964: data available
June 1, 1964 - August 31, 1964: no data
September 1, 1964 - December 31, 1969: data available

3) Resultant wind direction measured from north taken clockwise. (Northerly = 360, Easterly = 180, Westerly 270, 0 = calm).

January 1, 1961 - December 31, 1969: data available

4) Resultant wind speed (mph). Resultant wind movement is the vectorial sum of all surface wind directions and speeds for each day. It is obtained by resolving each hourly wind observation into components from north and east, summing over the day, and reconverting the summed components into a single vector. The daily resultant wind speed is obtained by dividing the total movement by 24.

All meteorological data reported were measured at the Sacramento Municipal Airport. (Name changed October 1, 1969 to Executive Airport).

Statistical analysis of the data

After the foregoing data were transferred to punched cards, a careful error check was made, followed by an extensive study of the elementary statistics which could be formed from these data including the arithmetic mean, the standard deviation, maximum and minimum values, and correlation coefficients between all input parameters. These calculations were made for the following groupings of data:

(1) Each individual month (108 months - no correlations)
(2) Each individual year (1961 to 1969)
(3) All nine years together
(4) All nine years together, Sunday only
(5) January - March
(6) January - March, with wind restrictions*(any day with wind directions between east and north were excluded)
(7) April - June
(8) April - June, with wind restrictions*
(9) July - September
(10) July - September, with wind restrictions*
(11) October - December
(12) October - December, with wind restrictions*
(13) December - February
(14) March - May
(15) June - August
(16) September - November

A few words regarding the limitations of these data are in order. The pollution data were available in the form of daily values of maximum hourly averages. For some applications relating to public health and human comfort, such information is quite useful. On the other hand, these data severely limits our ability to make detailed verification tests for model development. For this application, average daily values would be preferable and direct access to hourly averages would be ideal. However, these data are still useful as numerical baseline information in spite of the limitations. In this section, we shall give the principal results of our analysis. We have not yet subjected these data to more advanced statistical analyses, such as the higher moments, probability and joint probability density distribution, or spectral and cross-spectral analyses. In view of the fact that, in general, a daily hourly maximum for any one pollutant will not occur at the same hour as another, any correlation-type analysis must be viewed with caution. It should also be remembered that the particulate data, unlike the rest, exist in the form of daily mean hourly averages.

TABLE 2-1. MEAN VALUES 1961 - 1969

Quantity	Unit	Average Value	Maximum Value	Standard Deviation
Oxidant	ppm	0.055	0.290	0.0645
NO	ppm	0.113	1.50	0.145
NO_2	ppm	0.061	0.50	0.042
NO_x	ppm	0.158	1.19	0.159
Hydrocarbon	ppm	6.460	33.0	4.326
Particulates	COH	0.506	2.80	0.378
CO	ppm	6.700	55.0	6.472
Temperature	°F	60.2	91.0	12.2
Wind speed	mph	5.90	22.0	3.96
Wind direction	deg.	222	---	75.0

Note that temperature and wind velocity are also averaged over the entire day.

Inspection of Table 2-1 shows that the maximum hourly pollutant concentration is a highly variable statistic since most of the standard deviations are of the same order of magnitude as the mean value.

Sunday-only data, 1961 - 1969 - In order to begin to investigate the relationship between human activities and pollution concentration, we computed the mean values for all Sunday data over the same period. The results of this analysis are given below.

TABLE 2-2. POLLUTANT CONCENTRATIONS FOR SUNDAYS ONLY, 1961 - 1969

Pollutant	Unit	Mean Value	Standard Deviation	Percent Reduction
Oxidant	ppm	0.0497	0.0282	9.1
NO	ppm	0.0845	0.123	25.7
NO_2	ppm	0.0429	0.0317	29.5
NO_x	ppm	0.125	0.150	20.9
Hydrocarbons	ppm	6.040	4.042	6.5
Particulates	COH	0.373	0.321	26.3
CO	ppm	5.624	5.979	16.1

All the primary pollutants show reductions compared to the mean values computed for all days. The largest reductions appear for NO_2, particulates, NO, and NO_x with lesser reductions for the remainder. This result implies that those few pollutants are those which are most directly related to human activities on a 24-hour time scale.

Monthly variation - A tabulation of the mean monthly values of the various parameters is given below.

TABLE 2-3. MONTHLY AVERAGES 1961 - 1969

Month	Oxidant	NO	NO_2	NO_x	HC	Part	CO	Temp.	Wind Speed	Wind Direction
JAN.	0.0358	0.163	0.0645	0.203	7.306	0.762	7.983	43.65	4.90	206.6
FEB.	.0364	.1304	.0586	.1813	7.435	.5853	7.264	49.70	5.30	218.7
MAR.	.0425	.0740	.0526	.1211	6.404	.4308	5.720	52.63	6.14	215.8
APRIL	.0471	.0421	.0438	.0830	5.104	.3002	4.556	57.84	6.91	230.0
MAY	.0554	.0337	.0448	.0737	4.435	.2947	3.451	63.92	7.21	228.9
JUNE	.0563	.0336	.0488	.0718	3.971	.2740	3.449	70.49	7.45	227.4
JULY	.0728	.0299	.0572	.0792	4.000	.2984	3.711	74.87	6.93	213.3
AUG.	.0687	.0441	.0542	.0902	5.441	.3557	4.472	75.14	6.11	218.4
SEPT.	.0711	.0643	.0647	.1181	5.440	.5020	5.449	71.45	6.09	235.2
OCT.	.0605	.2202	.1000	.3240	10.72	.7902	13.81	63.86	4.85	239.2
NOV.	.0350	.2357	.0768	.2881	9.236	.7743	11.64	53.31	4.55	218.4
DEC.	.0240	.2075	.0637	.2363	7.094	.6991	8.307	44.84	4.61	210.4

These numbers are plotted in Figures 2-1 and 2-2. As can be seen, the average monthly pollution concentrations fall into two patterns. The majority of these pollutants show a maximum in October (November for NO) and a minimum in June (July for NO, April for NO_2). This pattern closely resembles the reciprocal of wind speed which shows a maximum in November and minimum in June (Figure 2-4) so that one would conclude that dilution due to the action of the wind is a dominant process for these pollutants. Oxidant displays an entirely different pattern. The annual maximum is reached in July, followed by decreasing values during the period when the other pollutants are increasing. The minimum for oxidant is reached in December close to the time of the maximum for the other pollutants. This different behavior on the part of oxidant most certainly is a reflection of the importance of its photochemical origin. The generation of oxidant is a function of the intensity of solar radiation and the concentration of the reagents which participate in this complex reaction (NO, NO_2, hydrocarbons). Evidently, conditions are optimum in July with decreasing generation of oxidant thereafter in spite of increasing concentrations of the input reagents due to decreasing radiation. The remaining meteorological parameters are plotted in Figure 2-3.

Seasonal statistics - Since air pollution is more of a seasonal phenomena than a monthly one, we computed the same statistics as before on a seasonal basis. We chose the periods January - March, April - June, July - September, and October - December for this analysis. Below are the results. These values show essentially the same pattern as our previous analysis and are not plotted. (See Table 2-4)

Correlation analysis - We have also subjected these data to a correlation analysis. In a sense, the limitations of daily-maximum hour-concentrations are an advantage here. The rate constants in the complex photochemical process are such that peak values in the various participants occur at different times. However, a bad day for one pollutant would be expected to be bad for one of the other chemical actors but with the maximum concentration occurring at a different time. Hence, correlations between the various pollutants without regard for the time of their maximum values may be more meaningful than if the analysis were done hour-by-hour without consideration of time-lags among the pollutants. Table 2-5 shows the correlation matrix for all data available for 1961 - 1969.

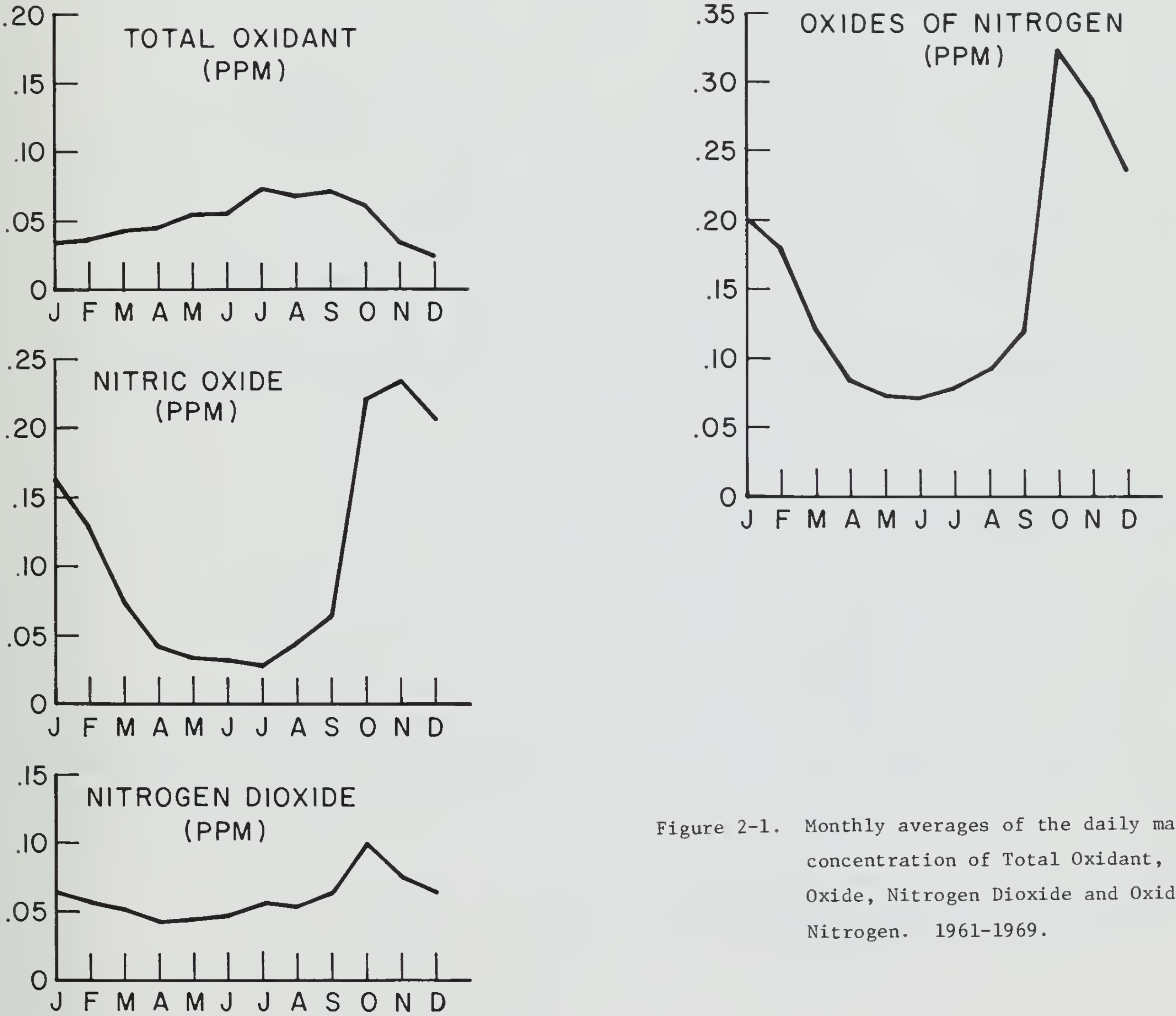

Figure 2-1. Monthly averages of the daily maximum concentration of Total Oxidant, Nitric Oxide, Nitrogen Dioxide and Oxides of Nitrogen. 1961-1969.

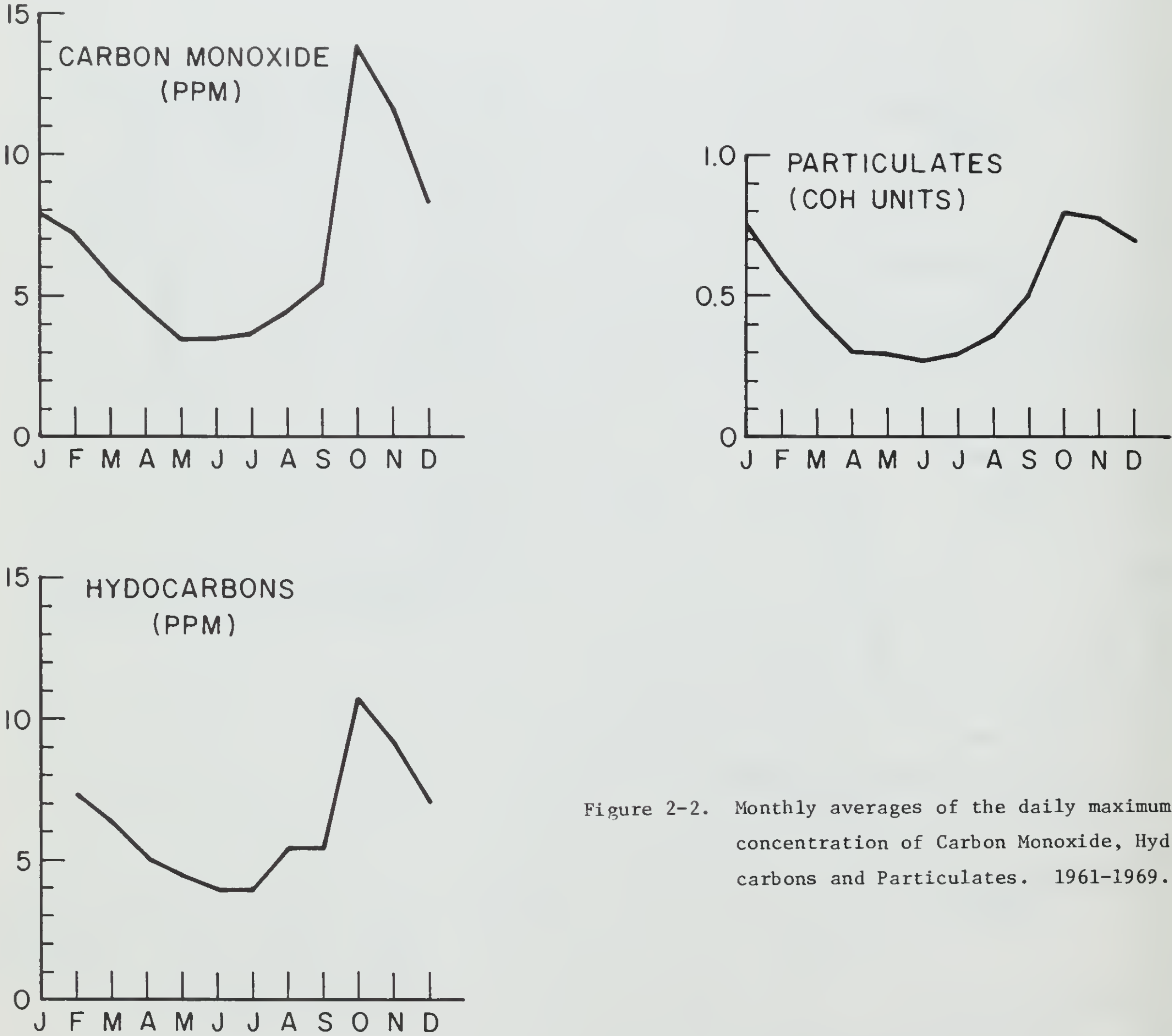

Figure 2-2. Monthly averages of the daily maximum concentration of Carbon Monoxide, Hydrocarbons and Particulates. 1961-1969.

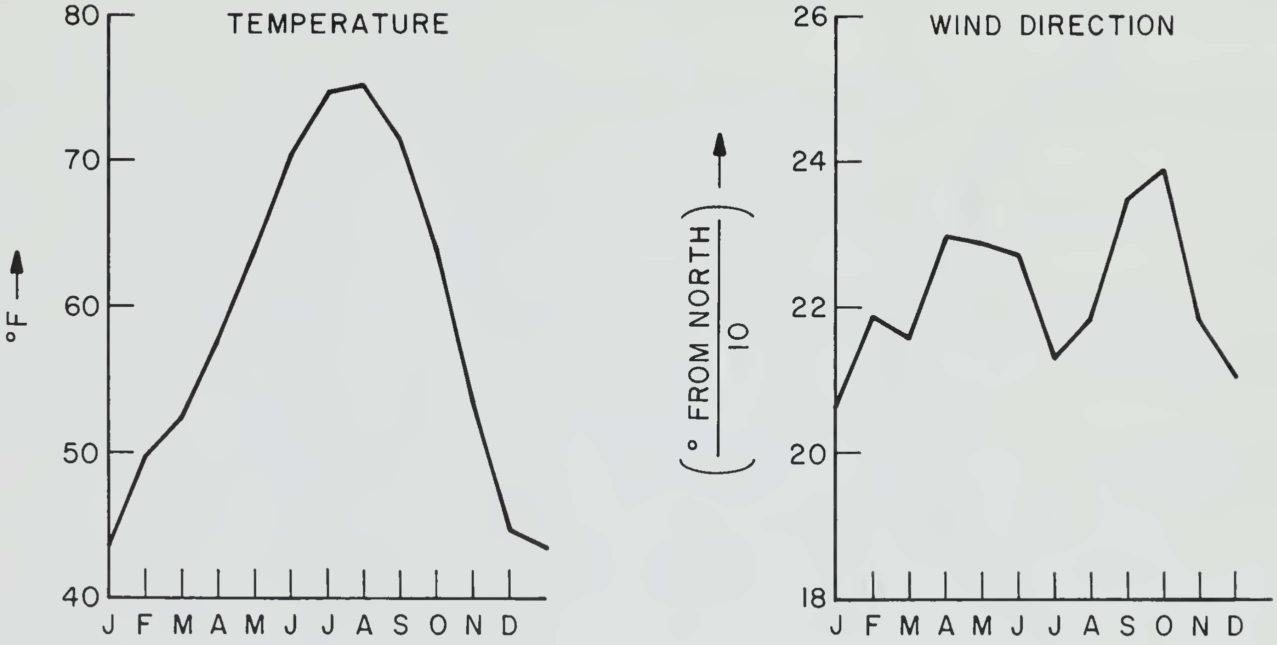

Figure 2-3. Monthly averages for temperature and wind direction. 1961-1969.

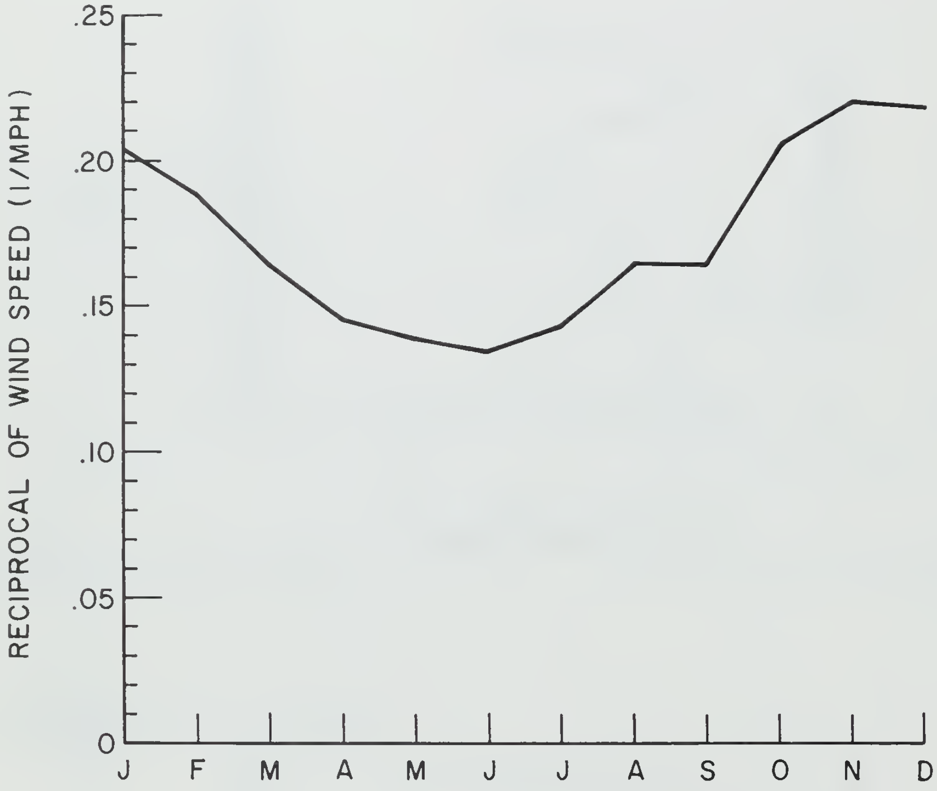

Figure 2-4. Monthly average of the reciprocal of wind speed. 1961-1969.

TABLE 2-4. SEASONAL STATISTICS 1961-1969

	Jan.-Mar.		April-June		July-Sept.		Oct.-Dec.	
Oxidant	Mean	σ	Mean	σ	Mean	σ	Mean	σ
Oxidant	.0401	.0241	.0536	.0264	.0728	.0360	.0399	.0319
NO	.1256	.1173	.0392	.0359	.0485	.0558	.2220	.2023
NO_2	.0565	.0346	.0471	.0226	.0591	.0396	.0805	.0540
NO_x	.1704	.1292	.0766	.0424	.0978	.0737	.2856	.2234
HC	7.082	3.739	4.538	2.302	5.011	2.559	8.058	5.821
Particulate	.5885	.3832	.2879	.1506	.3868	.2379	.7518	.4637
CO	7.035	4.916	3.799	2.225	4.586	3.554	11.290	9.527
Temp.	48.70	6.26	64.01	8.25	73.85	5.39	54.01	9.59
Speed	5.40	4.18	7.16	3.71	6.38	3.33	4.67	4.15
Direction	215.3	88.9	229.3	51.37	222.3	43.5	222.9	99.3

TABLE 2-5. CORRELATION COEFFICIENTS 1961-1969

	Oxidant	NO	NO_2	NO_x	HC	Part.	CO	Temp.	Speed	Direction
Oxidant	1	-.035	.286	.036	.104	.117	.108	.534	-.126	-.110
NO	-.035	1	.514	.981	.806	.690	.812	-.304	-.409	.070
NO_2	.286	.514	1	.604	.836	.571	.847	.018	-.375	.002
NO_x	.036	.981	.604	1	.836	.741	.847	-.246	-.442	.081
HC	.104	.806	.836	.836	1	.781	.866	-.144	-.480	.086
Part.	.117	.690	.571	.741	.781	1	.754	-.257	-.551	.051
CO	.108	.812	.847	.847	.866	.754	1	-.157	-.449	.067
Temp.	.534	-.304	.018	-.246	-.144	-.257	-.157	1	.120	.076
Speed	-.126	-.409	-.375	-.442	-.480	-.551	-.449	.120	1	.067
Direction	-.110	.070	.002	.081	.086	.051	.067	.076	.067	1

Due to the large number of degrees of freedom, the great majority of these correlations are significant at the 1% level or better. The following features are particularly noteworthy. For oxidant, the correlation coefficients are unifornly low except for temperature. Among the remaining pollutants, the correlations are, without exception, high. The highest correlations are between NO_x and NO (0.981), CO and hydrocarbon (0.866), CO and NO_2 (0.847), and CO and NO_x (0.847). Between pollutants and meteorological perameters, only wind speed shows a consistent pattern. With the exception of oxidant, the correlation between wind speed and pollution concentration tends to be about -0.5, with particulates yielding the largest negative correlation (-0.551). Oxidant is the only pollutant that shows a significant correlation with temperature and no significant correlations are found with wind direction.

Most of these results are unsurprising. The primary source for all these pollutants is the automobile, so they should be correlated. Similarly, the diluting effect of the wind would be expected to be reflected as a negative correlation. The low oxidant correlations are surprising at first glance because it is well known from the Los Angeles experience that high oxidant hays tend to be high in the other major pollutants. One hypothesis to explain the Sacramento data is that during the late fall months when most of the pollutants are building up due to lessening wind speed, oxidant decreases due to decreasing radiation. This effect is especially pronounced in Sacramento because of a maximum in fog in the late fall and early winter. However, sunny days do occur, even during the peak of the fog season. On these days oxidant could be high, along with temperature. Hence, the correlation between temperature and oxidant should persist throughout the year.

To test this hypothesis, we performed the correlation analysis for the various seasons, as defined above. For oxidant, we obtained the following results.

TABLE 2-6. SEASONAL CORRELATION COEFFICIENTS WITH OXIDANT 1961-1969

Quantity	Jan.-Mar.	April-June	July-Sept.	Oct.-Dec.
NO	0.1399	-0.0301	0.1515	0.2516
NO_2	0.3438	0.2220	0.3422	0.5336
NO_x	0.1760	0.0557	0.2331	0.3631
HC	0.2284	0.1292	0.2670	0.5020
Part.	0.3229	0.2889	0.3115	0.4160
CO	0.3464	0.1668	0.2197	0.4121
Temp.	0.2514	0.3833	0.2970	0.5525
Speed	-0.1509	-0.1997	-0.3384	-0.1435
Direction	0.0233	-0.0725	-0.0632	0.0219

As can be seen by comparing these values with those in the previous table, the correlation between oxidant and the other major pollutants is higher in almost every case than for the previous annual analysis. The correlations during the late fall are particularly high. For the other pollutants and meteorological parameters, the effect of seasonal grouping is not as pronounced. For instance, the following results were obtained for carbon monoxide.

TABLE 2-7. SEASONAL CORRELATION COEFFICIENTS WITH CARBON MONOXIDE 1961-1969

Quantity	Jan.-Mar.	April-June	July-Sept.	Oct.-Dec.
Oxidant	.3464	.1668	.2197	.4121
NO	.7235	.5695	.6823	.7933
NO_2	.4641	.3702	.4191	.5859
NO_x	.7602	.6558	.7349	.8369
HC	.8205	.6012	.8260	.8888
Part.	.6947	.5126	.6799	.7477
Temp.	-.0938	.0725	.1109	.2352
Speed	-.4743	-.3796	-.4394	-.4321
Direction	.0114	.1687	.3304	.0844

For particulate, the seasonal analysis yielded the following values.

TABLE 2-8. SEASONAL CORRELATION COEFFICIENTS WITH PARTICULATES 1961-1969

Quantity	Jan.-Mar.	April-June	July-Sept.	Oct.-Dec.
Oxidant	.3229	.2889	.3115	.4160
NO	.5414	.3361	.5658	.6703
NO_2	.4909	.3953	.4927	.6230
NO_x	.5707	.4742	.6810	.7604
HC	.6462	.4024	.7221	.8102
CO	.6947	.5126	.6799	.7477
Temp.	-.3010	.2351	.1708	.0758
Speed	-.5567	-.4494	-.5078	-.5639
Direction	-.0114	.1524	.3348	.0779

Finally, the seasonal correlation coefficients for wind speed are the following:

TABLE 2-9. SEASONAL CORRELATION COEFFICIENTS WITH WIND SPEED 1961-1969

Quantity	Jan.-Mar.	April-June	July-Sept.	Oct.-Dec.
Oxidant	-0.1509	-0.1997	-0.3384	-0.1435
NO	-0.3660	-0.3730	-0.3817	-0.4141
NO_2	-0.3017	-0.4081	-0.3891	-0.3378
NO_x	-0.3802	-0.4729	-0.4745	-0.4735
HC	-0.4683	-0.3304	-0.5209	-0.4504
Part.	-0.5567	-0.4494	-0.5078	-0.5639
CO	-0.4743	-0.3796	-0.4394	-0.4321
Temp.	0.1707	-0.1337	-0.3330	0.1047
Direction	0.0634	-0.0619	-0.2113	0.0907

Temporal variation - As we have mentioned earlier, one of the most important reasons for examining these statistics is to study whatever temporal trends may exist in air quality. We have found it useful in attempting to assess the existence of trends to keep in mind the major processes which effect air quality. During the decade 1960-70, in which population increased by 22% and energy consumption by 50%, the number of motor vehicals increased by approximately 30%. In the absence of emission control efforts, and all other factors being the same, one would expect air pollution concentrations to increase by about 3 or 4% per year during the period in question. We shall presently examine the variability of meteorological parameters. The control effort for automobile emission began about 1962 when crankcase systems began to be installed. The mechanism is thought to have become a significant factor in air quality by about 1965. This control approach is effective primarily for hydrocarbons so that impact would be expected only for the photochemical pollutants.

In the following sections we present the elementary temporal statistics. We have not subjected the data to an elaborate regression analysis. As will become apparent in the discussion, we do not feel that the evidence warrants such a treatment. Table 2-10 shows annual averages for the pollution and meteorological statistics and their standard deviations for each year. The standard deviations, it will be noted, are of similar magnitude to the averages in all cases for the pollutants. In the series of figures which follow, the annual average pollutant concentrations are shown plotted in groups with parameters which have previously been shown to have significant correlations.

TABLE 2-10. ANNUAL AVERAGES OF POLLUTION CONCENTRATIONS AND METEOROLOGICAL PARAMETERS 1961-1969

	1961	1962	1963	1964	1965	1966	1967	1968	1969
Oxidant	.0371	.0553	.0457	.0597	.0620	.0494	.0528	.0423	.0561
σ	.0310	.0332	.0284	.0364	.0341	.0310	.0344	.0271	.0332
NO	.1543	.0866	.1163	.1073	.1135	.1157	.1250	.0960	.1019
σ	.2153	.1045	.1423	.1330	.1514	.1317	.1496	.1267	.1281
NO_2	.0697	.0655	.0724	.0625	.0672	.0504	.0613	.0464	.0570
σ	.0559	.0446	.0444	.0431	.0402	.0391	.0400	.0261	.0306
NO_x			.1699	.1540	.1681	.1587	.1731	.1356	.1454
σ			.1573	.1568	.1731	.1596	.1748	.1401	.1444
HC					7.396	6.137	7.045	6.129	5.853
σ					4.734	3.927	5.156	3.782	3.939
Part.	.6063	.5268	.5008	.4874	.5183	.5112	.5970	.4635	.3587
σ	.3871	.4191	.4182	.3670	.3678	.3324	.432	.3346	.2681
CO		6.597	6.177	6.740	7.311	6.525	7.268	6.297	6.662
σ		6.349	4.841	6.587	7.264	6.139	7.159	5.974	7.048
Temp.	59.69	58.77	58.40	60.22	59.92	61.61	60.95	61.13	61.01
σ	12.88	11.95	12.09	11.28	11.72	12.00	13.39	12.12	12.41
Speed	5.76	5.42	4.60	7.97	6.14	6.00	5.26	5.94	6.05
σ	4.04	3.93	3.58	3.71	4.12	3.88	3.71	3.90	3.98
$(Speed)^{-1}$	.1736	.1845	.2174	.1255	.1629	.1667	.1901	.1683	.1653
Direct.	221.7	224.8	224.4	224.2	218.8	225.5	2.6.8	227.4	218.4
σ	76.2	70.3	70.0	72.0	81.4	75.7	76.5	79.0	75.03

In Figure 2-5 the annual data are shown for hydrocarbons, NO_2 and inverse wind speed. The data period for hydrocarbon is too short to permit conclusions, but a downward trend is suggested. The NO_2 data likewise show an apparent downward trend throughout the entire nine-year period. The small positive correlation with inverse wind speed can easily be seen. Figure 2-6 shows the data for oxidant, temperature and inverse wind speed. Disappointingly, no trend can be discerned for oxidant, and negligible interrelationships can be detected between these variables. Figure 2-7 shows the same analysis for carbon monoxide, particulate matter and inverse wind speed. No trend is evident for carbon monoxide. Particulates do indicate a decrease in the last three years of the data period, but this can be seen to be highly correlated with a decrease in the inverse wind speed at the same time.

Our previous analysis indicated that correlations among the pollution and meteorological variables were more apparent if the analysis was done on a seasonal basis. Accordingly, we have examined temporal variation on a mean monthly basis. Tables 2-11 and 2-12 show the monthly averages for June and October for each year in the study period. Figure 2-8 shows a plot of the June data for oxidant, temperature and inverse wind speed. No trend is evident for oxidant and interrelationships seem nil. The previous analysis had indicated weak

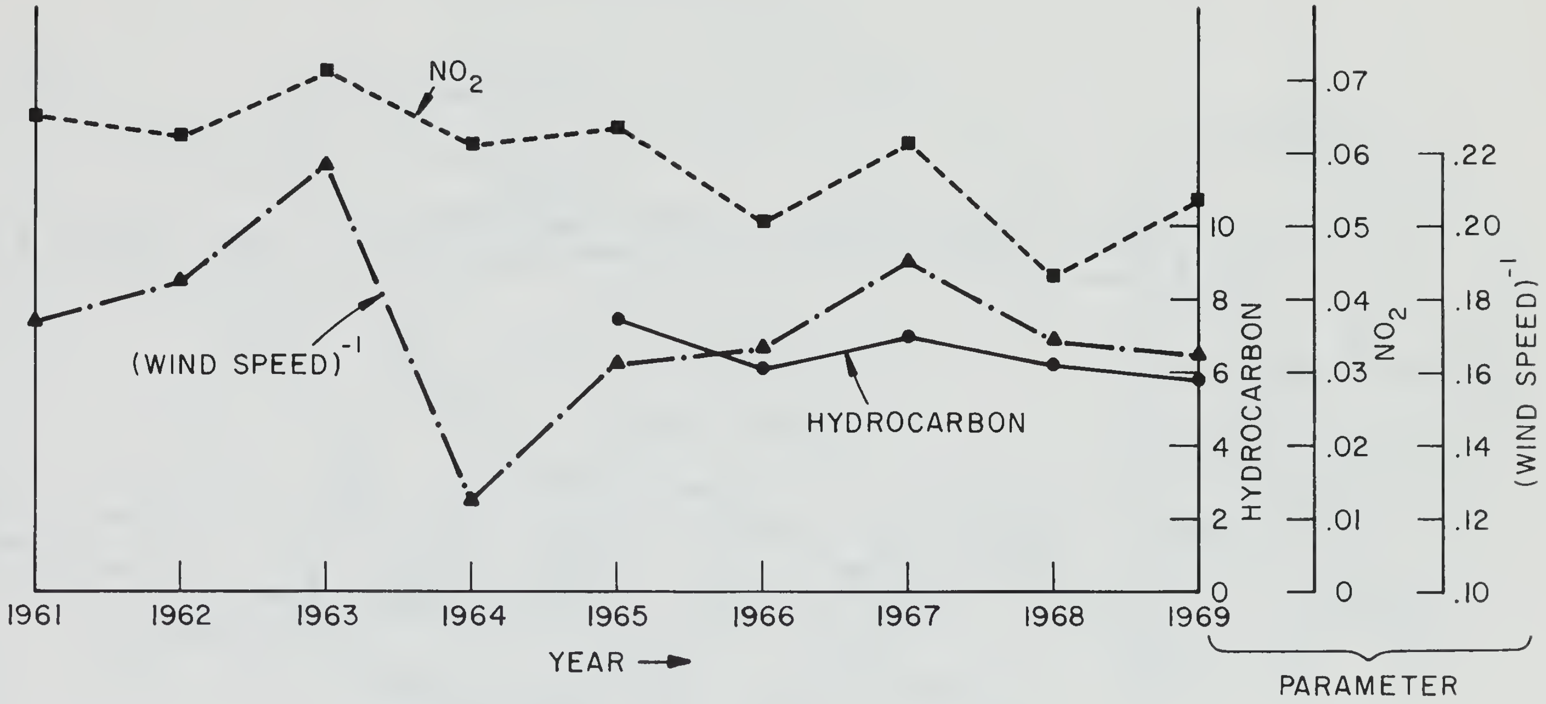

Figure 2-5. Annual averages of the maximum daily concentrations of Carbon Monoxide (ppm) and Nitrogen Dioxide (ppm) and 24 hour average Inverse wind speed (mph^{-1}).

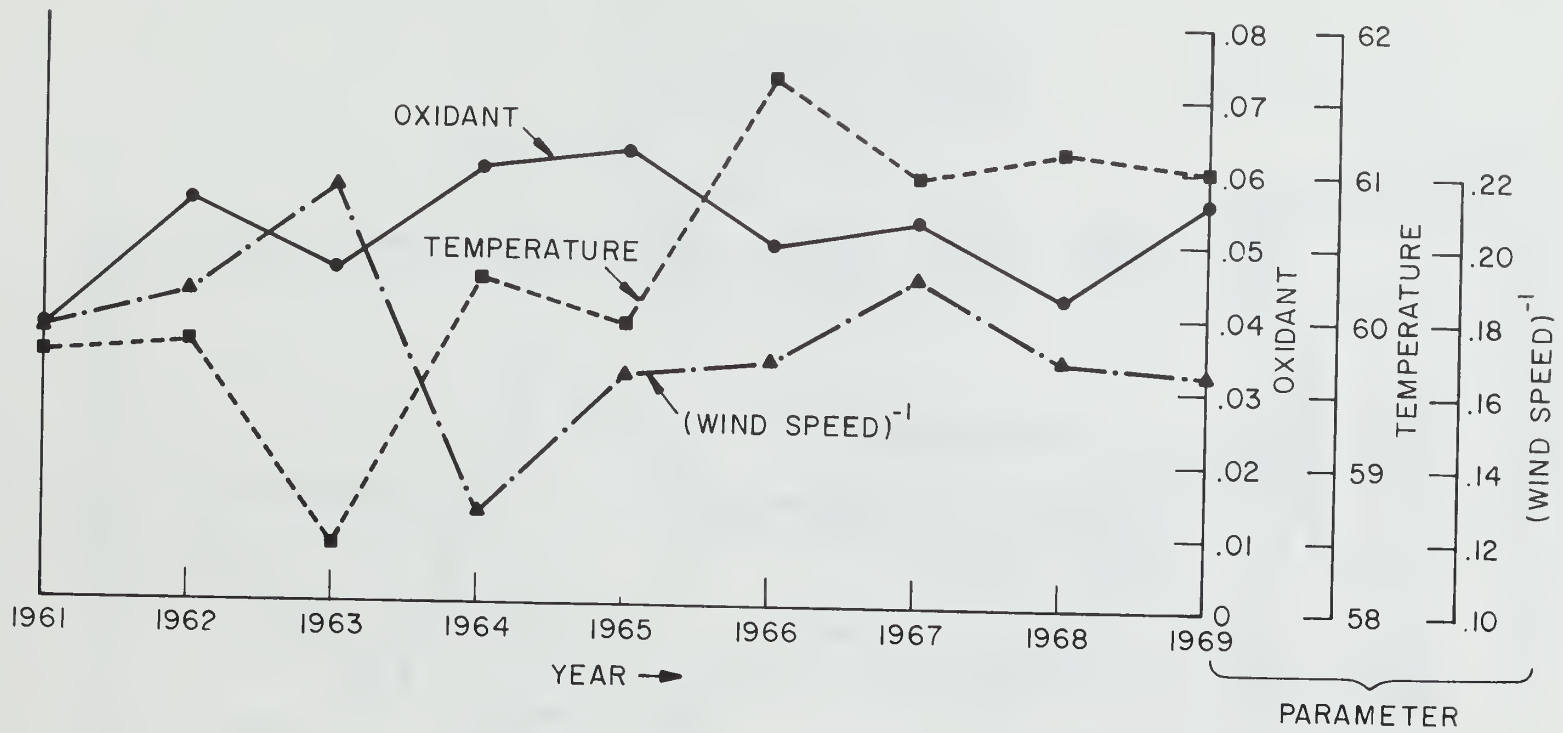

Figure 2-6. Annual averages of the maximum daily concentration of Total Oxident (ppm) and 24 hour average Temperature (°F) and Inverse Wind Speed (mph^{-1}).

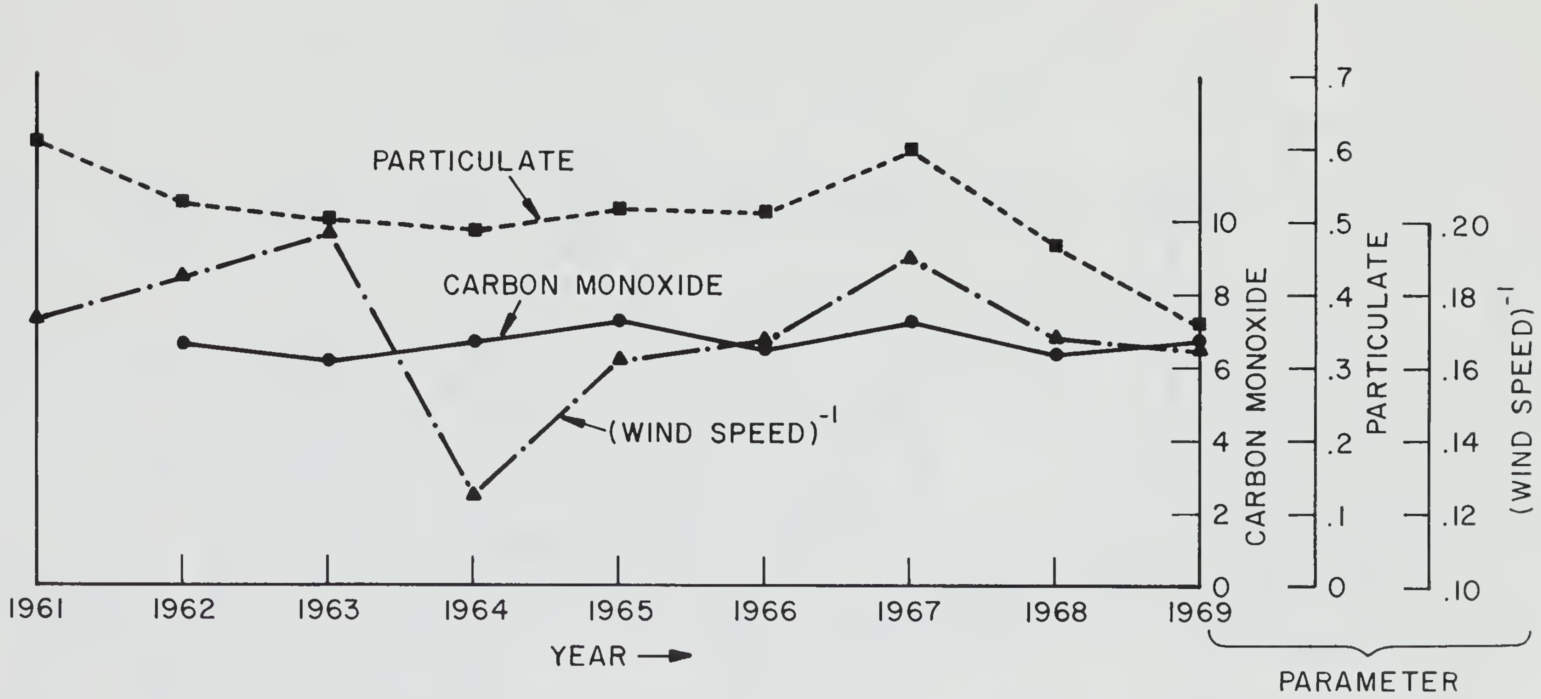

Figure 2-7. Annual averages of the daily maximum concentration of Carbon Monoxide and 24 hour average of Particulates and Inverse Wind Speed (mph^{-1}).

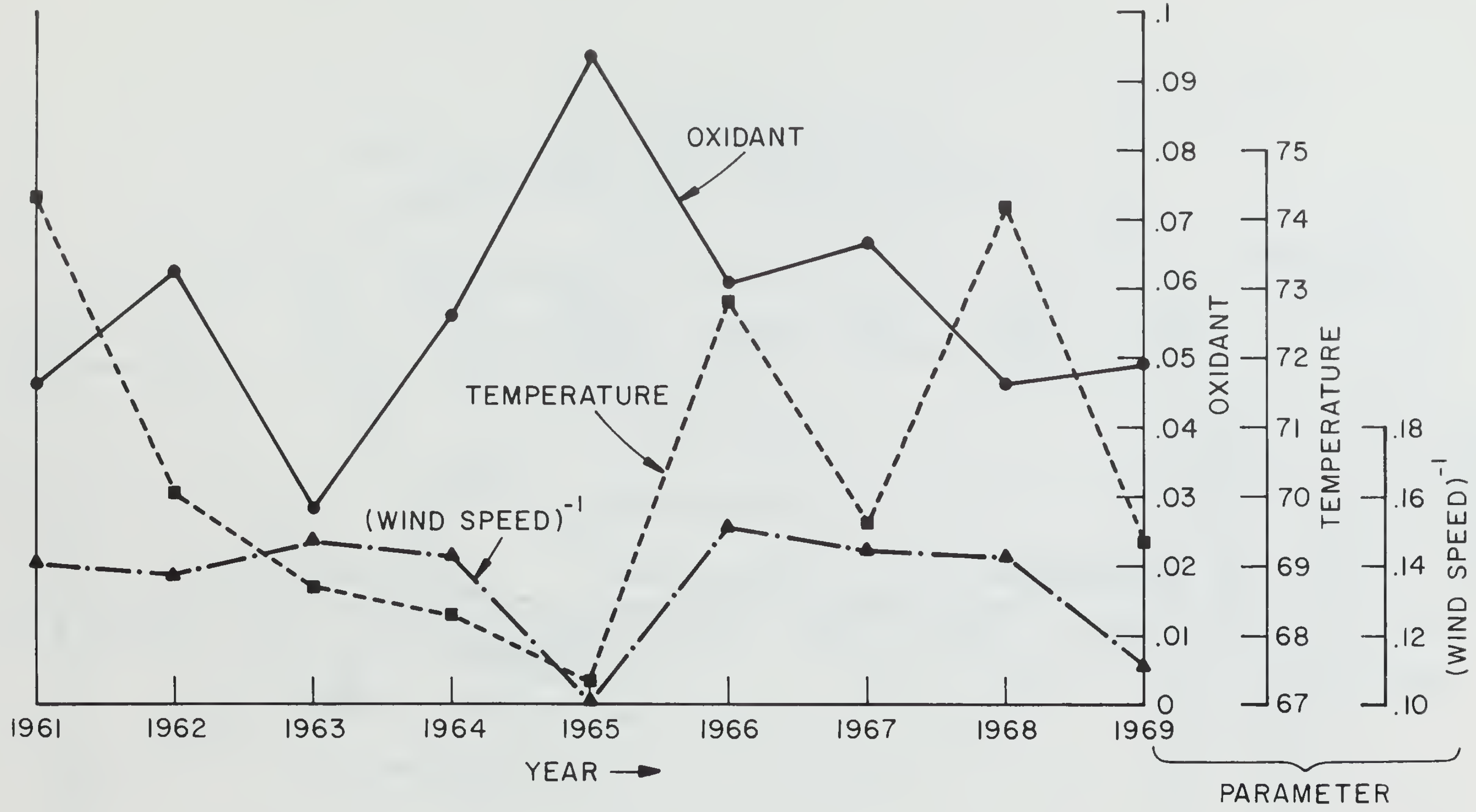

Figure 2-8. June averages of the daily maximum concentration of Total Oxidant (ppm) and 24 hour average Temperature (°F) and inverse wind speed (mph^{-1}).

positive correlations to exist among these variables but that is not apparent for this month. The year 1965 is particularly puzzling in that the highest June oxidant concentration is reached in this year despite the lowest values of temperature and inverse wind speed. It could be argued that this maximum is the result of increasing numbers of motor vehicles with, as yet, ineffective emission control. The decrease after 1965 would then reflect the increased effectiveness of the control technology. Figure 2-9 shows the June data for carbon monoxide, particulates and inverse wind speed. No trend is apparent and obvious correlations can be seen between these parameters.

TABLE 2-11. JUNE MONTHLY AVERAGES 1961-1969

	1961	1962	1963	1964	1965	1966	1967	1968	1969
Oxidant	0.0460	.0625	.0282	.0589	.0934	.0604	.0662	.0460	.0487
CO	--	3.759	2.700	4.103	3.233	4.133	3.200	3.172	3.310
Part.	.4286	.2567	.2033	.2464	.2300	.3321	.2960	.2714	.2033
Temp.	74.3	70.03	68.70	68.27	67.30	72.80	69.60	74.17	69.33
Speed	7.06	7.24	6.78	7.07	9.61	6.61	6.92	7.04	8.79
(Speed)$^{-1}$	.1416	.1381	.1474	.1414	.1040	.1512	.1445	.1420	.1137

TABLE 2-12. OCTOBER MONTHLY AVERAGES 1961-1969

	1961	1962	1963	1964	1965	1966	1967	1968	1969
Oxidant	.0321	.0493	.0568	.0865	.0800	.0694	.0766	.0559	.0397
CO	--	12.82	9.129	15.25	19.06	13.21	17.43	13.40	10.16
Part.	.9192	.5968	.6821	.9862	1.026	.7903	.9964	.7214	.3948
Temp.	62.58	61.00	64.48	66.90	66.22	64.26	65.74	62.35	61.26
Speed	6.26	4.87	4.12	5.70	3.75	5.21	4.20	4.39	5.21
(Speed)$^{-1}$	.1597	.2053	.2427	.1754	.2667	.1919	.2380	.2278	.1919

The next series of figures show the same analysis for the month of October. Data for oxidant, temperature and inverse wind speed are given in Figure 2-10. The oxidant profile for Ocrober can be seen to follow a pattern very similar to that for June except that the maximum is reached one year sooner. On the face of it, this could interpreted as an encouraging indication that the emission control program is having a significant effect since there is little meteorological reason for events in October to be correlated with those in June, on the average. However, further examination of this figure shows that a strong correlation exists between oxidant concentration and temperature. It appears that patterns of temperature, which presumably reflect fluctuations in radiation load, explain the oxidant variation. In addition, inverse wind speed, since 1965, also has correlated with the oxidant fluctuations. On the basis of this figure, it would be very difficult to demonstrate that the control technology was dominating the observed oxidant concentrations. Figure 2-11 shows the October analysis for carbon monoxide, particulate and inverse wind speed. Again the correlation among these variables is strong and no trend is apparent.

This elementary statistical analysis illustrates the fundamental difficulty of demonstrating improvement in air quality due to emission control. As can be seen from the October analysis, the most important meteorological variables, such as inverse wind speed and temperature, dominate the pollution data and are highly variable from year to year.

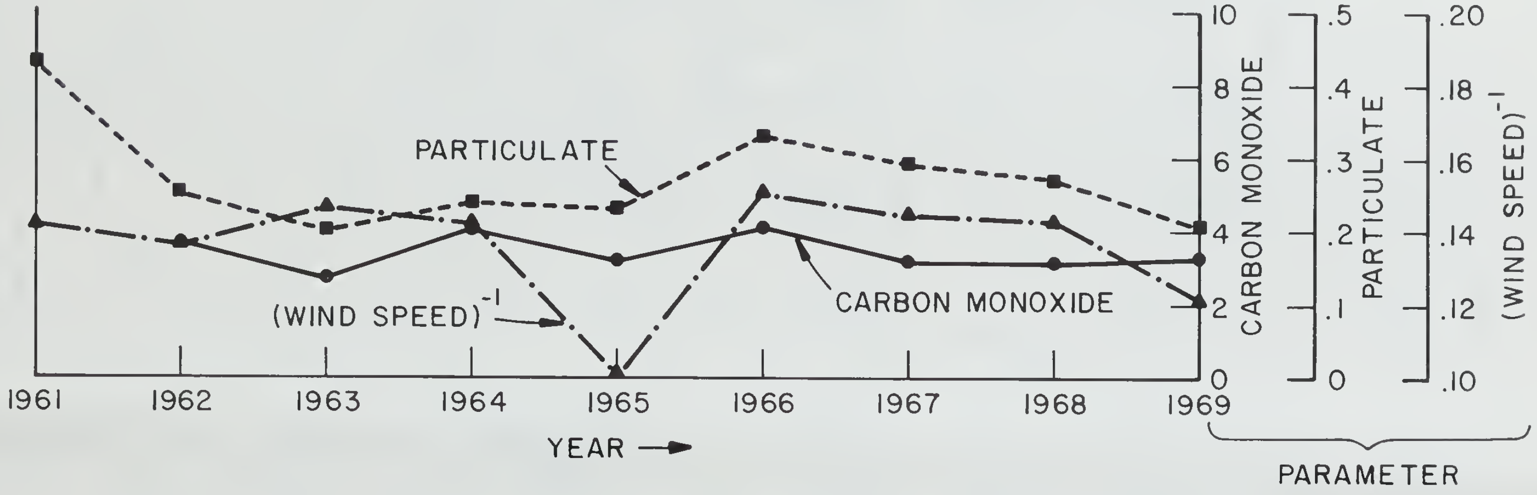

Figure 2-9. June averages of the daily maximum concentration of Carbon Monoxide (ppm) and 24 hour average Particulates (COH) and Inverse Wind speed (mph^{-1}).

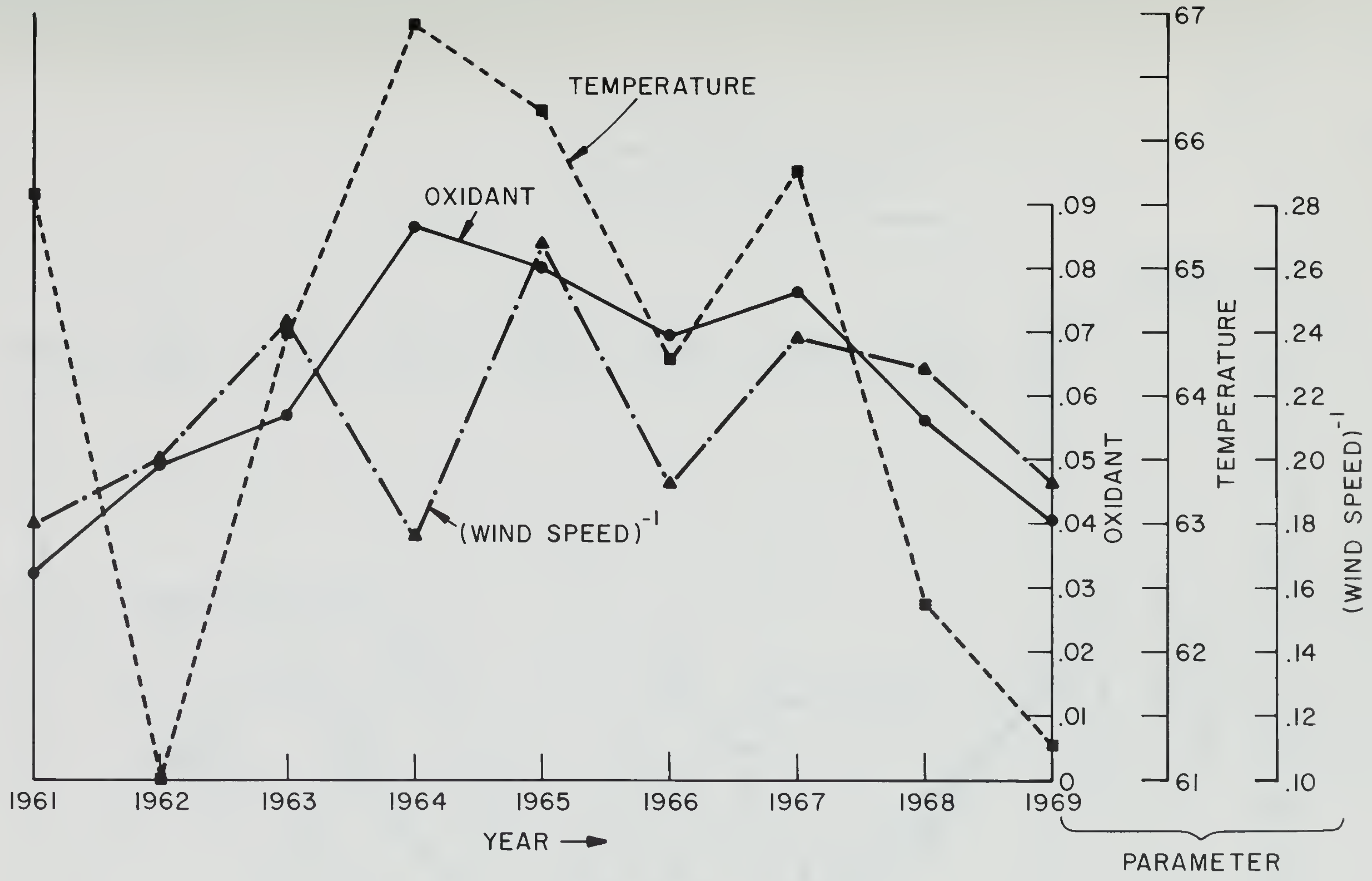

Figure 2-10. October averages of the daily maximum concentration of Total Oxidant (ppm) and 24 hour average temperature (°F) and inverse wind speed (mph^{-1}).

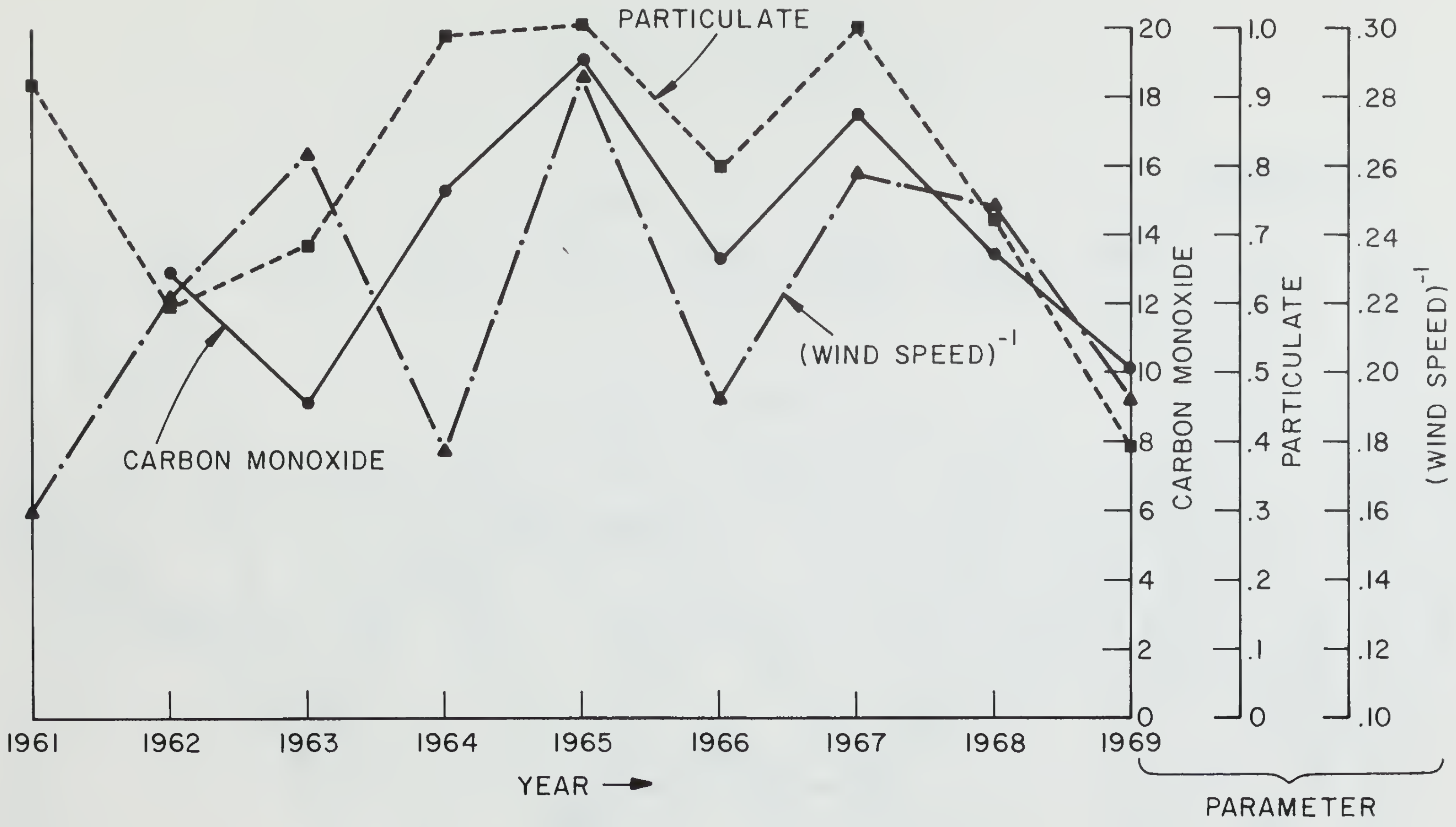

Figure 2-11. October averages of the daily maximum concentrations of Carbon Monoxide (ppm) and Particulates (COH) and 24 hour average inverse wind speed (mph^{-1}).

Consequently, significant improvement in quantity of pollutants emitted from motor vehicles could easily be masked by meteorological variability. We can state categorically that no temporal trend, either up or down, can be demonstrated for the majority of the pollutants found in the air above Sacramento. There is indication that hydrocarbon and NO_2 concentrations have been decreasing during our study period. The hopeful sign is countered by the fact that the associated pollutant, oxidant, does not show an unambiguous decrease for our study period.

CHAPTER 3

DRIFT, DIFFUSION AND FALLOUT OF AN INSTANTANEOUS LINE SOURCE OF HEAVY PARTICLES IN THE ATMOSPHERIC BOUNDARY LAYER

INTRODUCTION

In this chapter we shall discuss the development of a numerical model of the processes by which a line source of gaseous material or heavy particles, released in the atmospheric boundary layer, is diffused downwind and, in the case of particles, deposited at the surface of the earth. We have in mind two applications for this model: (1) a cloud of pesticide or herbicide released by a low flying aircraft for agricultural purposes and (2) gaseous pollutants and particulate matter emitted by motor vehicles moving on a highway. Both these cases are serious environmental problems involving the health and safety of individuals and ecosystems in the area downwind of the source of pollution. In the discussion which follows, we shall emphasize particulate pollution.

This problem is one of the most difficult conceivable in the field of turbulence and diffusion. Non-isotropic, boundary layer turbulence is known to differ in important ways (Townsend, 1956) from the case of homogenious turbulence, for which a satisfactory theory is available (Batchelor, 1953). In addition, for the two cases we are considering, the effects of unstable and stable stratification are known to be important (Slade, 1968; Yates, et al, 1964). When you add to this system the interaction between the turbulent wakes, formed behind the emitting bodies, and the boundary layer flow the problem becomes dishearteningly complex and well beyond the current state of knowledge in this field. Consequently, we adopted the idealization of the line source as one acceptable simplification. It should be noted that use of this initial condition restricts the applicability of the model to distances well downwind from the release point.

The development of this model has been guided primarily by data relating to the deposition of aircraft released agricultural chemicals very kindly supplied by Professors Akesson and Yates of the Department of Agricultural Engineering at the University of California, Davis. We found the experimental information available from the agricultural case far exceeded any that we were able to find for the highway particulate problem. We do not believe the problem of the drift, diffusion and fallout of agricultural chemical sprays differs in any important way from the same processes affecting particulate matter emitted from highways. If anything, the agricultural chemical problem is more complex due to the possible importance of evaporation in changing the size of the particles with time.

In this chapter we shall develop the model equations from the diffusion equations and micrometeorological theory. Our basic objective has been a model which will predict deposition of particulate information from detailed knowledge of the emitted particulate amount and size distribution and micrometeorological information. We feel that the successful formulation and testing of such a research model is the first step towards developing an operational model which would be capable of making useful estimates of deposition from commonly available source strength and meteorological information.

We have deliberately avoided the use of arbitrary and adjustable parameters. We prefer to use a two stage development in which we first formulate and test a model entirely from known micrometeorological principles. We will not introduce any corrections until the basic behavior of the model is revealed. It should be anticipated, however, that for operational use, corrections of some kind would be required by any model due to the great complexity of the system under consideration.

Discussion

The deposition of a cloud of particles released in the atmospheric boundary layer can be thought of as the net result of three processes. These are: gravitational settling, drift, and diffusion. The first, gravitational settling, is best known and easiest to calculate. In the size range of interest here, diameters from 1 to 100 microns (calculations for larger diameters can, of course, be made, but these larger drops settle so rapidly that the line source approximation becomes very dubious), the Stokes formula is valid only for the smallest particles (Goldstein, 1938). However, empirical information is plentifully available for the entire range (Perry, 1950) so we may regard the settling velocity itself as well-known given reliable data on the size distribution of the particles. Such information is only now becoming available for the highway case (Cahill, 1973). In contrast, detailed size distributions have been measured for some years by Akesson and Yates' group. As we shall see, size information is essential to calculations such as we attempt here.

It should also be noted that the possible effect of evaporation on droplet size for the agricultural case remains a problem that we do not consider in this chapter.

Even without the formidable effect of turbulent diffusion, very considerable dispersal in deposition can be achieved purely through the effect of the differential fallout associated with a size spectrum. This effect is illustrated below in Table 1 where we list the terminal velocities for particles of sizes ranging from 10 to 800μ and deposition point downwind where such a drop would land if it were released at a height of 2 meters with an average wind, from the surface to two meters, 2 ms^{-1}. As can be seen the dispersal of the smaller drops is quite large with the 10μ particles traveling over a kilometer before depositing.

Table 1

Particle Diameter (μ)	Terminal Velocity ($cm\ s^{-1}$)	Deposition Point (m)
10	0.3	1333
20	1.3	308
100	32.0	12.5
200	136.0	2.94
800	340	1.18

It is also apparent why we do not wish to consider particles above 100 . These sizes fall out so fast that they remain in the zone of influence of the turbulent wakes behind the emitting vehicles.

The second process, drift with the mean wind depends critically on the shear of the wind with height near the surface. This is a phenomena extensively studied in micrometeorology (Goddard, 1971; Morgan et al, 1971) and we can choose from several alternative formulations. Most generally,

$$\frac{\partial \bar{U}}{\partial Z} = \frac{U_*}{kZ}\,\phi(Z/L) \quad , \qquad (1)$$

where U is the wind speed, Z is the vertical ordinate, U_* is called the friction velocity, $U_* = (\tau_o/\rho)^{1/2}$ with τ_o the stress exerted by the wind on the surface, ρ is air density, k is the von Kārmān constant with a value of 0.4, L is stability parameter,

$$L = -\frac{\rho C_p T U_*^3}{kgH} \quad , \qquad (2)$$

with C_p the specific heat capacity at constant pressure, T air temperature in °K, g the acceleration of gravity and H the flux of sensible heat transferred upwards from the surface by turbulence, and the overbar indicates a time average of the order of a half-hour. The function $\phi(Z/L)$ is determined empirically, and various versions are available. We have chosen to use the "log + linear" approximation as the simplest which gives a realistic effect of stability on shear. That is,

$$\phi(Z/L) = 1 + \alpha \frac{Z}{L} \quad , \tag{3}$$

where α is a constant whose value has been discussed by Priestley (1963)
We are aware that other approximations to the "phi" functions are probably more accurate over a greater range of stabilities. At the current stage in the development of the model, however, it does not seem appropriate to introduce additional complexity in any individual component until the properties of the entire system are understood. In any event, other versions of the "phi" function can easily be introduced when it becomes apparent that additional accuracy in specifying the shear is warranted.

The mean wind speed between a release height, H, and a reference height Z_o, can easily be calculated from equations (1) and (3). Z_o has the significance of being the height where the mean wind goes to zero according to equation (1). Empirically, Z_o is found to be a strong function of the height of the predominant roughness elements of the surface (Sellers, 1965). Thus, this parameter offers the means of introducing an important aspect of the underlying surface, its roughness. Integration of equation (1) yields

$$U = \frac{U_*}{k} \left[\ln \frac{Z}{Z_o} + \frac{\alpha}{L} (Z - Z_o) \right] \quad , \tag{4}$$

where U_* and L are treated as constants. It has been found that for large canopies, equation (4) describes the mean wind profile accurately only if a "zero plane displacement", d, is used to shift the origin upwards to a height comparable to that of the canopy thickness. The displacement height, like the roughness parameter, Z_o, is empirically determined. It should be understood, therefore, in equation (4) that the origin of the vertical coordinate is at d. We define the mean wind speed between H as the catch height,

Z_c, as

$$\overline{U} = \frac{1}{H - Z_c} \int_{Z_c}^{H} u dZ \quad . \tag{5}$$

Evaluation of this integral with equation (4) substituted for the wind speed yields

$$\overline{U} = U_Z \left[\frac{\dfrac{(H \ln H - Z_c \ln Z_c)}{(H - Z_c)} + \dfrac{\alpha}{2L} (H + Z_c - 2Z_o) - \ln Z_o - 1}{\ln \dfrac{Z_w}{Z_o} + \dfrac{\alpha}{L} (Z_w - Z_o)} \right] , \tag{6}$$

where U_w is the wind speed measured at the height Z_w. Thus, from equation (6) the vertically averaged wind speed can be calculated given a wind speed measured at a single height, the surface roughness parameters Z_o and d, and the stability parameter, L.

The relative roles of stability and surface roughness in determining the transport speed, $\overline{U}$, may be illustrated by a few order-of-magnitude calculations with equation (6). However, some care is required in formulating the calculation in order to avoid misleading results. For instance, if we specify that the release height, H, is 6 meters, L = ∞ (neutral conditions), $U_w = 2 \text{ ms}^{-1}$ at $Z_w = 2$ m, and $\alpha = 2$, the numbers in Table 2 are obtained.

Table 2

Z_o(cm)	$\overline{U}$ (ms^{-1})	$(\overline{U})^{-1}$
0.1	2.026	0.493
1	2.041	0.490
10	2.112	0.473
100	3.318	0.301

We show the inverse of the transport speed because pollutant concentrations should be proportional to this parameter, other factors being the same. Inspection of these numbers would lead one to the anomalous conclusion that the transport speed increased with roughness. This is at variance with a physical concept of surface roughness being a major factor in bringing about the retardation of flow in the atmospheric boundary layer. The reason for this peculiar result lies in specifying the measured wind, U_w, within the layer of interest, $H - Z_o$. Other factors being equal, the speed would not be the same at this height as the boundary layer flows over surfaces of varying roughness. To do a complete examination of this problem would require a substantial detour into the theory of the planetary boundary layer since it is the gradient wind speed that should be held constant in the calculation. Since that problem is well beyond the scope of this chapter (discussed in Volume II of this report), we shall do a simpler calculation that reveals better the physics of the situation. The numbers shown in Table 3 result from specifying the release height, H, to be 2 meters, while the measured wind speed, U_w, is held constant at 2 ms^{-1} at a height of 6 meters. This gives us the problem of the response of the lower portion of the boundary layer to a change of roughness while the wind speed is held constant above. Here we also show an order-of-magnitude calculation as to the effect of stability on the transport speed for various stabilities. The case L = + 10 meters corresponds to moderately stable conditions while L = - 10 meters to moderately unstable conditions. These results are physically more satisfying. The transport speed decreases strongly with increasing roughness. In comparison, it can be seen that the effect of stability on the transport speed is quite small particularly for values of Z_o 10 cm and smaller.

Table 3

Z_o	L = + 10 m		L = ∞		L = - 10	
(cm)	$\overline{U}$ (ms^{-1})	$\overline{U}^{-1}$	$\overline{U}$	$\overline{U}^{-1}$	$\overline{U}$	$\overline{U}^{-1}$
0.1	1.512	0.661	1.518	0.658	1.525	0.655
1	1.351	0.740	1.352	0.739	1.353	0.739
10	1.068	0.936	1.052	0.951	1.033	0.967
100	0.476	2.099	0.431	2.319	0.371	2.693

The third process to be treated by the model, diffusion, is the most difficult of all. It is sometimes treated in air pollution studies by introducing turbulent diffusivities formally analogous to molecular diffusivities but orders-of-magnitude larger. We shall also adopt this procedure but first we shall discuss some of the limitations of the approach.

One of the fundamental properties of turbulent diffusion is that the diffusivity is a strong function of the scale of the diffusing "patch" of fluid. This is a consequence of the fact that for geophysical turbulence the maximum of the spectrum of turbulence is almost always found at quite long wavelengths. Consequently, as a patch of marked fluid grows by diffusion, it becomes subject to diffusion by more and more energetic scales of motion. As L. F. Richardson anticipated, the diffusivity increases roughly as the 4/3 power of the dimension of patch of marked fluid in question. Thus, diffusivity is not a constant as is most convenient mathematically. For the problem under consideration, this means that the diffusivity should increase with time as the cloud of particles moves downwind and increases in size due to turbulent diffusion. Under these conditions, the choice of a constant diffusivity leads to fundamental difficulties.

Another, more operational criticism that can be made of the diffusivity concept is that ordinarily no effort is made to relate diffusivities used in air pollution studies with micrometeorological processes. For instance, surface roughness and stability are known to exert great influence on turbulence in the atmospheric boundary layer yet these quantities are only rarely taken into account in choosing diffusivities. One of our objectives in the model under discussion was explicitly to include micrometeorological parameters, wherever possible, so that the influence of variable terrain, crops and stability could be taken into account in an objective fashion.

The model

We shall consider the intial cloud to be an instantaneous line source at height H. The wind is taken to be blowing perpendicular to the line of release and is measured to be U_w at height Z_w. The downwind coordinate direction is called X. The coordinates of the center Y, the plume at time t, are X_p and Z_p. The plume is considered to be infinite in the Y-direction.

We assume that the center of the cloud moves with the speed of the wind averaged from H to the surface, $\overline{U}$. Then

$$X_p = \overline{U}t \quad , \tag{7}$$

and

$$Z_p = H - ct \quad , \tag{8}$$

where c is the terminal velocity for a specified particle size and $X_p = 0$ and $Z_p = H$ at $t = 0$. In order to calculate the downwind drift of the remainder of the cloud after the center reaches the surface (or catch height) we shall continue to displace the center at speed U, "underground".

Since the terminal velocity, c, depends on particle size, the manner the size distribution is specified is critically important. We have developed two schemes. In one, we assume the particle size spectrum is Gaussian so that we need only specify the mean diameter and the standard deviation to determine the entire distribution. It is necessary to truncate the spectrum at zero diameter to avoid "negative" diameters. The continuous Gaussian distribution is approximated by a series of step functions, as the number of discrete steps is chosen according to the degree of approximation desired. In the second scheme for specifying the particle size spectrum, the distribution is completely arbitrary. Any number of discrete steps can be accommodated. In this way, if measurements of the size distribution are available, the observed spectrum may be approximated to whatever degree desired. Thus, in this model we replace the "real" cloud with a continuous size distribution with a series of homogenious clouds each falling with a different terminal velocity. As we will describe in the following pages, we repeat all our drift, diffusion and fallout calculations for each cloud and then sum them all to obtain the total effect.

We assume that the mass flux in the downwind direction, F_x, can be represented by

$$F_x = \overline{U}\,\overline{q} - K_x \frac{\partial \overline{q}}{\partial x} \quad , \tag{9}$$

Where $\overline{q}$ is the mass concentration in units of g cm^{-3} and K_x is the turbulent diffusivity in the x-direction in units of $cm^2 s^{-1}$. These two terms represent the contribution to the downwind flux of particles of mean drift and diffusion. The vertical mass flux is given by

$$F_z = - c\,\overline{q} - K_z \frac{\partial \overline{q}}{\partial z} \quad , \tag{10}$$

where c is the terminal velocity of a given size particle and is taken as a positive quantity. These two terms then represent gravitational settling and vertical diffusion.

These equations are formulated so as to give a positive flux in the x and z directions and, therefore, a deposition is a negative flux. The overbar indicates that the quantity $\overline{q}$ should be thought of as an averaged quantity either through executing a large number of trials or by averaging in the y (crosswind) direction.

The equation governing mass concentration at some downwind point is

$$\frac{\partial \overline{q}}{\partial t} = - \overline{U} \frac{\partial \overline{q}}{\partial x} + C \frac{\partial \overline{q}}{\partial z} + K \frac{\partial^2 \overline{q}}{\partial x^2} + \frac{\partial^2 \overline{q}}{\partial z^2} \quad , \tag{11}$$

where we have assumed

$$K_x = K_y = K = \text{constant.} \tag{12}$$

Solutions may be obtained for equation (11) using the boundary conditions,

$$\overline{q} \rightarrow 0 \text{ as } t \rightarrow 0 \text{ for } x, z > 0$$

$$\overline{q} \rightarrow 0 \text{ as } t \rightarrow \infty$$

and defining a "source strength", Q, such that

$$Q = \int_{-\infty}^{+\infty}\int \overline{q} \, dxdz \quad , \tag{13}$$

i.e. Q is the total amount of material released in units of grams per unit length along the release line.

By direct substitution into equation (11) it may be verified that the solution is

$$\overline{q} = \frac{Q}{4\pi K t} \exp \left\{ - \frac{\left[(x - \overline{U}t)^2 + (z - H + ct)^2 \right]}{4Kt} \right\} \tag{14}$$

Differentiation of $\overline{q}$ with respect to z and x and use of equations (9) and (10) gives

$$F_z = Q \left(\frac{z - H - ct}{8\pi K t^2} \right) \exp \left\{ - \frac{\left[(x - \overline{U}t)^2 + (z - H + ct)^2 \right]}{4Kt} \right\} \tag{15}$$

$$F_x = Q\left(\frac{x + \overline{U}t}{8\pi Kt^2}\right) \exp\left\{-\frac{\left[(x - \overline{U}t)^2 + (z - H + ct)^2\right]}{4Kt}\right\} \quad (16)$$

The total mass deposition, per unit area and normalized with the source strength, at catch height, Z_c, and distance downwind, x, is given by

$$\frac{D}{Q} = \int_0^\infty \left(\frac{Z_c - H - ct}{8\pi Kt^2}\right) \exp\left\{-\frac{\left[(x - \overline{U}t)^2 + (Z_c - H + ct)^2\right]}{4Kt}\right\} dt \quad (17)$$

which we will call the normalized deposition.

It should be noted that we are identifying the total downward flux, calculated with equation (15), with deposition at the catch height. This is in marked contrast with the usual procedure in which the air concentration is calculated from equation (14), or its equivalent, at the catch height. This number is multiplied with a "deposition velocity", an additional empirical parameter which supposedly takes into account the properties of various surfaces in regard to impact geometry and other processes of deposition. Our general strategy has been to avoid the introduction of free parameters. Therefore, we have chosen not to use the deposition velocity concept.

The total transport, or drift, past point x is given by

$$\frac{T}{Q} = \int_0^\infty \int_0^\infty \left(\frac{x + \overline{U}t}{8\pi Kt^2}\right) \exp\left\{-\frac{\left[(x - \overline{U}t)^2 + (z - H + ct)^2\right]}{4Kt}\right\} dtdz \quad , \quad (18)$$

where the normalized drift is given in units of mass per unit length in the y-direction.

We have developed a numerical technique for integrating these integrals. However, the algorithm was so consuming of machine time that we found the economics of systematically investigating the properties of the model prohibitive. Consequently, we developed the following analytic scheme for integrating equation (17). The right side of equation (17) is of the form

$$\int_0^\infty \frac{F_x}{Q} dt = \int_0^\infty \left(\frac{C_1}{t} + \frac{C_2}{t^2}\right) e^{\frac{B^2 + C^2}{-4Kt}} dt \quad , \quad (19)$$

where $C_1 = {}^{c}/8\pi K$ $C_2 = H - {}^{Z}c/8\pi k$ $B = x - \overline{U}t$ and $C = Z_c - H + ct$. The integral may be further transformed,

$$\int_o^\infty \frac{F_x}{Q}\,dt = \int_o^\infty C_6\left(\frac{C_1}{t} + \frac{C_2}{t^2}\right) e^{-\frac{C_3}{t} - C_5 t}\,dt \quad , \qquad (20)$$

where $C_3 = (Z_c^2 + H^2 + X^2 - 2\,Z_cH)/4K$ $C_5 = (\bar{U}^2 + c^2)/4K$, $C_6 = e^{C_4}$ and $C_4 = [\bar{U}x - c(Z_c - H)]/2K$. From the Bessel function literature (Dwight, 1955), we have the relation

$$\int_o^\infty X^{\nu-1} \exp\,(-\beta\,X^p - pX^{-p})\,dx = \underline{2}\,\left(\frac{\gamma}{\beta}\right)^{\nu/2p} B_{\nu/p}\,(2\sqrt{\beta\gamma}\,) \quad , \qquad (21)$$

for $\beta < 0$ and $\gamma < 0$, where $B_n(Y)$ is a modified Bessel function of Y of order n. Our integral may be written as

$$\int_o^\infty \frac{F_x}{Q}\,dt = \int_o^\infty C_6\,\left(\frac{C_1}{t} + \frac{C_2}{t^2}\right) e^{-\frac{C_3}{t} - C_5 t}\,dt = C_6C_1\int_o^\infty t^{0-1}\exp(-C_5t^1 - C_3t^{-1})\,dt$$
$$+\,C_6C_2\int_o^\infty t^{-1-1}\exp(-C_5t^1 - C_3t^{-1})\,dt \quad , \qquad (22)$$

which are two integrals of the proper form. We can now write

$$\int_o^\infty \frac{F_x}{Q}\,dt = 2\,C_6C_1\,B_o\,(2\sqrt{C_3C_5}\,) + 2\,C_6C_2\left(\frac{C_3}{C_5}\right)^{-\frac{1}{2}} B_1\,(2\sqrt{C_3C_5}\,) \quad , \qquad (23)$$

where

$$2\,C_6C_1 = 2\,C_1C_6 = \frac{c}{4\pi K}\exp\left[\frac{c(Z_c - H) - x\bar{U}}{-2K}\right]$$

$$2\,C_6C_1 = 2\,C_1C_6 = \frac{H - Z_c}{4\pi K}\exp\left[\frac{c(Z_c - H) - x\bar{U}}{-2K}\right]$$

$$2\,\sqrt{C_3C_5} = \frac{1}{2K}\left[(Z_c^2 + H^2 + X^2 - 2\,HZ)\,(c^2 + \bar{U}^2)\right]$$

and

$$C_3/C_5 = (Z_c^2 + H^2 + X^2 - 2\,HZ)/(c^2 + \bar{U}^2).$$

The final form, then, which we now use in the model is

$$\int_0^\infty \frac{F_x}{Q}\, dt = (4\pi K)^{-1} \exp\left[\frac{C(Z_c - H) - x\bar{U}}{-2K}\right]$$

$$\left\{ C\, B_o \left[\frac{1}{2K} \sqrt{(Z_c^2 + H^2 + X^2 - 2HZ_c)(c^2 + \bar{U}^2} \right] \right\}$$

$$+ (H - Z_c) \left[\frac{Z_c^2 + H^2 + X^2 - 2HZ_c}{c^2 + \bar{U}^2}\right]^{-\frac{1}{2}}$$

$$+ B_1 \left[\frac{1}{2K} \sqrt{(Z_c^2 + H^2 + X^2 - 2HZ_c)(c^2 + \bar{U}^2)}\right] \qquad (24)$$

We have incorporated tables from Dwight (1955) for the modified Bessel functions of order 0 and 1 into our algorithm for calculating normalized deposition. Excellent agreement was achieved between the numerical and analytic integration schemes. The analytic algorithm was found to be two orders of magnitude faster than the numerical scheme.

The last important parameter to specify in the model is the diffusivity which we have assumed constant in order to be able to use an analytic solution. We have chosen to assume that the diffusivity for the diffusivity for the small particle we are considering is the same as that for momentum. This cannot strictly be true but we have adopted the assumption as a useful first approximation. From equation (1), we have

$$K = \frac{kU_* Z}{\phi(Z/_L)} \qquad (25)$$

We choose to evaluate the diffusivity at $(H + Z_c)/2$. Using equation (4) to specify the friction velocity, we obtain

$$K = \frac{k^2\, U_w\, (H + Z_c)}{2\left[\ell n \frac{Z_w}{Z_o} + \frac{\alpha}{L}\,(Z_w - Z_o) \qquad 1 + \frac{\alpha}{2L}\,(H + Z_c)\right]} \qquad (26)$$

In summary, the following information must be specified in order to calculate downwind deposition: (1) the wind speed, U_w, at a particular height, Z_w, (2) the atmospheric stability either by means of the parameter L or some other measure of stability which can be converted to L such as the Richardson number or the Stability Ratio, (3) the canopy roughness characteristics as specified by Z_o and the zero-plane displacement height, (4) the properties of the cloud of particles, i.e., particle density, size distribution, and release height, H, and (5) the catch height, Z_c. It should be evident that, in so far as the state of the art allows, we have successfully avoided use of arbitrarily determined parameters in this model. This may be regarded as an excessively purest strategy and our results may indeed not be as good as those achieved with models in which various parameters are available, such as diffusivity or deposition velocity, to adjust the calculation to correspond with observation. We feel that more may be learned from discrepancies than from agreement in this case.

Analysis and preliminary validation

In this section we shall illustrate the use of the model and the kind of analysis which may be performed with the output information. We do not pretend that the analysis is complete. It is our opinion that far too little attention is usually paid the analysis of the properties of models, considered apart from the accuracy of their predictions. In many cases, detailed studies such as systematic sensitivity analyses yield information which may be more valuable than a bare validation effort, particularly considering the general difficulty of securing definitive experimental data.

At this time we have carried out one validation study. It is helpful to discuss the nature of the data which Professors Akesson and Yates have made available to us. Their experiments are aimed at understanding the nature of all the processes, from the nozzle to the plant, by which aircraft-released agricultural chemicals are deposited in a target area and dispersed into the environment. The objective is to assist in the development of systems which minimize drift beyond the target area and maximize the effectiveness of the application. In these experiments, the aircraft makes repeated passes at an altitude of about 10 feet upwind of the instrumented area. The multiple passes greatly increase the reliability of the experimental statistics. The released material is designed to simulate the physical properties of various pesticides and herbicides and contains accurately known amounts of fluorescent dye. Downwind deposit is measured by determining the amount of fluorescent dye deposited on mylar plates, while air concentrations are measured by means of high volume samplers. Cascade impactors are used to determine the size distribution of the particles. The deposition measurements are accompanied by micrometeorological measurements of the temperature and wind speed profile and turbulence level. The Stability Ratio, SR, is used as a measure of atmospheric stability, where

$$SR = \frac{\overline{T}_2 - \overline{T}_1}{\overline{U}^2} \times 10^5 \quad , \qquad (27)$$

where the mean temperature, in °C, is measured at 32 and 8 feet, the mean wind speed is measured at 16 feet in units of cm s^{-1}.

Model verification

We had hoped to include in this chapter a comprehensive analysis of the model's behavior relative to observed data. Unfortunately, the experimental effort and analysis of the data is so difficult and time consuming that we have been able to complete only one case. The difficulty lies in measuring the size distribution of the emitted particles. Inasmuch as we have no idea how representative this single case is, we have chosen not to present the analysis at this time. We would have preferred to delay publication of this report until comprehensive verification information was available. However, since the delay in publishing this report has already been extensive, we have decided to present the model without verification at this time.

REFERENCES

Batchelor, G. K. (1953): *The Theory of Homogenious Turbulence*. Cambridge University Press.

Cahill, T. A. (1973): *Contribution of Freeway Traffic to Airborne Particulate Matter*. Final Report to the California Air Resources Board, Contract ARB-502, Crocker Nuclear Laboratory, University of California, Davis.

Dwight, H. B. (1961): *Mathematical Tables*. Dover Publications, New York.

Goddard, W. B. (1971): *Heat, Mass and Momentum Transfer*. Ph.D. Dissertation, Department of Agricultural Engineering, University of California, Davis.

Godstein, S., Editor (1938): *Modern Developments in Fluid Dynamics*. Oxford at the Clarenton Press.

Morgan, D. L., W. O. Pruitt, F. J. Lourence (1971): *Analysis of Energy, Momentum and Mass Transfers Above Vegetative Surfaces*. Department of Water Science and Engineering, University of California, Davis.

Perry, J. H. (1950): *Chemical Engineers Handbook*, 3rd Ed. McGraw-Hill Book Co.

Priestley, C. H. B. (1963): Recent flux and profile measurements in Australia. Abstracted in *Proc. 13th Assembly IUGG-IAMAP*, Berkeley, California.

Sellers, W. D. (1965): *Physical Climatology*. University of Chicago Press.

Slade, D. H., Ed. (1968): *Meteorology and Atomic Energy 1968*. U.S. Atomic Energy Commission, Division of Technical Information.

Townsend, A. A. (1956): *The Structure of Turbulent Shear Flow*. Cambridge at the University Press.

Yates, W. E., N. B. Akesson, H. H. Coutts (1966): Evaluation of drift residuals from aerial applications. Trans. Am. Soc. Agr. Engin., 9, 389-397.

RETURN TO the circulation desk of any
University of California Library
or to the
NORTHERN REGIONAL LIBRARY FACILITY
University of California
Richmond Field Station, Bldg. 400
1301 South 46th Street, Richmond, CA 94804-4698

ALL BOOKS MAY BE RECALLED AFTER 7 DAYS

To renew or recharge your library materials, you may
contact NRLF 4 days prior to due date at (510) 642-6233

DUE AS STAMPED BELOW

OCT 26 2011

DD20 10M 4-10

Book Slip–Series 458

3 1175 00650 8538